UNIVERSITÉ LAVAL

Studies on the role of the Extended-Synaptotagmin Gene Family in vivo

Thèse

Prakash Mishra

Doctorat en biologie cellulaire et moléculaire

Philosophiae Doctor (Ph.D.)

Québec, Canada

Résumé

La signalisation cellulaire est un processus fondamental par lequel les organismes multicellulaires assurent un développement normal et maintiennent leur homéostasie. La communication entre les divers organites joue un rôle crucial en ce sens. Les sites de contact membranaires (SCM), régions de proche apposition entre deux organites (environ 20 nm), sont importants dans le maintien de la communication inter-organite. Une étude minutieuse de cette communication est indispensable pour comprendre certains fascinants mystères de la nature. Récemment, les protéines apparentées aux synaptotagmines (ESyt) ont été identifiées comme étant des protéines résidentes au niveau du Réticulum Endoplasmique (RE) et impliquées dans le maintien des sites de contact entre le RE et la Membrane Plasmique (RE-PM). Trois protéines appartiennent à cette famille, dénommées ESyt1-3. Celles-ci sont également impliquées dans la reconnaissance des récepteurs conduisant à l'endocytose du récepteur et la signalisation en aval.

Dans ce manuscrit, nous présentons l'interaction des ESyt avec FGFR1-4, EGFR ainsi que le récepteur MET et proposons que les ESyt interagissent avec de nombreux récepteurs tyrosine-kinases (RTK). Nous avons montré que les membres de la famille ESyt (ESyt1, ESyt2a et ESyt2b (variant d'épissage) et ESyt3) sont capables d'homo- et hétéro-dimérisé via leurs séquences proximales à, ou chevauchantes leur domaine transmembranaire (TM) (a.a. 88 à 138). De plus, il a été montré que l'interaction de ESyt2 avec FGFR1 est dépendante de l'état actif du récepteur. Cependant, l'autophosphorylation du récepteur ou son activation catalytique *per se* ne sont pas requises. Le site de liaison à ESyt2 sur FGFR1 est proche du site de liaison à l'ATP au sein du lobe supérieur du domaine catalytique du récepteur. Il devient accessible lorsque la boucle d'activation est déplacée dans sa conformation active. Le site d'interaction sur ESyt2 se situe dans la même région que la séquence nécessaire à la dimérisation de ESyt (a.a 88 à 138) et ne requière pas le domaine SMP adjacent. Finalement, nous montrons que la perte de ESyt2 et Esyt3 n'affecte ni le

développement ni la viabilité chez la souris, malgré que la migration cellulaire et la survie sont affectées suite à des stress *in vitro*.

Abstract

Cellular signaling is one of the fundamental process by which multicellular organisms maintain their normal development and homeostasis. Inter-organelle communication plays a crucial role in governing such processes. Membrane contact sites (MCS), a region where two organelles come in close proximity (within ≈20nm), helps in maintaining the inter-organelle communication. A thorough study of inter-organelle communication is required to understand some of the wonderful mysteries of nature. Recently Extended Synaptotagmin-like proteins (ESyts) have been found to be Endoplasmic Reticulum (ER) resident proteins that have been attributed the function of maintaining the ER-Plasma Membrane (ER-PM) contact sites. Three proteins belong to this family, namely ESyt1 to 3. Further, ESyts have been implicated in receptor recognition, receptor endocytosis and downstream signaling.

Here I present the interaction of ESyts with FGFR1-4, EGFR and the MET receptor and propose that ESyts interact with a broad range of receptor tyrosine kinases (RTKs). The members of ESyt family (ESyt1, ESyt2a and ESyt2b (spliced variants), and ESyt3) are shown to homo- and heterodimerize via sequences proximal or overlapping their transmembrane domains (TM) (a.a. 88 to 138). It is shown that the interaction of ESyt2 with FGFR1 is dependent on the active state of the receptor. In contrast, neither receptor autophosphorylation nor catalytic activation *per se* is required. Rather, the interaction depends upon the active conformation of the receptor catalytic domain. The ESyt2 binding site on FGFR1 lies close to its ATP binding fold within the upper lobe of the receptor catalytic domain and is revealed when the receptor activation loop is displaced into the active conformation. The interaction site on ESyt2 lies within the same sequences that are required for ESyt dimerization (a.a. 88 to 138) and does not require the adjacent SMP homology domain. Finally, it is shown that the loss of ESyt2 and ESyt3 does not affect mouse development or viability. However, in vitro cell migration and survival under stress are affected.

Table of Contents

List of figures

Abbreviations

AP-2	Adaptor Protein 2
Atg18	Autophagy-related protein 18
ATP	Adenosine triphosphate
CHD	CAM-homology domain
DAG	Diacyl glycerol
EGF	Epidermal Growth Factor
EGFR	Epidermal Growth Factor Receptor
ER	Endoplasmic Reticulum
ERK	Extracellular signal-regulated kinase
ERMES	Endoplasmic Reticulum (ER)-Mitochondria Encounter Structure
ESyt	Extended Synaptotagmin like protein
FGF	Fibroblast Growth Factor
FGFR	Fibroblast Growth Factor Receptor
FGFR1-3P	Fibroblast Growth Factor 3 Phosphate
FGFRL1	Fibroblast Growth Factor Receptor like protein 1
FRS2	FGF Receptor Substrate 2
GAB	GRB2-associated-binding protein
GAP	GTPase-activating protein
GEF	Guanine nucleotide exchange factor
GRB2	Growth factor receptor-bound protein 2
GTP	Guanosine-5'-triphosphate
HSPG	Heparin sulfate proteoglycan
IP3	Inositol trisphosphate
IP3R	Inositol trisphosphate receptor
JNK	c-Jun N-terminal kinase
LTP	Lipid-transfer proteins
MAPK	Mitogen-activated protein kinase

MAPKAP	Mitogen-activated protein kinase
MAPKK	Mitogen-activated protein kinase kinase
MAPKKK	Mitogen-activated protein kinase kinase kinase
MAPPER	Membrane attached peripheral ER
MEK	MAPK-ERK kinase
MEKK	MEK kinase
MCS	Membrane Contact Sites
MCTP	Multiple C2 domain and transmembrane region protein
MSK	mitogen- and stress-activated kinases
NGF	Nerve growth factor
NLK	Nemo-Like Kinase
NVJ	Nucleus-Vacuole Junction
PAK1	p21 activated kinase
PE	Phosphatidylethanolamine
PH	Pleckstrin homology
PI3K	Phosphoinositide-3 kinase
PIP2	Phosphatidylinositol 4,5-bisphosphate
PKA	Protein kinase A
PKC	Protein kinase C
PLA	Phospholipase A
PLC	Phospholipase C
PLD	Phospholipase D
PM	Plasma membrane
PROPPIN	β-propeller that bind phosphoinositide
PTB	Phosphotyrosine-binding domain
PtdIns	Phosphatidylinositol
PtdIns (3,4,5)P3	Phosphatidylinositol (3,4,5)-trisphosphate
PtdIns4P	Phosphatidylinositol 4-phosphate
PX	Phox homology
RSK	Ribosomal s6 kinase
RTK	Receptor tyrosine kinase

SEF	Similar expression to fgf
SH2	Src Homology 2
SH3	SRC Homology 3
SMP	Synaptotagmin-like-mitochondrial-lipid binding protein
SNAP-25	Synaptosomal-associated protein 25
SNARE	Soluble N-ethylmaleimide attachment protein receptor
SOC	store-operated ca^{2+} channels
SOS	Son of sevenless
SV	Synaptic vesicles
Syt1	Synaptotagmin 1
TCB	Tricalbin
TCR	T cell receptors
TK	Tyrosine kinase
TMD	Transmembrane domain
TULIP	Tubular lipid-binding proteins
VAMP	Vesicle-associated membrane protein
Vps15	Vacuolar protein sorting-associated protein 15
Vps34	Vacuolar protein sorting 34
WIPI	WD40 repeat protein interacting with phosphoinositides

Acknowledgement

The work presented in this thesis reflects the four and half years of work during my doctoral study. I must say that my work was not easy and remained complicated and confusing right from the start of my PhD and all the way till the end. It wouldn't have been possible for me to write my thesis without the kind help and support from my supervisor, colleagues, friends and family. So, here in this section of my thesis, I would like to acknowledge all those excellent people around me and would like to thank all of them from the core of my heart.

First of all, I would like to thank my supervisor Dr. Tom Moss. I am really grateful to him for providing me the opportunity to work in his lab. I truly admire him for the vast knowledge and passion for the science that he has. Although working in his lab is not easy and that it is close to impossible to convince him about anything new! I would never forget few of the things that he used to say in the lab often and one of them is "Ideas are cheap to buy but very expensive (in terms of difficulty) to get it done" I am really thankful to him for his help, patience, guidance and valuable advice throughout my doctoral work.

I would also like to thank all the past and present lab members who have always been supportive. I would like to give special thanks to Victor Stefanovsky (or Saint Fanovsky) for all of his general theories, not only about science but about almost everything in life, and to Michel Tremblay (or Super Mike) from whom I have learned a lot and without whose help, it would have been impossible for me to finish my work. I would like to thank Alexander Mikryukov for helping me during the early phase of my doctoral work and for all his valuable comments and advice, I learned much from him. I also thank François Guillou. He was the first person with whom I worked, and I am grateful to him for helping me learn several techniques. I would also like to thank Fred Lessard for his wonderful thoughts and motivating advice. Also, I thank all those wonderful people, both past and present lab members, who

were there around me: Nourdin Hamdane, Sabrina Bellenfant, Chelsea Herdman, Ines Bacher, Joël Boutin and Jean-Clément Mars.

Further, I thank all those in our research center, they have been so friendly to me and I wish to express my appreciaton to each and everyone of them. I would like to give a special thanks to Katia Mercier for being such a good friend. She is continuously trying to help anybody and everybody. I also thank Lucie Marcoux for being so friendly and helpful.

I wish to thank all of my Indian friends, Ranjan Maity, Wajid Bhat, Irfan Bukhari, Hemanta Adhikary, Priyanka Patel, Jayesh Patel, Niraj Joshi, Pallavi Jain, Kallol Dutta, Sai Sampath, Senthil Krishnaswami and Arojit Mitra and the many others whose names I missed out here. I would also like to thank all those friends I have made in Quebec City. I have met so many nice and friendly people here that neither I can write all their names here but nor can I ignore them. I am really glad that I chose Quebec City to do my Doctoral studies. It's a wonderful city.

Finally, I would like to thank my parents and family members for their unconditional love and support throughout my life!

Foreword

The work presented in this thesis is the outcome of my four and half years of PhD work. I have divided this thesis into four chapters. The first chapter- Introduction is further divided into six sections. In the first section, section 1.1, I present an overview of the Extended Synaptotagmins (ESyts). The ESyts contain only two types of known structural domain, the C2 domain and the SMP domain, discussed in sections 1.2 and 1.3. The functional aspects of ESyt point towards their action at membrane contact sites (MCS) and in receptor tyrosine kinase (RTK) signaling. Section 1.4 describes an overview of MCS while section 1.5 covers RTKs signaling in detail. Finally, the majority of my work is related to the fibroblast growth factor receptor (FGFR) and it's signaling, hence in section 1.6 I describe cell signaling via this receptor. The second chapter describes the major interaction and localization of the ESyts (submitted article). In the third chapter I describe the deleterious effects of ESyt 2/3 gene inactivation in mouse embryonic fibroblasts (MEFs) on survival under stringent culture conditions or oxidative stress. The data presented in chapter 3 is already published as part of an article that I have attached to this thesis as an annex. The final chapter, chapter 4 provides a general discussion and the conclusion of this thesis.

Chapter 1: Introduction

1.1) The Extended Synaptotagmin Proteins

Extended Synaptotagmin Proteins (or ESyts) are C2 Domain containing proteins that are similar to the Synaptotagmins, a C2 domain containing family of proteins involved in calcium mediated secretion. So far, three proteins have been discovered that belong to this class, namely ESyt1, ESyt2 and ESyt3. ESyt1 was discovered by Morris et al in 1999, in the vesicles prepared from rat adipocytes and termed it as vp115 for vesicular protein that migrates at 115kDa in SDS gel electrophoresis (Morris et al., 1999). Already in 2004, our laboratory presented data at the 10th International Xenopus Meeting, (Marine Biology Laboratory, Woods Hole, Massachusetts) identifying the interaction of a conserved Synaptotagmin-like protein, at the time named N126 but later to be called ESyt2, with the cytoskeletal and signaling kinase PAK1. The data suggested a role in FGF signaling during embryogenesis, a finding later confirmed (Jean et al., 2010 and 2012). However, in 2007, Min et al described the structure and subcellular localisation of three related human proteins and coined the term ESyt, for extended synaptotagmin-like, due to their similarity to the synaptotagmins. Since then, a variety of studies have been published on the structural, physical and biological properties of the ESyts. Min et al in 2007, presented data on the architectural domain organisation and intracellular localization of the three ESyts. Our laboratory then showed that Xenopus and human ESyt2 functioned as adapter proteins required for endocytosis of the FGF receptor, for functional signaling via the ERK MAP-kinase pathway and was involved in regulating cytoskeletal dynamics in conjunction with PAK1 (Jean et al. 2010 and 2012). Most recently ESyts were shown to be endoplasmic reticulum (ER) resident proteins that help in the formation of ER to Plasma Membrane contact sites or bridges (Giordano et al., 2013; Chang et al., 2013). The structurally related yeast Tricalbins had been shown to play a similar role the year before (Manford et al., 2012).

Given the relevance of the most recent published data from laboratories other than our own, I have integrated this data into the following sections without respect to the time-line of discovery. However, I wish to remind the reader that at the start of my PhD very little was understood of the ESyt proteins beyond the publications and unpublished data from our laboratory. Only 5 manuscripts had been published. One solely describes the isolation and sequencing of a cDNA, two concern the structures of C2 domains of ESyt2, one describes the primary structures of the three human ESyt proteins and provides data on their subcellular localization, data that was later found to be at least in part incorrect, and one manuscript indirectly suggesting a possible role in the insulin response via CDK5 kinase. Our laboratory published significant data in 2010 and again in 2012, but it was not until 2013 and 2014 that the subcellular localization of the ESyts was mostly resolved. Thus, while reading the following sections I wish the reader to bear in mind that no relevant data from laboratories other than our own was available to guide my PhD studies until mid 2013.

1.1.1) The discovery of Xenopus ESyt2 and its role in FGF signaling.

During the first year of my PhD studies, our laboratory published a key manuscript (Jean et al., 2010) showing that the Xenopus ESyt2 (xESyt2) was required for FGF-dependent cellular signaling in early Xenopus embryos. Depletion of ESyt2 was shown to inhibit the induction of the early mesodermal marker Xbra by FGF. This was shown to be due to a delay in endocytosis of the activated FGF receptor (FGFR) that inhibited activation of the ERK MAP-kinase pathway. The data showed that ESyt2 interacts selectively with activated form of FGFR and with Adaptin-2, required for Clathrin-dependent endocytosis and in this way acts as an endocytic adapter. Depletion of ESyt2 then appeared likely to change the subcellular targeting of FGFR and hence the activation of the ERK/ MAP-Kinase cascade. The results had also shown that both Xenopus and human ESyt2 selectively interact with all four activated

FGF receptors (FGFR1-4). It was proposed that ESyt2 functioned as an endocytic adapter for the FGFRs endocytosis via clathrin-coated pit and downstream signaling (Figure 1).

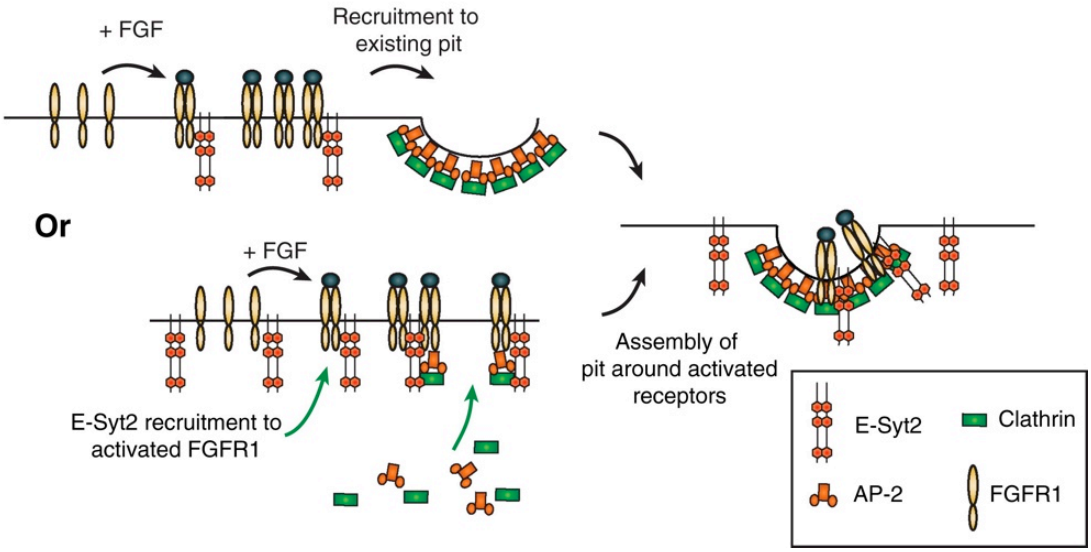

Figure 1. ESyt2 as an endocytic adapter (Jean et al., 2010).

Two possible modes of ESyt2 action in which either ESyt2 hands over the activated receptor to an existing clathrin pit or recruit the activated receptor and other proteins to assemble new pit.

Another study published from our lab (Jean et al., 2012) had shown that ESyt is also an interaction partner for the p21-GTPase Activated kinase PAK1. The PAK family of protein kinases has been shown to play crucial roles in cytoskeletal regulation and phosphorylates important cytoskeletal regulators such as LIM kinase, MLCK and MLC (Bokoch, 2003; Edwards et al., 1999; Sander et al., 1999; Bisson et al., 2003). In addition, PAK also plays a non-catalytic role in driving actin depolarization by locally sequestering the active GTPases Cdc42 (GTP bound) and Rac (Bisson et al., 2007). Jean et al (2012) showed that the C2C domain of ESyt2 binds to a CRB/GBD adjacent site within the regulatory N-terminal domain of PAK1, and they proposed a hypothetical model for the role of ESyt2 in FGF receptor endocytosis by locally

regulating actin cytoskeleton to permit endocytosis (Figure 2). PAK1 binds to the ESyt2 and then both are recruited to the FGF receptor upon its activation. ESyt2 binding supresses actin polymerization and inhibits the activation of PAK1 by the GTPases Cdc42 and Rac. Inhibition of wound healing in Xenopus by ESyt2, a processes dependent upon F-actin polymerization, supports the idea that the ESyt binding supresses the activation of PAK1. The hypothetical model presented by Jean et al (2012) proposes that the recruitment of PAK1 to the ESyt2 could cause the local cortical actin depolymerisation or displacement and open the way for the assembly of a clathrin-coated pits for the receptor endocytosis and signaling.

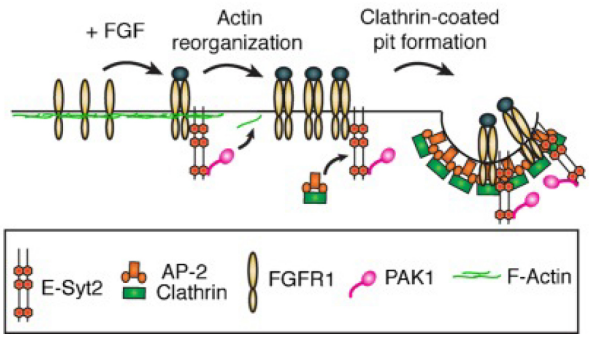

Figure 2. A hypothetical model of the chain of events occurring at the plasma membrane during FGF receptor activation (Jean et al., 2012).

1.1.2) The ESyts are ER proteins.

The data presented by Min et al in 2007 had argued that ESyt2 and ESyt3 are inserted in the plasma membrane, since they were detectable on the cell surface without permeabilizing the transfected cells in immunolabelling experiments. However, data from our lab (Chapter 2) and other labs (Chang et al., 2013; Giordano et al., 2013) suggest that this is not the case. As described in Chapter 2, the N-terminally tagged ESyt2b was not detected before cell permeabilization in immunolabelling experiments, but could be detected after extended fixation that also revealed other

cytoplasmic factors (unpublished data of F. Guillou). Yet, when the N-terminal trans-membrane domain (TMD) of ESyt2b was replaced by the N-terminal TMD of Syt1, the fusion protein obtained can be detected on the cell surface. Data from our lab (Chapter 2) are consistent with the fact that ESyts are ER resident proteins that have a non-penetrating mode of membrane association, as was proposed recently (Chang et al., 2013; Giordano et al., 2013). The immunofluorescence data presented by Giordano et al (2013) showed that the ESyts localize to the ER and that their overexpression in cell lines induces cortical localization. Further, using immunogold electronmicroscopy they found that the ESyt2 and ESyt3 localize at the ER-PM contact sites. Chang et al in 2013 used a genetically encoded marker, 'MAPPER' (for membrane attached peripheral ER) to show that the connection between ER and PM was dynamically regulated by the Ca^{2+} signaling. They showed that the elevation of cytosolic Ca^{2+} levels triggers the translocation of ESyt1 to the ER-PM junction in order to enhance the ER-to-PM connection that facilitates the recruitment of Nir2, a phosphatidylinositol transfer protein (PITP) to ER-PM junction following receptor stimulation. Nir2 then helps in the replenishment of plasma membrane levels of PIP2 (see Figure 6)

1.1.3) ESyt domain structure.

The domain architecture of ESyts comprises a short N-terminal domain preceding a putative transmembrane domain, an SMP domain and C-terminally to this, multiple C2 domains (Figure 1). ESyt2 and ESyt3 have three C2 domains (C2A, C2B and C2C) while ESyt1 has five C2 domains (C2A to C2E domain). The sequences of the individual C2 domains in ESyt 2 and 3 show good homology. In the case of ESyt1, its C2E domain closely resembles the C2C domains of ESyt2 and 3, suggesting that it is related to the other ESyts by internal C2 domain insertion/deletions (Figure 3, 28 and 37)

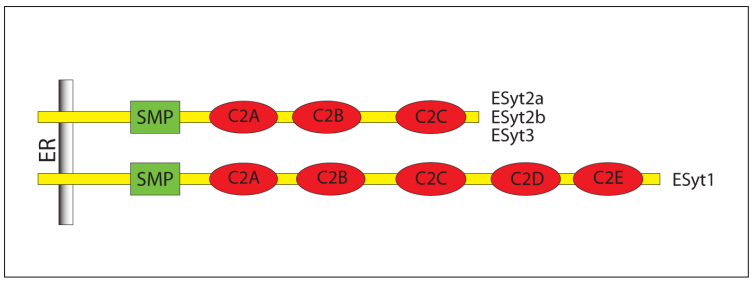

Figure 3. The domain architecture of ESyts.

The SMP (Synaptotagmin-like Mitochondrial lipid-Binding Protein) domains are conserved from yeast to humans (Lee and Hong, 2006). They are believed to be involved in lipid exchange and targeting to membrane contact sites, (MCSs) (Creutz et al., 2004; Toulmay and Prinz, 2012; Kopec et al., 2010). Recently, Schauder et al (2014) presented the crystal structure of ESyt2 SMP domain with the two adjacent C2 domains (C2A-C2B). They reported the presence of glycerophospholipids in a channel formed within the SMP domain, thereby suggesting a direct role of ESyts in lipid transport, and proposed models for the tethering of ER-PM by ESyt2 to transfer lipids between them. Figure 4a shows the representation of a cell with ER-PM contact site. Figure 4b shows the 'Tunnel' model of ESyt2 where ESyt2 bridges the ER and PM to transfer the lipids between them. Figure 4c shows a second model, the 'Shuttle' model where ESyt2 SMP shuttles between ER and PM in order to transfer lipid. A third model is also presented where SMP transfers lipids between the ER and PM with the help of some possible partner protein labeled as question mark in Figure 4c

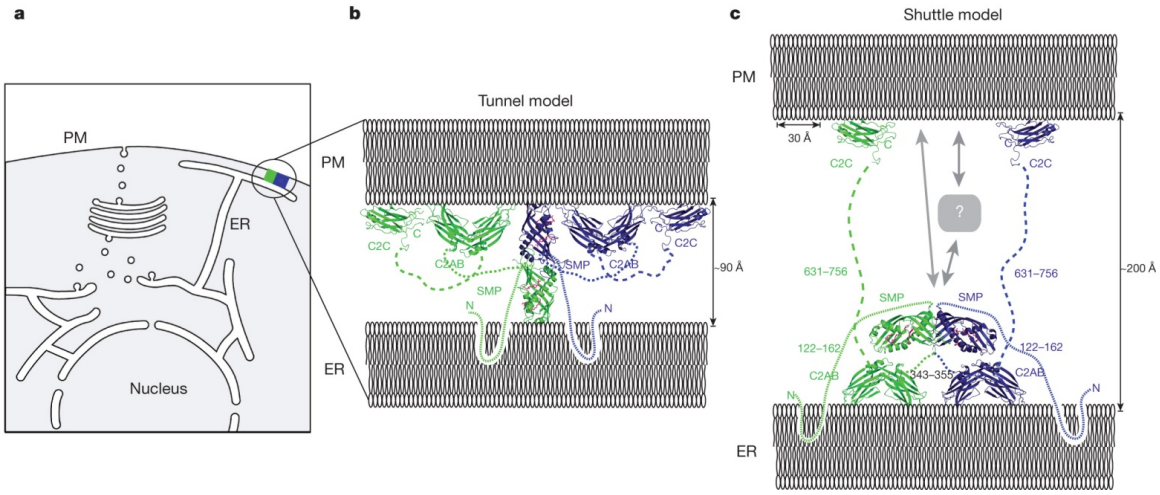

Figure 4. ER–PM contact site and a model of ESyt2 (Schauder et al., 2014).

(a) Representation of a cell with ER-PM contact site. (b) The 'Tunnel' model of ESyt2 where ESyt2 bridges the ER and PM to transfer the lipids between them. (c) The 'Shuttle' model where ESyt2 SMP domain shuttles between ER and PM in order to transfer lipid.

In addition to the lipid transfer role, ESyt2 C2A domain has been shown to bind up to 4 Ca^{2+} ions, which suggests that ESyt2 and ESyt3 may have Ca^{2+} dependent functions that still remain unknown (Xu et al., 2014). On the other hand, the ESyt2 C2B domain does not binds Ca^{2+} ions. The function of ESyt C2B domain is yet to be discovered, although a direct role in interaction with other proteins cannot be ruled out. The C2C domain of ESyt2 and ESyt3 is responsible for its plasma membrane localization (Min et al., 2007) (and F. Guillou unpublished). Moreover the formation of ER-PM contacts requires the C2C domain of ESyt2 and ESyt3 and this function is dependent on a Ca^{2+} -independent interaction with phosphatidylinositol 4,5-bisphosphate.

Figure 5 shows a proposed model of ESyt function incorporating a Ca^{2+} -dependent function of the C2A domain (taken from Xu et al., 2014). The model shows that in addition of promoting the ER-PM contact via C2C domain (Ca^{2+} independent), the C2A domain of ESyt2 and ESyt3 may have a Ca^{2+}-dependent function. It was

suggested that the C2A domain might bind to the plasma membrane in a Ca^{2+} -dependent manner and thus bring the SMP domain close to the plasma membrane. Moreover, the C2B domain could bind unknown protein targets (denoted as X) on the plasma membrane.

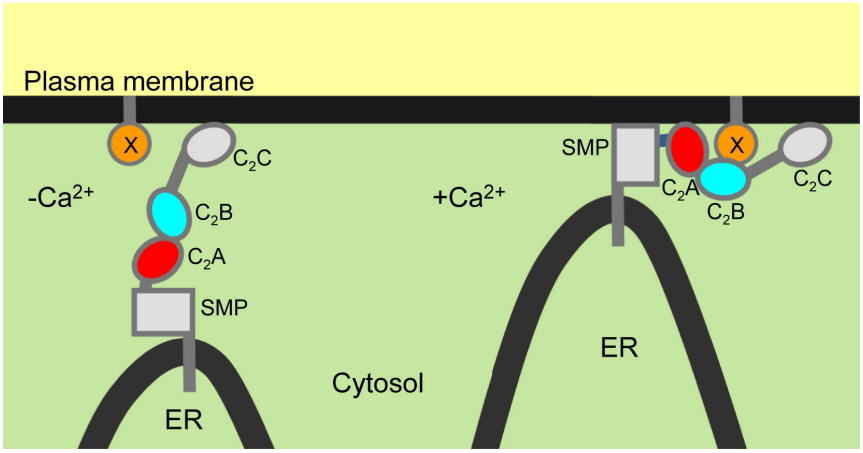

Figure 5. Model of ESyt function incorporating a Ca^{2+} -dependent function of the C2A domain (Xu et al., 2014)

At the resting unstimulated cellular Ca^{2+} levels, ESyt2 and ESyt3 strongly bind to the plasma membrane, whereas the Ca^{2+} dependent plasma membrane localization and tethering has been attributed only to ESyt1 (Giordano et al., 2013; Chang et al., 2013). Chang et al recently presented another interesting model in 2013. These authors proposed a feedback mechanism for receptor-induced Ca^{2+} signaling (Figure 6). Cell surface receptor activation upon stimulation leads to the activation of PLC which then hydrolyzes PIP2 at the plasma membrane to produce IP3. The IP3 then binds to the IP3 receptor inducing a release of Ca^{2+} into the cytosol. ESyt1 binds Ca^{2+} in response to the elevation of cytosolic Ca^{2+} and translocates to the ER-PM junction thereby forming new ER-PM junctions and decreasing the gap between the ER and plasma membranes. This enhanced ER-PM connection induced by ESyt1 then results in Nir2 recruitment (a phosphatidylinositol transfer protein (PITP)) to ER-PM junction and PI transfer from the ER to PM. The PI transferred to the PM is then converted back to PIP2 by PM-associated PI kinases to support further receptor

induced Ca^{2+} signaling. It is also possible that Nir2 replenishes PIP2 on the PM by enhancing PI metabolism or by stimulating PI kinases.

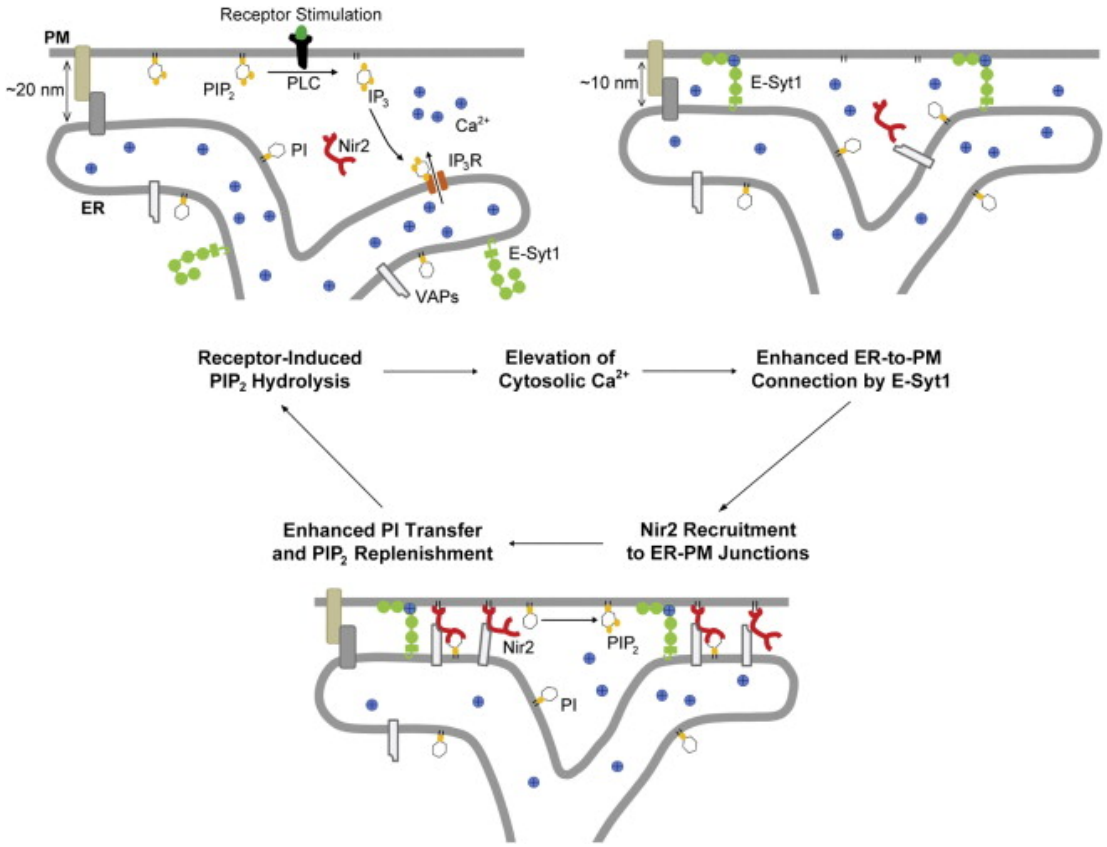

Figure 6. Model of a feedback mechanism for receptor-induced Ca^{2+} signaling (Chang et al., 2013).

1.2) C2 Domain containing proteins

The C2 domain was first identified in Ca^{2+} dependent protein kinase C PKC (Nishizuka, 1988; Kikkawa, 1989), which contains two conserved regulatory sites (C1 and C2 domains). Thereafter, many proteins have been found that contain C2 domains. C2 domain containing proteins can function in both Ca^{2+} -dependent and -independent pathways, and the number of C2 domains in a single protein can vary from one to six. Figure 7 shows the domain architecture of multiple C2-domain containing proteins. These proteins may or may not contain a transmembrane domain. Four classes of multiple C2-domain containing transmembrane region are coded in mammalian genome: synaptotagmins (Syt1-16), extended synaptotagmins (ESyt1-3), multiple C2-domain and transmembrane proteins (MCTP1-2), and ferlins. Syt17 is not shown as it lacks a transmembrane region and is anchored to the membrane via palmitoylated cysteine residues.

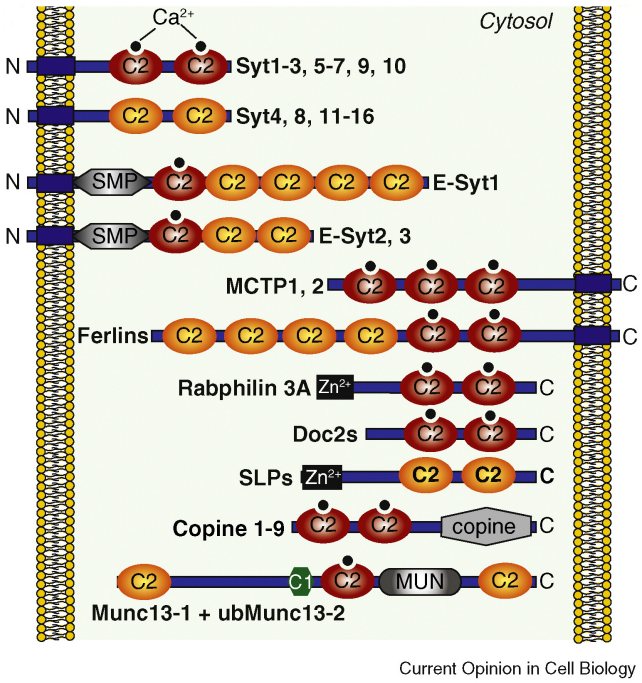

Figure 7. Multiple C2-domain containing proteins (taken from Pang Z. P. and Sudhof T. C., 2010).

1.2.1) The C2 domain

The crystallographic structure of C2A domain of Synaptotagmin 1 (Syt1) was reported in 1995 (Sutton et al., 1995). Later, analysis of other C2 domains revealed a common overall structure having a compact eight-stranded β-sandwich, in which the β- strands are connected by loops that in some instances contain insertions (Chapman, 2002). Based upon simple change in the connection patterns of the β- strands, C2 domains exists in two topologies, Type I and Type II. The connections of the β-strand can be in such a way that the amino and carboxyl termini exit the domain either at the 'top' (towards the Ca^{2+} binding sites) or towards the 'bottom' (away from the Ca^{2+} binding sites) of the C2 domain. Many proteins contain more than one C2 domain and in some cases the structure of the second C2 (C2B) domain has been determined. C2B domain differs from C2A domain in that it has one or two short α-helices at the 'bottom' of the domain. Figure 8 (taken from Fernandez et al., 2001) shows the ribbon diagrams of the C2A and C2B domains of Syt1. The C2A domain of Syt1 can bind up to three Ca^{2+} ions whereas C2B domain can bind only two Ca^{2+} ions.

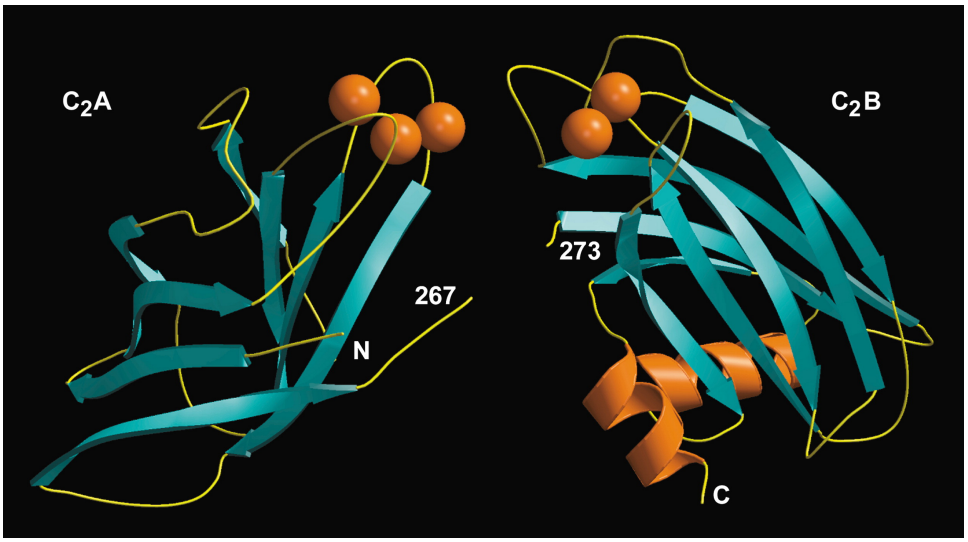

Figure 8. Ribbon Diagrams of the C2A- and C2B-Domains of Synaptotagmin 1 (Fernandez et al., 2001).

1.2.2) Membrane Associated C2 domain proteins:

There are four classes of membrane-associated proteins containing C2 domains:

Synaptotagmins
ESyts (ESyt1, ESyt2 and ESyt3), and Tricalbins
Ferlins (dysferlin, otoferlin and myoferlin), and
Multiple C2 Domain and Transmembrane Region Proteins (MCTPs, MCTP1 and MCTP2).

1.2.3) Synaptotagmins

The Synaptotagmins represent a large family of C2 domain containing proteins that are characterized by having a single trans-membrane region (TMR), two C2 domains and variable inter-domain linkers. Of the 17 Synaptotagmins (Craxton M, 2007), functions are known for only few of them. Syt1 is the first Synaptotagmin to be discovered and has been widely studied. It is the most abundant Ca^{2+} -sensing protein on the surface of synaptic vesicles, SV (~ 7% of the total vesicle protein) and functions in rapid neurotransmitter release and SV recycling (Chapman, 2002). Syt1 seems to bind a total of five Ca^{2+} ions (three with C2A domain and two with C2B domain) and these domains can also bind to membrane phospholipids. The fusion of SV with the pre-synaptic membrane requires the formation of the SNARE (soluble N-ethylmaleimide-sensitive factor attachment protein receptor) complex that is composed of vesicle protein Synaptobrevine (or VAMP, vesicle-associated membrane protein) and the plasma-membrane proteins Syntaxin and SNAP-25 (synaptosome associated protein of 25kDa). The complex formed carries out the exocytosis process either by the “kiss-and-run” mode in which vesicle fusion with the PM is for a very short period, or by “kiss-and-stay” in which the fusion is much longer lived. Synaptic transmission requires a rapid release of neurotransmitter and for that it requires a rapid fusion of SV with the synaptic membrane. This rapid vesicle fusion is dependent upon the pre-synaptic rise in Ca^{2+} concentration. Gene

disruption studies of Syt1 presented by Geppert et al in 1994 reported a loss of rapid exocytosis, which did not depend upon the reduction in the total releasable vesicles. This and other data suggests that Syt1 acts as a Ca^{2+} sensor and regulates the vesicle fusion and hence neurotransmitter release. Further studies have reported that the loss of Syt1 leads to a defect in SV recycling. Syt1 has been reported to interact with the adapter protein complex AP-2, which in turn mediates the assembly of clathrin coat onto the fused vesicle membrane and helps in endocytosis. Thus a loss of Syt1 clearly affects the recycling of SVs.

1.2.4) Tricalbins, the probable yeast ESyt orthologs

Tricalbins constitute another class of proteins that contain C2 domains, having domain organisation highly similar to the ESyts. Tricalbins contain a probable transmembrane domain in the N-terminal region, an SMP domain and three C2 domains in case of Tricalbin1 and 2 (Tcb1 and Tcb2), and five C2 domains in case of Tricalbin3 (Tcb3) (Figure 9 taken from Manford et al., 2012). The name Tricalbin was suggested for Tri (three) CA (calcium) L (lipid) BIN (binding) and the corresponding genes are *Tcb1, Tcb2, and Tcb3* (Creutz et al., 2004). The Tricalbins were suggested to play a role in membrane trafficking and may interact with each other to form heteromeric complexes in performing their functions in yeast cell.

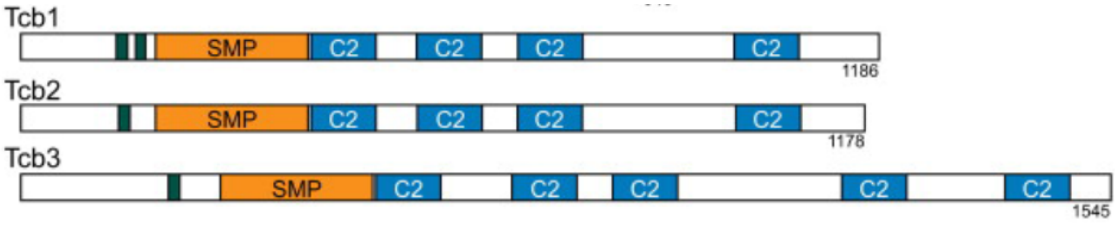

Figure 9. Tricalbin domain architecture (Manford et al., 2012).

In 2012, Manford et al published a report on three families of ER-PM tethering proteins in yeast, namely: Ist2 (related to mammalian TMEM16 ion channels), the tricalbins (Tcb1/2/3, orthologs of the extended synaptotagmins), and Scs2 and Scs22 (vesicle-associated membrane protein-associated proteins). They showed that the loss of all the six proteins results in the separation of the yeast ER from the PM and the accumulation of the cytoplasmic ER. They also showed that the phosphoinositide signaling at the PM was misregulated by the loss of these proteins.

1.2.5) Ferlins

Ferlins belong to a family of multiple C2 domain containing proteins. In mammals, there are six genes (*Fer1-L1 to -L6*) that encode multiple C2 domain containing transmembrane proteins with possible roles in vesicle trafficking and fusion (Angela Lek et al., 2011). The C. elegans ferlin *Fer-1* was the first to be discovered and was found to be a fertilization factor required for fusion of membrane vesicles with the plasma membrane during spermatogenesis (Achanzar et al., 1997).

Ferlins are large proteins (around 200-240 kDa) that undergo alternate splicing to generate multiple paralogues. Based upon the presence or absence of the DysF (Dysferlin) domain, they are divided into two sub-groups, Type I and Type II (Figure 10 taken from Angela Lek et al., 2011).

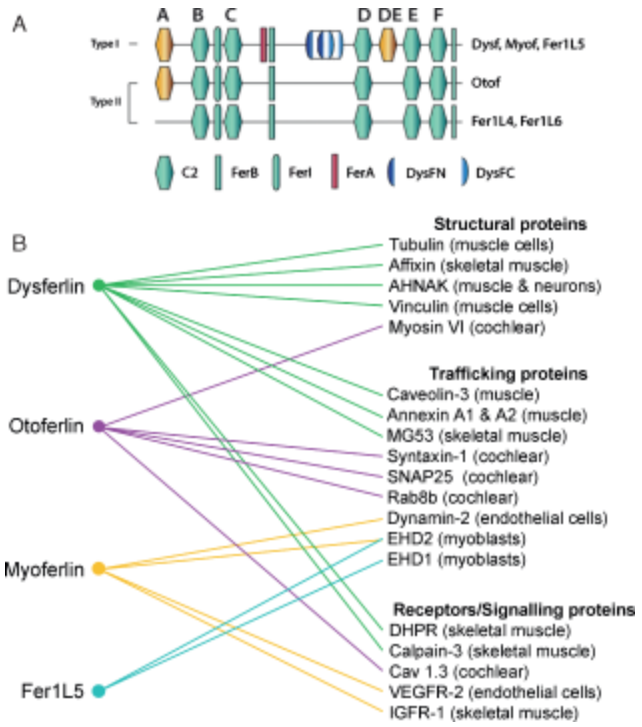

Figure 10. Classification, domain topology and interacting partners of ferlins (Angela Lek et al., 2011).

In general, invertebrates possess only two ferlins, one with DysF domain and one without it, whereas most of the vertebrates possess six ferlins, *Fer1L1, L3* and *L5* with DysF domain and *Fer1L2, L4* and *L6* without DysF domain (Angela Lek et al., 2011). Figure 10 (taken from Angela Lek et al., 2011), shows classification, domain topology and interacting partners of ferlins.

Apart from multiple C2 domains, ferlins have other FER domains: FerI, FerA and FerB. They are small (60-70 residues) consensus motifs with no known function.

The importance of ferlins in normal cellular signaling comes from the fact that they have been associated with muscular dystrophy (dysferlin) and deafness (otoferlin) in humans, and infertility in *C. elegans* (Fer-1) and *Drosophila* (misfire)

1.2.6) MCTPs

MCTPs are Multiple C2 Domain and Transmembrane Region (TMR) Proteins, as at least some of the splice variants of these proteins contain multiple trans-membrane domains or TMRs in addition to the C2 domains. The importance of MCTPs is highlighted by the RNA interference experiments in *C. elegans* performed by Maeda et al in 2001. These revealed the *C. elegans* MCTP homolog (1H206) is an essential gene, the ablation of which leads to early embryonic lethality. The domain structure of MCTPs consists of a variable N-terminal sequence, three C2 domains, two transmembrane regions, and a short C-terminal sequence. Only one MCTP gene is expressed in the case of the invertebrate organisms *C. elegans* and *Drosophila melanogaster*, whereas vertebrates express two MCTP genes (*MCTP1* and *MCTP2*) (Shin et al., 2004). The MCTPs contain two TMRs that can be alternatively spliced resulting in a single TMR that is sufficient for anchoring the protein to the plasma membrane. MCTPs have a very strong affinity for binding to the Ca^{2+} but they do not bind to phospholipids (Shin et al., 2004).

Figure 11 summarises the four classes of C2 domain containing proteins (taken from Shin et al., 2004).

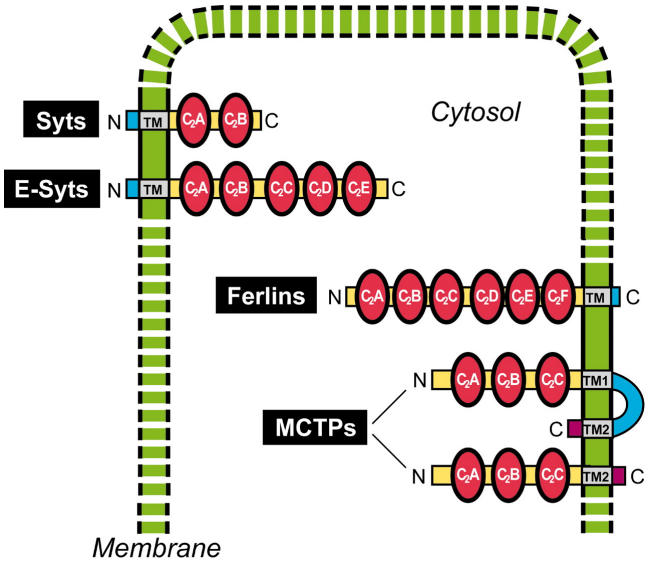

Figure 11. C2 domain containing proteins (Shin et al., 2004).

1.3) The SMP Domain containing proteins

Inter-organelle communication plays a crucial role in maintaining homeostasis in cells. Compartmentalization in eukaryotic cells has promoted the development of mechanisms of inter-organelle communication in which membranes of two organelles are brought in close proximity, within ~20nm (Toulmey and Prinz, 2011; Lebiedzinska, 2009; Levine and Loewen, 2006). These regions are called Membrane contact sites (MCSs) and play a role in functions such as lipid exchange (Voelker, 2009) and exchange of calcium (Lewis, 2007).

In yeast *Saccharomyces cerevisiae* very extensive MCSs occur between the ER and plasma membrane (PM), the ER and mitochondria, and the nucleus and vacuoles (nucleus-vacuole junction, NVJ) (Toulmey and Prinz, 2011). One complex that facilitates the contact between ER and mitochondria, named ER-mitochondrion encounter structure (ERMES) (Kornmann et al., 2009), consists of four proteins: Mdm10p and Mdm34p in the mitochondrial outer membrane, Mdm1p in the ER and the soluble protein Mdm12p. Out of these four ERMES proteins, three contains a domain of unknown function that has been termed as synaptotagmin-like mitochondrial-lipid binding protein (SMP) domain (Lee and Hong, 2006). The SMP domains are predicted to belong to a superfamily of lipid/ hydrophobic ligand-binding domains of known structure that have been called TULIP for tubular lipid-binding proteins, and has been proposed to play a role in phospholipid traffic (Kopec et al., 2010).

Several proteins have been identified that contains SMP domain. The SMP domain is a stretch of amino acids ~300 amino acids (Lee and Hong, 2006). The SMP domain containing proteins may additionally have one or more transmembrane domains (TMDs), and/ or other domains. Based upon the organization of the domains, the SMP-containing proteins are classified into four major families: C2 domain containing synaptotagmin like proteins, pleckstrin homology (PH) domain containing proteins, mitochondrial family of proteins and proteins with C1 and PDZ domains. Figure 12 (taken from Lee and Hong, 2006) shows domain architecture of some of the SMP-domain containing proteins.

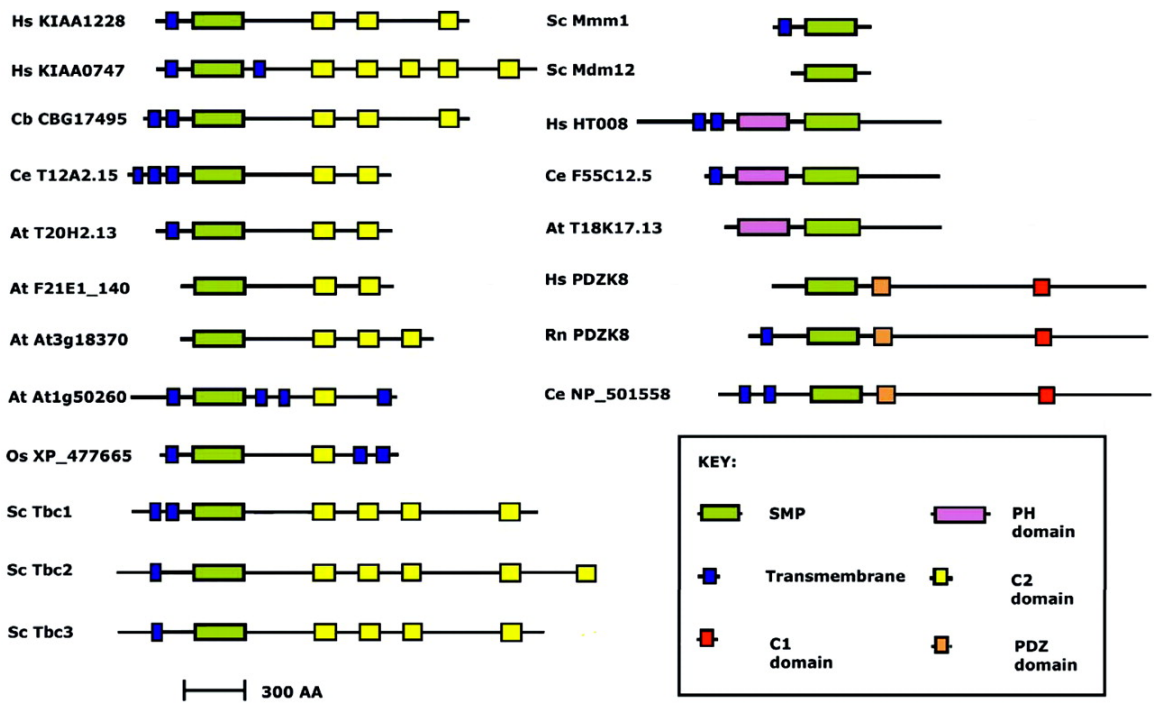

Figure 12. Domain architecture of the SMP-domain containing proteins (Lee and Hong, 2006).

1.4) Membrane Contact Sites (MCSs)

Through the evolutionary process, eukaryotic cells have compartmentalized the specific microenvironments for incompatible biochemical processes. These individual membrane bound compartments or cell organelles play individual roles in maintaining the normal cellular activity and homeostasis. Even though this compartmentalization has numerous advantages, it hinders free diffusion and trafficking of important metabolites or signaling molecules. In order to regulate such processes, these organelles form several contacts with each other. The membrane contact sites or MCSs bring two membrane bound structures close enough for exchange of macromolecules. In general MCSs serve in Ca^{2+} and protein trafficking, and in lipid exchange. The various contact sites formed are: ER- PM contact sites, ER- Mitochondria contacts, ER- Nuclear contact sites, ER- Golgi, ER- Vacuoles, ER- Lipid Droplets and ER- Late Endosomes.

Figure 13 shows a network formed by the ER with other organelles to facilitate diffusion of material (taken from Holthuis and Levine, 2005). Figure 13a shows a lipid transport network based on the ER, where lipids are selectively transported by lipid-transfer proteins (LTPs) across various MCSs (red in Figure 13a). Lipids can use the ER as a superhighway for their transport by crossing one MCS into the ER, diffusing through the ER and then crossing another MCS. As an example, phosphatidylethanolamine (PE) is synthesized in the mitochondrial matrix and moved to the plasma membrane potentially crossing two MCSs on route, i.e. a mitochondrion–ER and an ER–plasma membrane MCS. (Figure 13b and 13c shows the shuttling of LTP across MCS).

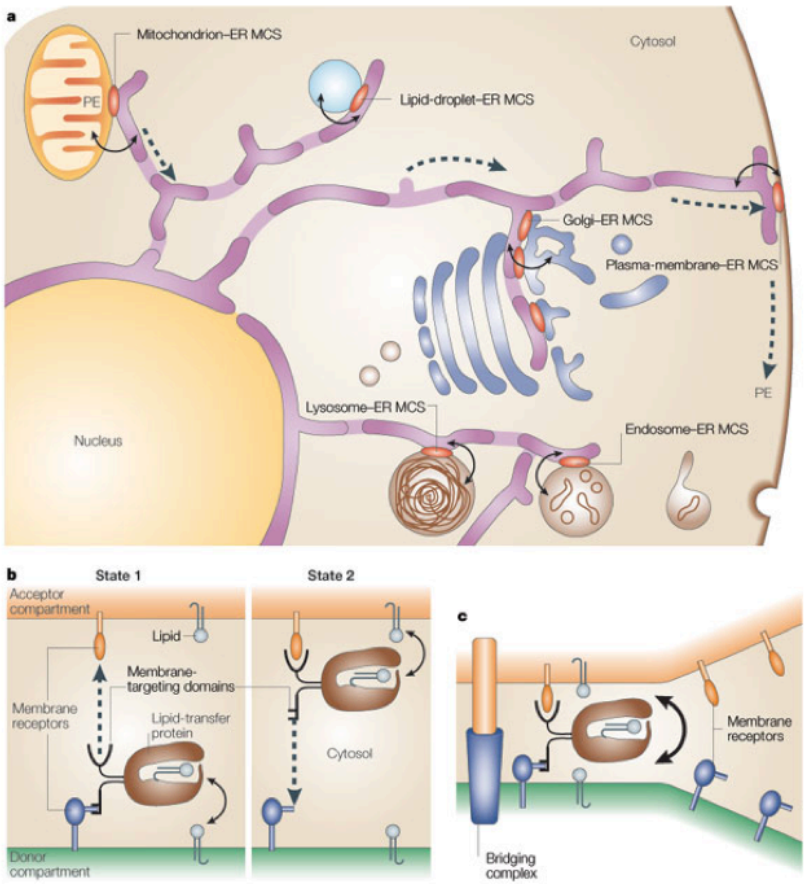

Figure 13. The endoplasmic reticulum (ER) network (Holthuis and Levine, 2005).

(a) A lipid-transport network based on the ER. (b) An LTP shuttling across an MCS. (c) An LTP that bridges an MCS.

1.5) Receptor Tyrosine Kinase

1.5.1) RTKs Family

Receptor tyrosine kinases (RTKs) constitute a large family of cell-surface proteins that act as key regulators of critical cellular processes such as proliferation, differentiation, cell survival, metabolism, cell migration, and cell-cycle control. Depending upon their structural characteristics, they can be divided into 20 subfamilies (Figure 14), which share a homologous domain that specifies the catalytic tyrosine kinase function (van der Geer et al., 1994; Zwick et al., 2001; Lemmon and Schlessinger, 2010). All RTKs have similar molecular plan having extracellular ligand binding domains, a single transmembrane helix, and a cytoplasmic region containing a tyrosine kinase (TK) domain plus additional carboxy (C-) terminal and juxta-membrane regulatory regions. The binding of ligand generally activates the RTKs by inducing receptor dimerization, leading to internalization. This leads to the activation of the kinase domain and autophosphorylation of the RTK on Tyr residues

Although all RTKs induce a specific cellular response, they signal via mostly three major pathways and this remains still a question, how different receptors can induce different cellular responses? In large part the answer involves the ability of RTKs to direct their signals to different subcellular compartments via distinct endocytic pathways. Previously endocytosis was thought to be a means to diminish the receptor signaling and hence permitting an appropriate response to sequential signaling events. However, active signaling may continue well after RTK internalization (Baass et al., 1995) and the choice of endocytic pathway can often determine the response to growth factors (Miaczynska et al., 2004). Thus, the exact manner in which RTKs are internalized will more often determine the outcome of growth factor signaling. Despite the wide-ranging biological importance of FGF signaling, the role of receptor endocytosis in determining its physiological outcome is still very poorly understood. (Wiedlocha et al., 2004). It is known that both the catalytic activity and intracellular

domains of the FGFRs are necessary for receptor endocytosis (Sorokin et al., 1994; Citores et al., 2001). Recent work has suggested that targeting activated RTKs to the clathrin-dependent endocytic pathway rather than to non-clathrin pathways is necessary if signaling is to be sustained (Sigismund et al., 2008). But, it is still far from clear how activated RTKs in general, and the FGFRs in particular, are selectively recognized and targeted to any endocytic pathway. Yet, a further complication in understanding FGF signaling is that, depending upon cell type, it activates to different degrees three distinct downstream pathways, each having specific function in regulating cell adhesion, growth and gene expression. Understanding the mechanisms that are used to decide which of these pathways are activated is of key importance to being able to specifically inhibit those effects of FGF signaling that enhance tumour formation and progression while stimulating those that limit tumour growth. Hence, it is very important that we understand how an RTK activated on the plasma membrane decides which endocytic pathway to take.

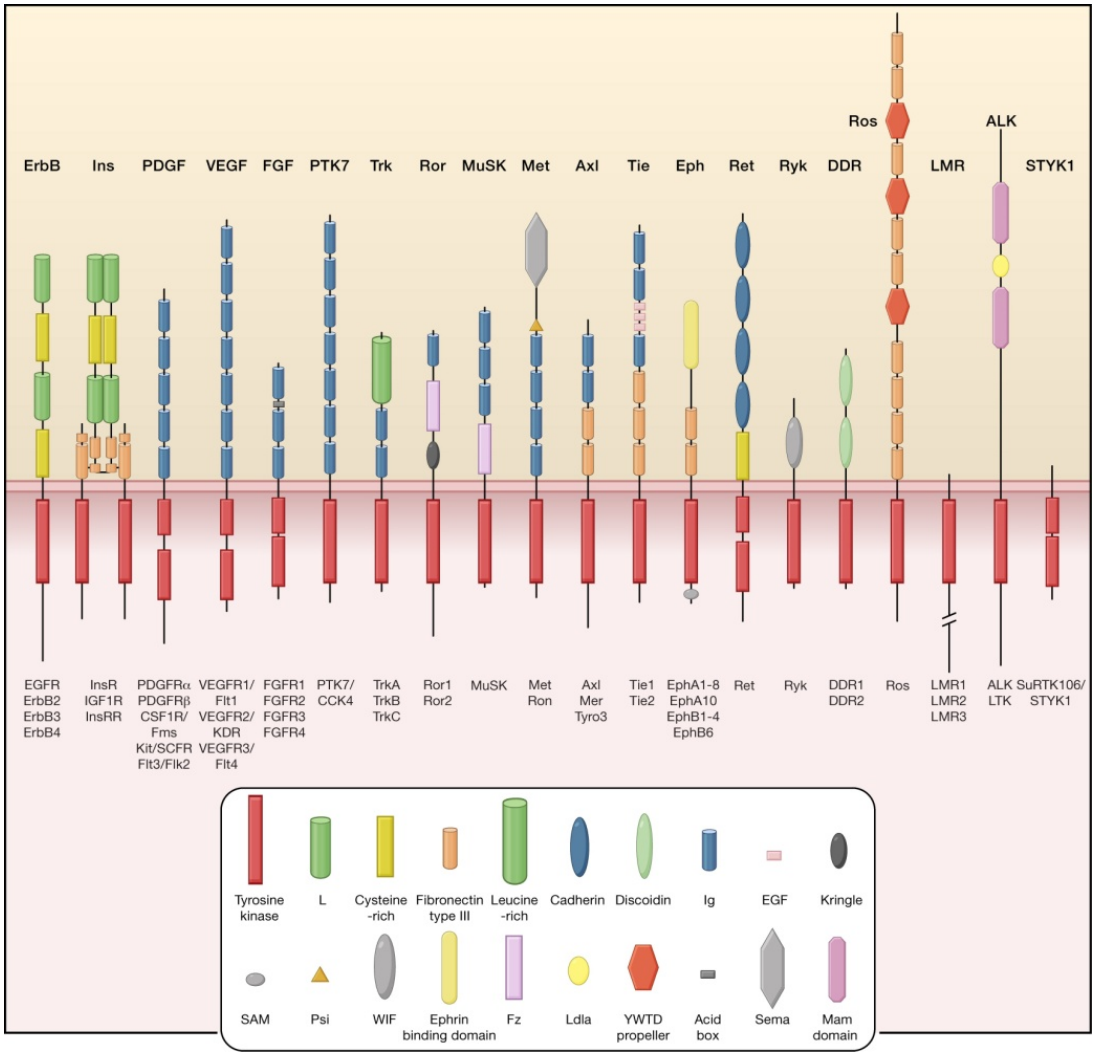

Figure 14. Receptor tyrosine kinase families (taken from Lemmon M.A. and Schlessinger J, 2010).

1.5.2) Major Signaling Pathways

1.5.2.1) MAP Kinase pathway

Mitogen-activated protein kinases (MAPKs) are protein Ser/Thr kinases that are highly conserved proteins involved in regulating a variety of key cellular processes such as cellular proliferation, differentiation, cell motility, stress response, apoptosis and cell survival. These MAPKs have been divided into conventional and non-convention (atypical) categories (Cargnello M and Roux PP, 2011). The 14 know mammalian proteins have been characterized into seven groups shown in Figure 15. The conventional MAPKs include extracellular signal-regulated kinases 1/2 (ERK1/2), c-Jun amino (N)-terminal kinases 1/2/3 (JNK1/2/3), p38 isoforms (α , β , Υ, δ) and ERK5, whereas the lesser known atypical MAPKs includes ERK3/4, ERK7/8 and Nemo-like kinase (NLK)

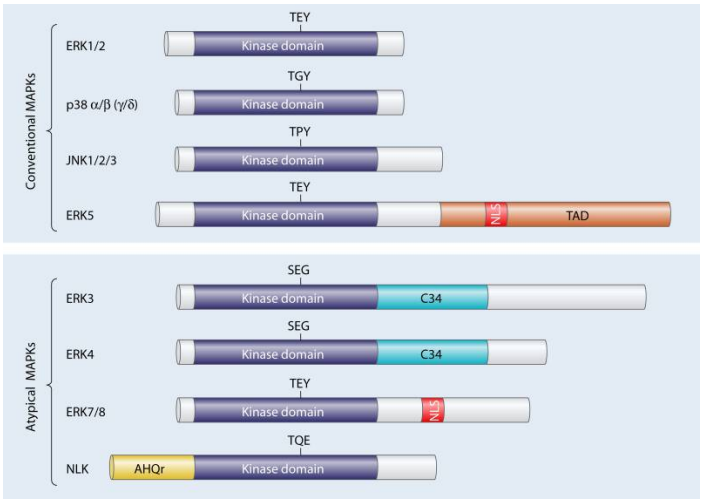

Figure 15. Schematic representation of the conventional and atypical MAPKs (Cargnello M and Roux PP, 2011).

Signaling via the conventional MAP kinasess involves an evolutionary conserved three-tiered kinase cascades, consisting of a MAP-kinase (MAPK), a MAP kinase kinase (MAPKK, MAP2K), and a MAP kinase kinase kinase (MAPKKK, MAP3K). In response to extracellular stimuli, the Ser/Thr kinase MAP3Ks become activated through phosphorylation mediated by their association with a small GTP-binding protein of the Ras/Rho family. The activation of MAP3K leads to the phosphorylation and activation of MAP2k, which in turn phosphorylates and activates the MAPK. The conventional MAPKs contain a Thr-X-Tyr motif in the activation loop of the kinase domain, and the phosphorylation of these residues is essential for their enzyme activity. The MAPKs respond to a broad range of extracellular stimuli such as growth factors, cytokines, mitogens, cellular stress such as heat shock and UV-radiation etc.

The activation mechanism for the atypical MAPKs is lesser known. In many aspects, they differ from the conventional MAPKs. For example, most of them lack the Thr-X-Tyr motif and they don’t get organised as the classical three-tiered kinase cascade modules.

Upon activation these MAPKs phosphorylate their substrates at Ser-Pro or Thr-Pro motifs. Specificity towards their substrates is further provided by the recognition of specific interaction domains termed docking sites. Scaffolding proteins that bind several components of a cascade together also provide signaling specificity by organizing the cascades coponents into specific modules.

The target substrate of MAPKs varies broadly. They include members of a family of proteins called MAPK activated protein kinases (MAPKAPK) that comprises the p90 ribosomal S6 kinases (RSKs), mitogen- and stress-activated kinases (MSKs), MAPK-interacting kinases (MNKs), MAPK-activated protein kinase 2/3 (MK2/3), and MK5.

Figure 16 summarizes the signaling cascade by MAPKs. The MAPKAPK further amplifies the signal from the MAPKs and increases the target range of biological functions of MAPKs.

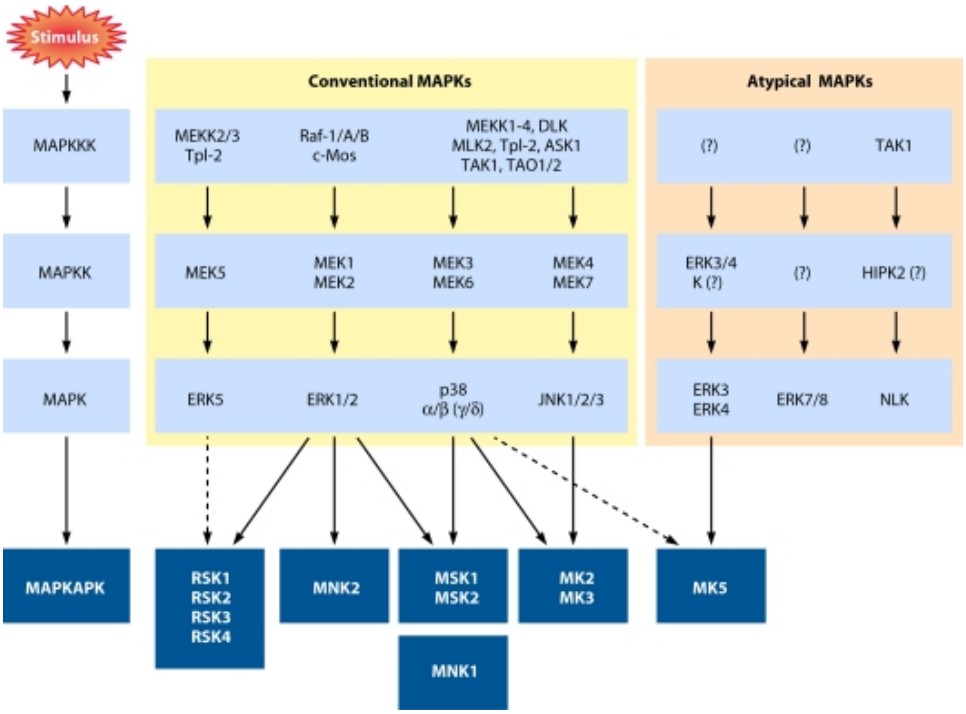

Figure 16. Signaling cascades involving MAPKs (Cargnello M and Roux PP, 2011).

1.5.2.2) Phospholipases and PLC gamma pathway

The importance of phospholipids are becoming much more evident through recent research focusing on their functional roles. Apart from being a major component of cell membrane (Phospholipids such as phosphatidylcholine, phosphatidylethanolamine, phosphatidylserine, phosphatidylglycerol and phosphatidylinositol), they can be hydrolyzed into bioactive lipid mediators by

phospholipases. These bioactive lipids participate in intercellular and intracellular signaling and regulate a wide range of cellular processes such as cell migration, proliferation, survival, vesicular trafficking, tumorigenesis and inflammation.

Based upon the type of reaction catalyzed, phospholipases are categorized in three sub categories i.e. Phospholipase A (PLA1 and PLA2), PLC and PLD. As shown in Figure 17 adapted from Park et al 2012, PLA1 and PLA2 target the sn-1 and sn-2 positions of the glycerol moieties of the phospholipids, yielding free fatty acids and 2-acyl lysophospholipid or 1-acyl lysophospholipid, respectively.

Hydrolysis of Phosphatidylinositol by PLC results in the cleavage of the bond between the glycerol and phosphate moieties. This reaction generates the phosphorylated base inositol-1,4,5-triphosphate (or IP3) and diacylglycerol (DAG). PLD acts upon Phosphatidylcholine and hydrolyses the phosphodiester bond between glycerol phosphate and the substituent resulting in the generation of a free base (choline) and phosphatidic acid.

Phospholipases subcategorized can further exist in many isotypes that can functionally vary and have different domains and regulatory mechanisms.
The calcium-binding C2 domain containing proteins, cytosolic PLA2 (cPLA2) and PLCδ1, require the binding of calcium for their activation. In the case of PLCδ1, it can exist as a ternary complex composed of the enzyme, phosphatidylserine and calcium. The C2 domains of PLCβ1 and PLCβ2 do not bind membrane lipids as PLCδ1 does, but instead in the presence of calcium, PLCβ1 and PLCβ2 associates with the GTP-bound Gαq, resulting in their activation.

The pleckstrin homology (PH) domain is yet another important domain present in PLC (except PLCζ) and PLD. The PH domains are important for binding various lipids and proteins, and that the PH domain of each phospholipases can bind to different molecules. In the case of PLCβ2, the heterotrimeric G protein subunit Gβγ binds with the PH domain and activates the catalytic core of PLCβ2. The PH domain

of PLCγ1 binds to the phosphatidylinositol-3, 4, 5-trisphosphate (PtdIns (3,4,5)P3) in a PI3K-dependent manner. On the other hand, the PH domain of PLD1 is important for its intracellular localization by binding with phosphatidylinositol-4,5-bisphosphate (PtdIns(4,5)P2) and thus regulating PLD activity. PLD1 contains another domain, the phox homology (PX) domain that has been reported to bind to PtdIns (3,4,5)P3, as well as to phosphatidylinositol-5-phosphate (PtdIns5P). The PLD PX domain may serve as a GTPase-activating protein (GAP) for dynamin, and a guanine nucleotide exchange factor (GEF) for RHOA, while the PLD PH domain acts as a GEF for RAC2.

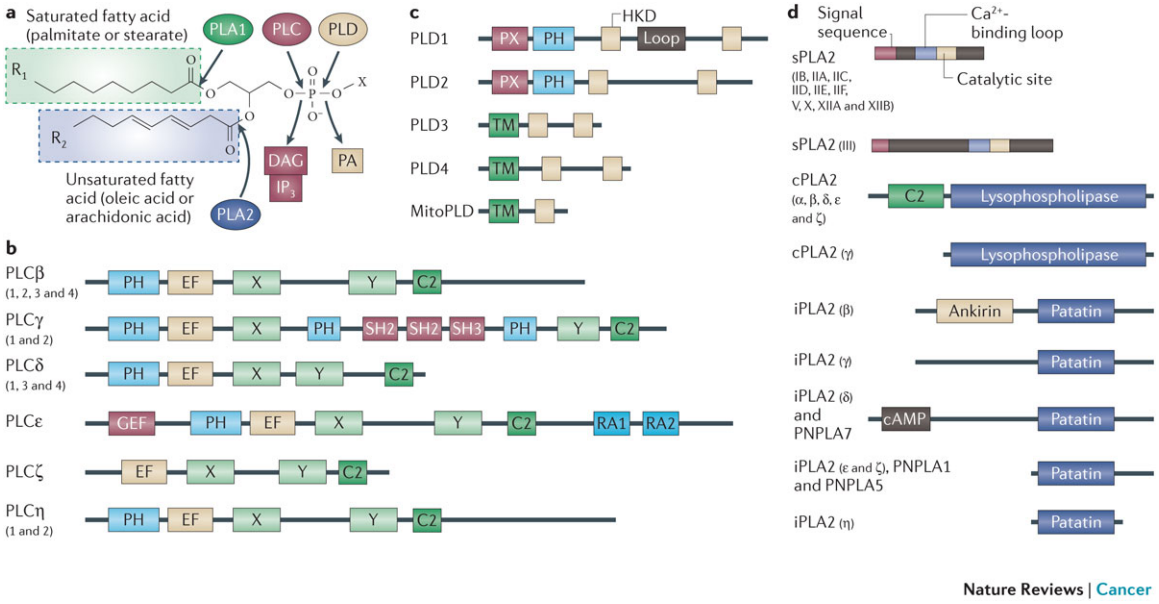

Figure 17. Overview of phospholipases (Park et al., 2012).

(a) Phospholipases are classified into three major types, PLA1/2, PLC and PLD. (b) Thirteen mammalian PLC isotypes are subdivided into six groups. (c) In mammals, PLD1 and PLD2 hydrolyse phosphatidyl-choline (PC). (d) The three major types of PLA2 include secretory PLA2 (sPLA2), cytosolic PLA2 (cPLA2) and calcium-independent PLA2 (iPLA2).

The PLC Family:

The PLC protein family contains 13 isozymes that have been divided into six sub types. The X and Y domains form the catalytic domain of PLC isozymes and are

higly conserved. The regulatory domains include C2 domain, PH domain (except PLCζ), and the EF-hand motif. PLC isozymes hydrolyses the phosphatidylinositol-4,5-bisphosphate (PIP2) to produce inositol-1,4,5-triphosphate (or IP3) and diacylglycerol (DAG). IP3 binds to its receptor and opens the intracellular calcium store, whereas DAG activates protein kinase C (PKC). The mobilization of the intracellular calcium ions and activation of PKC, are involved in a wide variety of cellular signaling processes.

The PLCγ:

The PLCγ1 and PLCγ2 are the two PLCγ isozymes that have been discovered in maamals so far. The basic structure of the isozymes is shown in the Figure 18 (adapted from Carpenter and Ji, 1999). The X and Y domain constitutes the catalytic domains, that hydrolyses PIP2. In addition, they contain two SH2 domains and one SH3 domain residing between the X and Y domains (Katan, 1998). The SH2 domain serves as the binding site of phosphotyrosine residue of target proteins, whereas the SH3 domain interacts with proline rich sequence (PXXP motifs) containing proteins (Pawson and Gish, 1992; Pawson and Nash, 2000). The N-terminal SH2 domain is believed to play a major role that mediates the interaction with several growth factor receptors while the C-terminal SH2 domain is considered to play a minor role (Larose et al., 1993; Chattopadhyay et al., 1999). The SH3 domain of PLCγ binds to the SOS1, c-Cbl, dynamin, and SLP76 (Yang et al., 2011; Seedorf et al., 1994; Graham et al., 1998; Kim et al., 2000a; Yablonski et al., 2001; Tvorogov and Carpenter, 2002) and can function as a guanine nucleotide exchange factor (GEF) for dynamin-1 in the regulation of EGF receptors endocytosis (Choi et al., 2004).

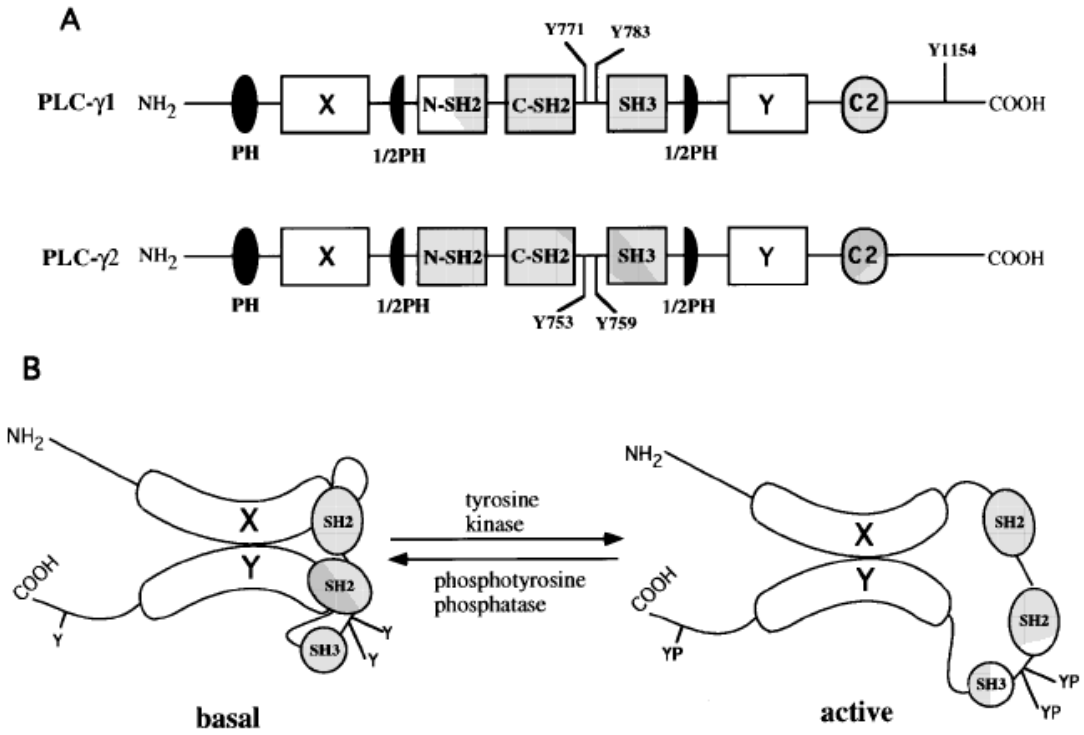

Figure 18. Organization of domains in PLC-γ isozymes (Carpenter and Ji, 1999).

(A) The linear arrangements of catalytic domains (X and Y) and regulatory domains (SH2, SH3, PH, and C2) for PLC-γ 1 and PLC-γ 2. (B) A model for the inactive or basal state and the activated state of the enzyme.

The central region PLCγ containing SH domain, are also believed to have a role in regulating the enzyme activity of PLCγ (Figure 18). The proposed model is that the catalytic domains of the PLCγ must fold together to create the catalytic site and in the inactive state of PLCγ, the SH domain region may act as a cap or lid to block the catalytic site (Kamat and Carpenter, 1997). Upon tyrosine phosphorylation and/or protein binding to the SH domain, the PLCγ acquires an active state where the SH domain region no longer blocks the catalytic site of the enzyme.

1.5.2.3) PI3 Kinase pathway

Since the discovery of PI3 kinase by Cantley's group in the late 1980's, it has been the subject of a very interesting field of research. The PI3K's have been shown to be involved in a wide varity of cellular processes, including cell cycle progression, cell growth, survival and migration, and intracellular vesicular transport (Bart Vanhaesebroeck et al., 2010). The PI3Ks phophorylate PtdIns, PtdIns-4-phosphate (PtdIns4P) and PtdIns-4,5-bisphosphate (PtdIns (4,5)P2), the three species of phosphatidylinositol (PtdIns) , at the 3-hydroxyl group of the inositol ring (Figure 19). These three species coordinates the localization and functions of multiple effector proteins by binding through specific lipid-binding domains such as the PH domain, the PX domain and the FYVE domain (Figure 19).

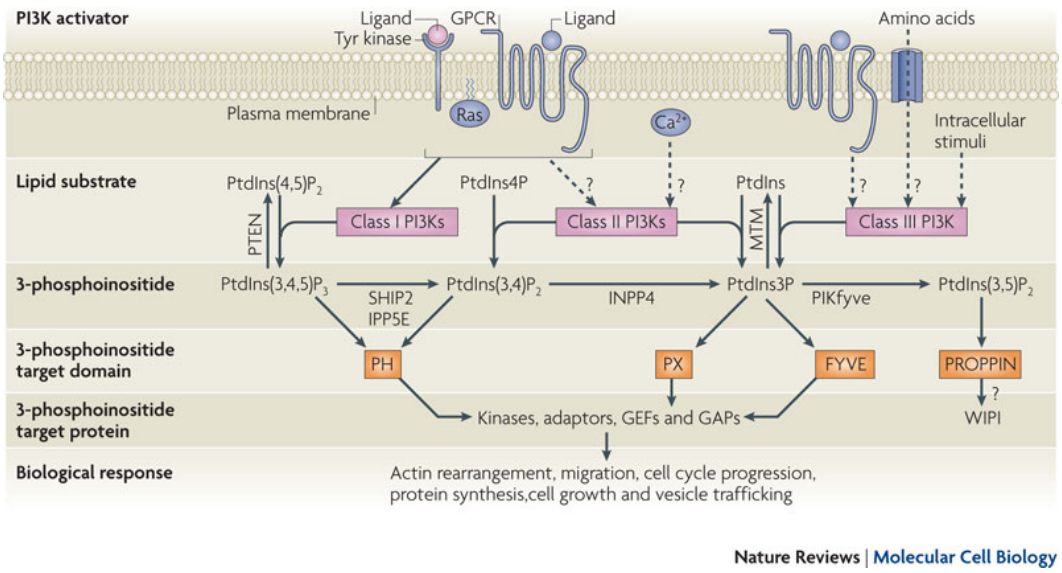

Figure 19. The 3-phosphoinositide lipid network (Bart Vanhaesebroeck et al., 2010).

PI3Ks when activated, generates phosphatidylinositol-3,4,5-trisphosphate (PtdIns (3,4,5) P3), PtdIns-3,4-bisphosphate (PtdIns (3,4) P2) and PtdIns-3-phosphate (PtdIns3P) from their lipid substrates. The fourth 3-phosphoinositide species found in

cells, PtdIns (3,5) P2, is generated by 5-phosphorylation of PtdIns3P by FYVE finger-containing phosphoinositide kinase. PtdIns (3,5) P2 interacts with the PROPPIN (β-propeller that bind phosphoinositide species) domain that is found in the four mammalian WD40 repeat protein interacting with phosphoinositides (WIPI) proteins that are related to yeast autophagy related 18 (Atg18).

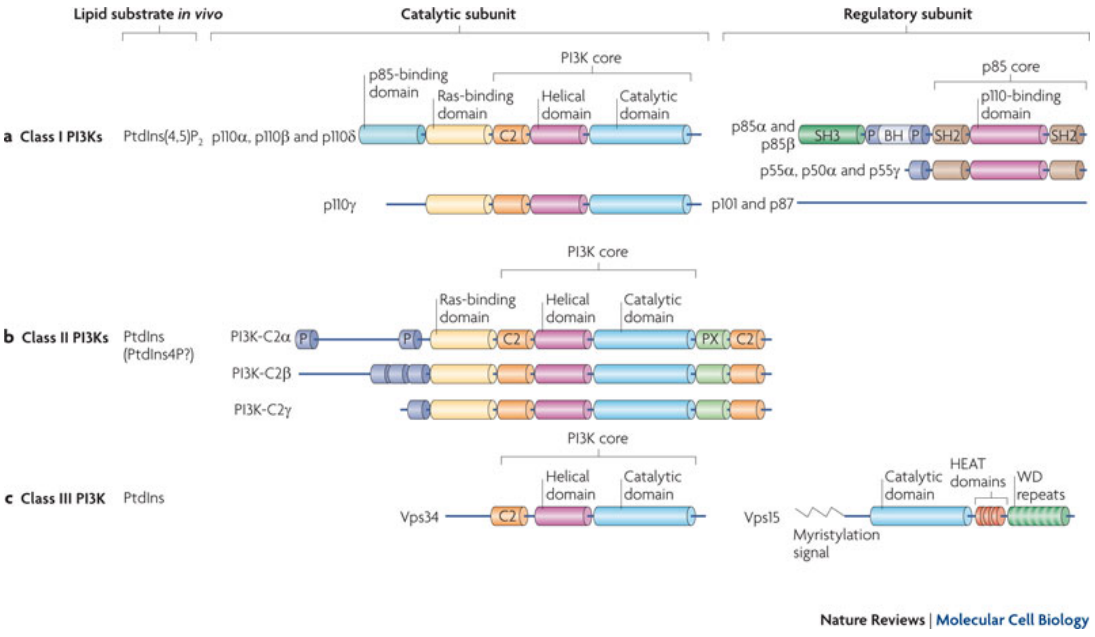

Figure 20. Classification and domain structure of mammalian PI3Ks (Bart Vanhaesebroeck et al., 2010).

Based upon the structural and biochemical features, PI3Ks are divided into three classes: Class I, Class II and Class III (Figure 20) (Bart Vanhaesebroeck et al., 2010). The basic structure of all PI3K catalytic subunits has a PI3K core structure consisting of a C2 domain, a helical domain and a catalytic domain. Class I PI3Ks (Figure 20a), use phosphatidylinositol-4,5-bisphosphate (PtdIns(4,5)P2) as their substrate and exist in complex with a regulatory subunit, either a p85 isoform (for p110α, p110β and

p110δ) or p101 or p87 (for p110γ). All p85 isoforms have two SH2 domains whereas p101 and p87 do not contain any SH2 domains. In addition, p101 and p87 have no identifiable domains and do not show any homology to other proteins. Class II PI3Ks (Figure 20b) use PtdIns and PtdIns-4-phosphate (PtdIns4P) as a substrate. Although they lack regulatory subunits, they do have amino- and carboxy-terminal extensions to the PI3K core structure that might be involved in mediating protein–protein interactions. Class III PI3Ks (Figure 20c), consists of one catalytic member, vacuolar protein sorting 34 or vps34 (PIK3C3 in mammals), which uses PtdIns as a substrate and binds Vps15 (PIK3R4 in mammals). Vps15 consists of an inactive catalytic domain, HEAT domains (involved in mediating protein–protein interactions) and WD repeats that are structurally and functionally similar to a Gβ subunit.

The activation of PI3K pathway can occur in three independent pathways. All three pathways involve the dimerization, autophosphorylation and activation of RTKs, which then recruit SH2 domain-containing molecules. In the first pathway (left side of Figure 21, taken from Cully et al., 2006), the 85 kDa regulatory subunit of PI3K (p85) binds directly to phospho-YXXM motifs (where X can be any amino-acid) on the RTK (Cully et al., 2006; Domchek et al., 1992) resulting in the activation of PI3Ks 110 kDa catalytic subunit (p110). The second pathway (the middle pathway in Figure 21) involves the adapter protein GRB2 (growth factor receptor-bound protein 2) protein that binds to the scaffolding protein GAB (GRB2-associated binding protein), which in turn can bind to p85. GRB2 binds preferentially to phospho-YXN motifs of the RTKs (Cully et al., 2006; Pawson et al., 2004).

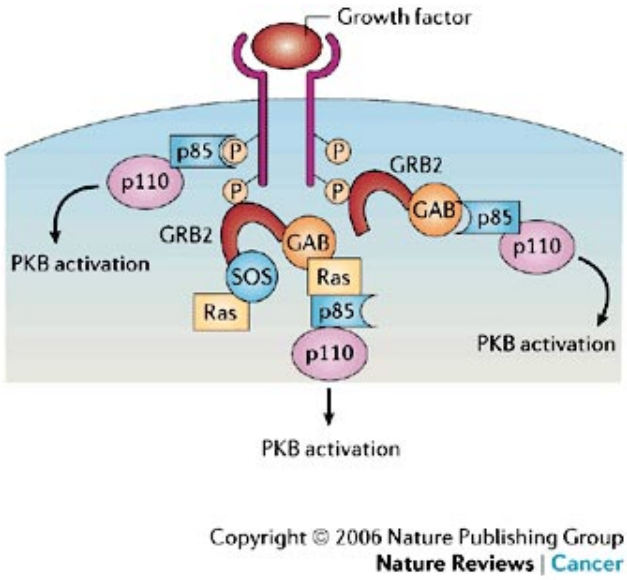

Figure 21. Mechanisms of PI3K activation (Cully et al., 2006).

Finally, GRB2 can also activate Ras via the activation of SOS, and in turn Ras can activate p110 independently of p85. In the third way (right side of Figure 21), GRB2 exists in a large complex that contains SOS, Ras and GAB or other scaffolding proteins that can interact with p110 PI3K (Cully et al., 2006; Ong, S. H. et al., 2001).

1.6) Fibroblast Growth Factor Receptor (FGFR) Family

The fibroblast growth factors (FGFs) are a family of growth factors with a wide variety of effects and are considered as powerful mitogens. Disregulation of FGFs has been associated with multiple forms of cancers (Eswarakumar et al., 2005), and with cell transformation (Dvorak et al., 2006), angiogenesis (Murakami and Simons, 2008) and metastasis (Chaffer et al., 2007). The signaling of FGF occurs via one of the four RTKs, the FGF receptor 1 to 4 (FGFR1-4), which transduce the FGF signal to the ERK- MAP Kinase (Umbhauer et al., 1995)/ PI3K/AKT and PLCγ (Sivak et al., 2005) pathways.

1.6.1) FGFs and FGFRs

Fibroblast growth factor belongs to a large family of polypeptide growth factors that are found throughout the species ranging from nematode to human, although it hasn't been yet identified in unicellular organisms (Itoh and Ornitz, 2004). Till date a large number of genes have been found in vertebrates: 22 genes in human (FGF1–14, 16–23), 22 genes in mouse (FGF1–18, 20–23), 6 in Xenopus (FGF2–4, 8–10), 13 in chicken (FGF1–4, 8–10, 12, 13, 16, 18–20), 10 FGFs in zebrafish (FGF2–4, 6, 8, 10, 17a, 17b, 18, 24) (Itoh and Ornitz, 2004; Bottcher and Niehrs, 2005; Thisse and Thisse, 2005).

In vertebrates the molecular weights of FGFs range from 17-34 kDa. Some of the FGFs are subjected to alternate splicing which can alter their affinity towards the receptor (Olsen, S. K. et al., 2006). Most of the FGFs are secreted constitutively and have classical N-terminal signal peptides whereas others that lack an obvious signal peptide (particularly FGF9, FGF16 and FGF20) are efficiently secreted. Some of the FGFs (FGF11-14) localizes to the nucleus of the cell rather than being secreted and thus are not involved in the activation of the receptor (Goldfarb, M, 2005; Ivor Mason, 2007). Certain FGFs (FGF2 and FGF3) can work in both secretory as well as nuclear pathways (Ornitz and Itoh, 2001)

In vertebrates, there are four *Fgfr* genes (*Fgfr1-4*) that code for the FGFR 1-4 proteins. But multiple spliced variants do exist that generate the diversity. An FGFR5 (also know as FGFR like protein 1 or FGFRL1) has been reported that lacks the C-terminal tyrosine kinase domain and thus serves as the negative regulator of FGFR signaling pathway (Sleeman et al., 2001). This protein is encoded by *FGFRL1* gene and also exists in multiple spliced variant forms.

The structural features of FGFs and FGFRs are shown in Figure 22 (taken from Böttcher R T and Niehrs C, 2005). Briefly, the FGFs contain a signal peptide sequence that precedes the N-terminal region, a central core region that binds to FGFR and heparin sulfate proteoglycans (HSPG) (Figure 22A). The basic structure of FGFRs (Figure 22B) comprises an N-terminal signal peptide sequence, followed by three Ig domains (Ig I-III). In between the IgI and IgII, there is an acidic box, a heparin-binding domain and CAM-homology domain (CHD). The middle region contains a single transmembrane domain followed by a juxtamembrane domain. Finally, the C-terminal region contains a split tyrosine kinase domain. The FGF binding is required for the receptor dimerization and activation. HSPG mediates the effective binding and activation of FGFR by FGF (Lin, 2004). HSPG binds to the core region of FGF and interacts with the FGFRs via its heparin-binding domain and forms a ternary complex involving FGFR-FGF-HSPG/Heparin in 2 :2 :1 ratio. Although, IgII and IgIII domain of FGFR is sufficient for the binding and specificity of the ligand, but it has been shown that the IgI domain alters the specificity of the ligand binding (Wang et al., 1995). The IgI and the acidic box are also involved in the autoinhibitory function of the receptor (Olsen et al., 2004).

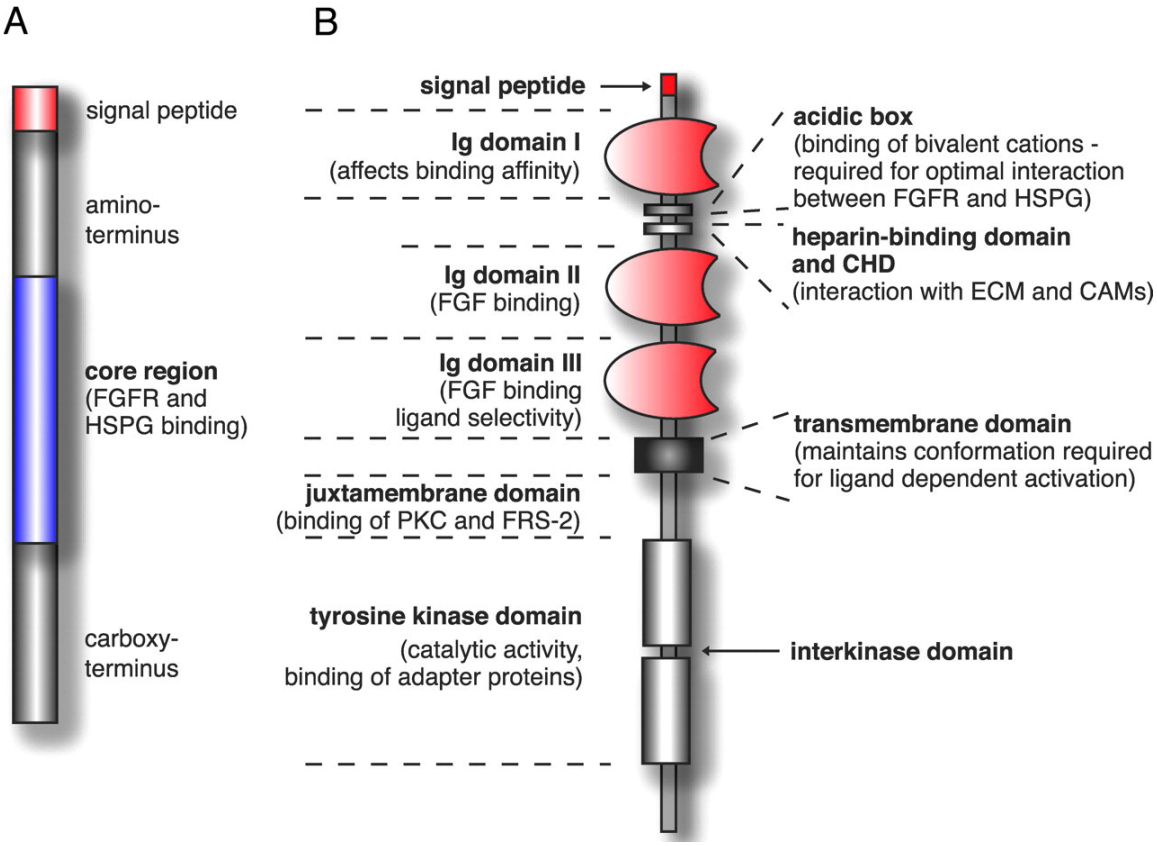

Figure 22. The structural features of FGFs and FGFRs (Böttcher and Niehrs, 2005). (A) Structure of a generic FGF protein. (B) The main structural features of FGFRs.

1.6.2) FGFR signaling pathway

The binding of FGF results in dimerization and autophosphorylation events, that lead to the activation of the receptor. Upon activation, FGFR follows one of the three major pathways (Figure 23 taken from Böttcher R T and Niehrs C, 2005), the MAPK pathway, the PLC pathway and the PI3K/ Akt pathway. These major pathways are already described in section 1.5.2. Briefly, the MAPK signaling cascade is the main pathway activated by FGF. The FGF Receptor substrate 2 (FRS2) is the constitutively binding partner of the FGFR. FRS2 serves as the docking protein for multiple RTKs

such as FGFR (Xu et al., 1998), Insulin receptor (Delahaye et al., 2000), NGF receptor (Ong et al., 2000; Zeng and Meakin, 2002; Dhalluin et al., 2000), and RET receptor (Kurokawa et al., 2001). FRS2 is a lipid-anchored protein, that binds to the FGFR juxtamembrane region via its protein tyrosine binding (PTB) domain. The activated receptor phosphorylates multiple tyrosine residues of FRS2, which is recognized by SH2 domains of the small adapter protein Grb2 that exists in a complex with the nucleotide exchange factor Son of Sevenless (SOS). The recruitment of SOS results in the activation of the membrane bound GTPase Ras, which further activates Raf. Thus the three tiered MAPK cascade Raf/MEK/ERK becomes activated (Sternberg and Alberola-Ila, 1998). The resulting activated ERK then translocate to the nucleus and phosphorylates the Ets domain containing transcription factors Erm and Pea3 (Wasylyk et al., 1998).

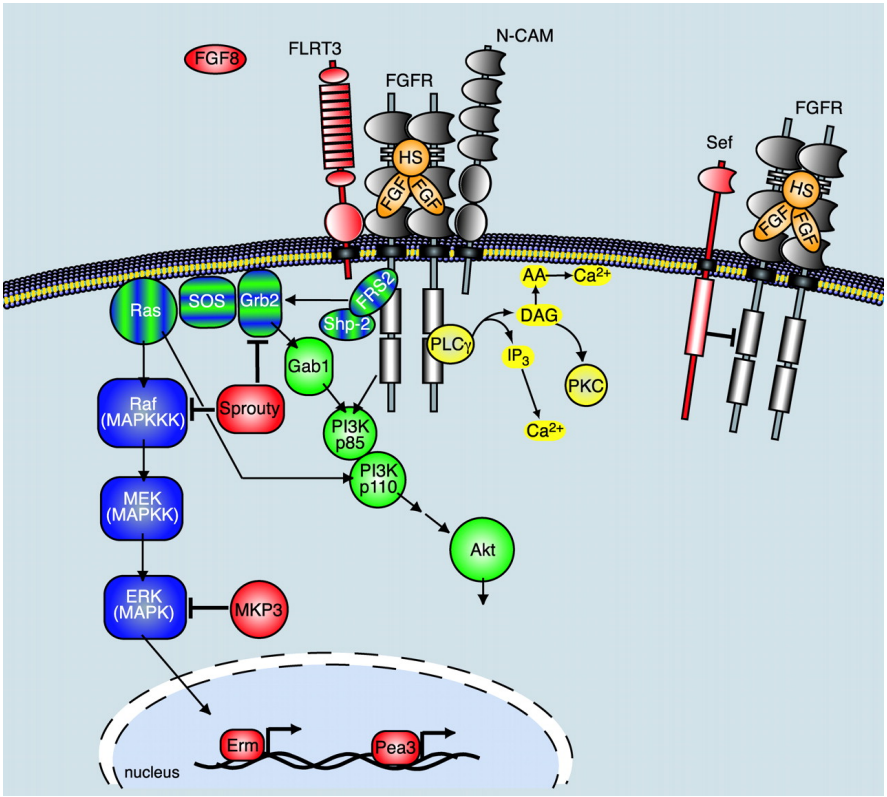

Figure 23. FGF Receptor signaling pathway (Böttcher and Niehrs, 2005).

The second major pathway, the PLCγ/ Ca^{2+} pathway is activated upon binding of the SH2 domain of PLCγ to phosphorylated Tyr766 of FGFR (Mohammadi et al., 1992; Peters et al., 1992). The activated phosphorylated PLCγ hydrolyzes PIP2 to IP3 and DAG. IP3 initiates Ca^{2+} release from the intracellular stores, whereas DAG activates PKC. PKC can stimulate Raf in a Ras-independent manner, thus connecting the two major pathways of FGF signaling (Ueda et al., 1996).

The PI3K/Akt pathway can be activated downstream of FGFR in one of the three following ways: (i) the p85 subunit of PI3K can bind to a phosphotyrosine of the activated FGFR; or (ii) it can be activated by Gab1, which is activated in turn by indirectly interacting with FRS2 via Grb2; or (iii) the p110 subunit of PI3K can be activated by Ras (Bottcher and Niehrs, 2005).

1.6.3) Modulators of FGFR signaling

Negative modulators of FGFR function: Proteins such as SEF, SPROUTY/SPRED, and FLRT belong to this class. These proteins either inhibit the receptor signaling or check signaling strength and thus maintain normal homeostasis (Figure 24 taken from Mason I, 2007). "Similar Expression to FGF" or SEF is a member of the FGF Synexpression group. Genes that are expressed in a similar spatiotemporal pattern comprise a Synexpression group whose members are co-regulated and may hence function in a common pathway (Niehrs and Meinhardt, 2002). SEF was originally discovered in zebrafish and since then, chick, mouse and human orthologues have been found (Harduf et al., 2005; Kawakami et al., 2003; Kovalenko et al., 2003; Lin et al., 2002; Preger et al., 2004; Xiong et al., 2003; Yang et al., 2003). SEF acts as a negative feedback inhibitor of FGF-induced MAPK signaling. There are 2 known isoforms: a long isoform and a short isoform. The site of action of SEF remains

controversial as some groups have reported it to act at the receptor level (Preger et al. 2004; Yang et al., 2003), while others have reported it to act within the ERK cascade at the level of MEK (Torii et al., 2004). Both SEF isoforms have been shown to directly interact (co-localisation and immunoprecipitate) with the FGFR across different species and cell type and have the ability to inhibit the FGFR and FRS phosphorylation (Tsang et al., 2002; Ren et al., 2007; Ziv et al., 2006; Ren et al., 2008). SEFs have been shown to inhibit FGF induction of the PI-3 kinase pathway (Kovalenko et al., 2003; Harduf et al., 2005) but they may also inhibit NGF and EGF dependent signaling (Xiong et al., 2003; Torii et al., 2004; Ziv et al., 2006). SEFs have been also reported to interact and co-localise with the EGFR (Ren et al., 2008)

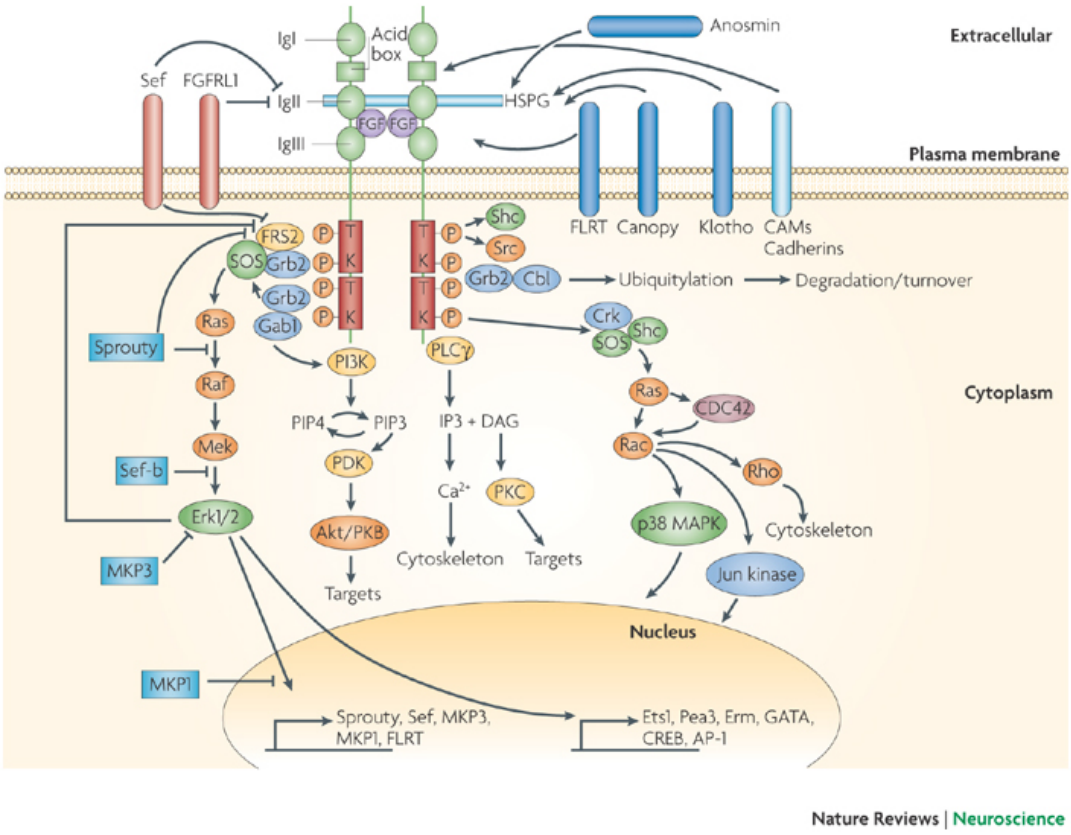

Figure 24. Signaling through fibroblast growth factor receptors (FGFRs) (Mason I, 2007).

1.6.4) FGFR1 Autophosphorylation

The tyrosine autophosphorylation of RTKs represent one of the critical step in regulating the kinase activity of the receptor and further recruitment and activation of intracellular pathways (Bae et al., 2010). The autophosphorylation of FGFR1 is a sequential and precisely ordered intermolecular reaction that occurs in three phases. The trans-phosphorylation of the tyrosine residue Y653, located in the activation loop marks the first phase that results in 50-100 fold stimulation of the kinase activity (Furdui et al., 2006). Next phase involves the phosphorylation of Y583 and Y585 in the kinase domain, Y463 in the juxtamembrane region, and the Y766 residue in the C-terminal tail of the FGFR1. The tyrosine residues involved in the second phase serve as the docking sites for the signaling proteins. In the final phase, the second tyrosine residue Y654 within the activation loop is phosphorylated. This step further increases the kinase activity by 10-fold. The order of trans-phosphorylation sites of FGFR1 was shown as: Y653, Y583, Y463, Y766, Y585, and Y654 as shown in Figure 25 (adapted from Bae et al., 2010). These sequentially autophosphorylated tyrosine residues are not adjacent to each other, being separated by distances of 35-50 Angstrom.

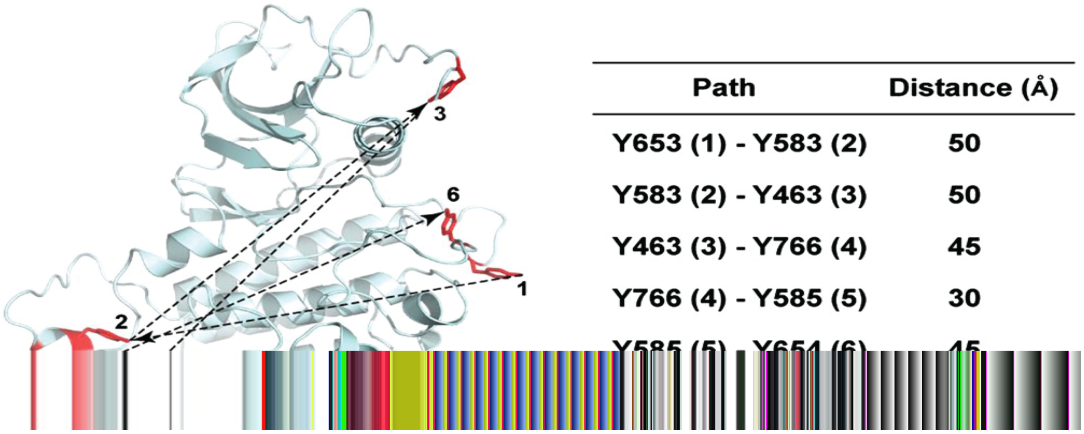

Figure 25. A model of FGFR1 sequential autophosphorylation (Bae et al., 2010).

In 2010, Bae et al had shown that the tyrosine autophosphorylation of FGFR in living cells requires the asymmetric receptor contact. Upon re-examination of the crystal structure of FGFR1 kinase domain (PDB code 3GQI) (Bae etal, 2009), they found that there is a substantial crystallographic interface between the N-lobe of the kinase molecule, which serves as an active enzyme, and specific docking sites on the C-lobe of the second kinase molecule of an FGFR1 dimer, which serves as a substrate.

1.6.5) The R577E FGFR1 Mutant:

The crystallographic studies performed by Bae et al in 2010 had shown that arginine 577 (R577) is involved in creating, in vivo, an asymmetric FGFR1 dimer that allows transphosphorylation of Y583 and probably other tyrosine autophosphorylation sites in FGF-stimulated cells. A single point mutation of R577 to glutamic acid residue was predicted to prevent asymmetric dimerization, and this mutation, R577E, was found to drastically reduce autophosphorylation in live cells. But, interestingly R577E hFGFR1 retains full kinase activity in vitro.

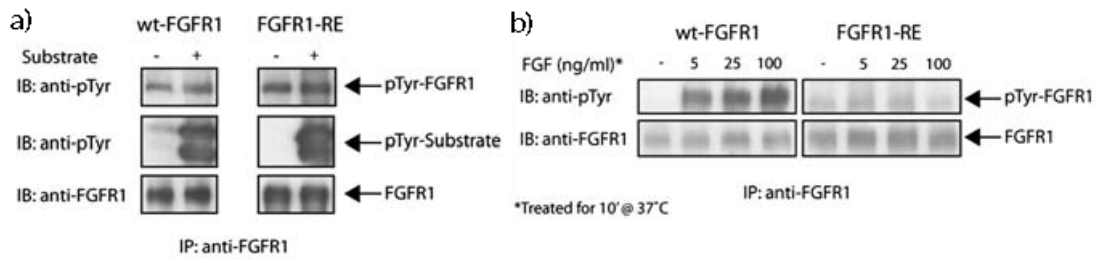

Figure 26. Autophosphorylation of FGFR1 in vitro and in vivo.

(a) The R577E mutant of FGFR1 (FGFR1-RE) is able to phosphorylate a fragment of PLCγ in vitro, but (b) its ability to autophosphorylation is severely compromised in vivo.

In Figure 26, the in vivo kinase activity of FGFR1-RE can be seen to be significantly reduced or lost. Compared to wt FGFR1, FGFR1-RE does not respond to dose dependent activation by FGF and fails to autophosphorylate. However, the same immunoprecipitated mutant receptor is fully active in phosphorylating an FGFR1 substrate in vitro.

Surprisingly, the FGFR1 R577E mutant (FGFR1-RE) was shown to lock the kinase domain activation loop in its open "active" conformation, explaining why it was catalytically active in vitro. Bae et al. (2010) concluded that the asymmetric dimerization of the FGFR1 catalytic domains is essential for receptor activation in vivo, and this is sterically prevented in the R577E mutant due to the restraints imposed by its manner of insertion in plasma membrane.

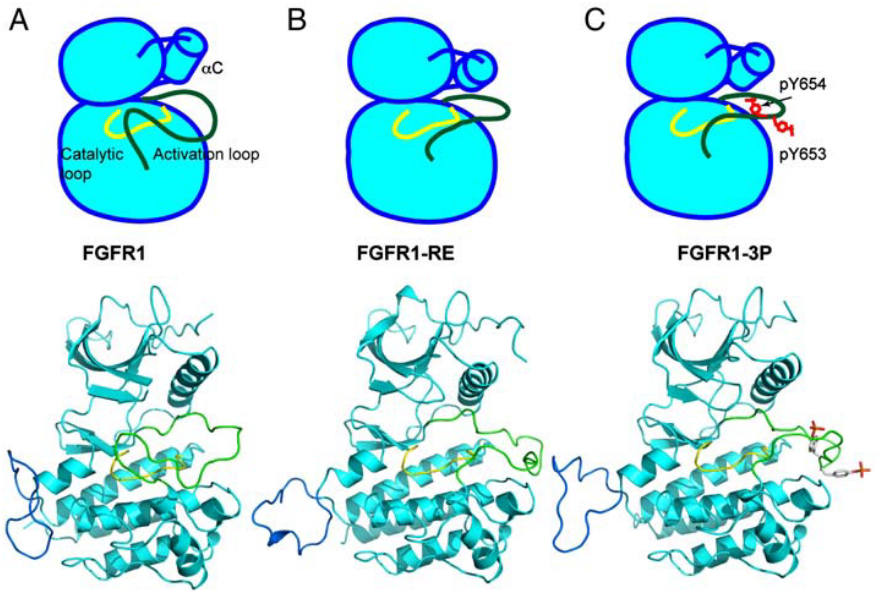

Figure 27. The structures of kinase domains of (A) wt-FGFR1, (B) FGFR1-RE mutant, and (C) activated FGFR1 (FGFR1-3P) shown as both cartoon and ribbon diagrams. The activation loop is shown in green and the catalytic loop in yellow. Figure taken from (Bae et al., 2010).

1.7 Objectives

The main objectives of my studies are:

- To study the interaction patterns of the different ESyts with RTKs in general, and with FGFR1 in particular, in order to better understand the role and importance of the ESyts in RTK signaling and receptor endocytosis.

- To study the effects of loss of ESyt 2/3 in mouse embryonic fibroblasts (MEFs).

Chapter 2

Extended Synaptotagmin Interaction with the FGF Receptor Depends on Receptor Conformation, not Catalytic Activity.

[#]François Guillou, [#]Chelsea Herdman, [#]Prakash K. Mishra, [#]Michel G. Tremblay, Joëlle Baril, Sabrina Bellenfant and Tom Moss*.

Laboratory of Growth and Development, St-Patrick Research Group in Basic Oncology, Cancer Division of the Québec University Hospital Research Centre. Department of Molecular Biology, Medical Biochemistry and Pathology, Faculty of Medicine, Laval University, ~~Edifice St Patrick~~, 9 rue McMahon, Québec, QC, G1R 3S3, Canada.

# These authors contributed equally to this work, (equal First Authors).

*To whom correspondence should be addressed,

E-mail. Tom.Moss@crhdq.ulaval.ca

Tel. 1 418 691 5281

FAX 1 418 691 5439

Keywords: Extended-Synaptotagmin, Esyt1, Esyt2, Esyt3, Dimerization, ESyt-FGFR complex, FGFR activity, FGFR conformation.

Foreword

After joining the lab I started working on ESyts. This chapter is based on my major work in the lab. I was involved mostly in checking the interactions of ESyts with different receptors, ESyt dimerization and mapping of the ESyt binding domain in FGFR1. Apart from working with FGFR1 mutants and construction of FGFR1 R577E and FGFR1 deletion mutants, I have contributed to work presented in Figure 29, Figure 31 (B and C) Figure 34 (B) and Figure 35 of this chapter.

Résumé

Nous avons précédemment démontré que ESyt2 interagit spécifiquement avec le récepteur de FGF activé et est nécessaire pour une rapide internalisation du récepteur et la signalisation fonctionnelle via la voie ERK dans les premiers stades embryonaires de *Xenopus*. ESyt2 fait partie d'une famille de trois membres des *Extended* synaptotagmines pour laquelle il a été récemment démontré qu'elle est impliquée dans la formation de la jonction entre le réticulum endoplasmique (RE) et la membrane plasmique (PM) ainsi que dans la régulation dépendente du Ca^{++} de ces jonctions. Ici, nous démontrons que ESyt2 est dirigée vers le RE par son domaine transmembranaire putatif, que les ESyts hétéro- et homodimerisées, ainsi que l'homodimérisation *in vivo* de ESyt2 nécessitent une séquence transmembrane (TM) adjacente, mais pas le domaine SMP. ESyt2 et ESyt3, mais pas ESyt1, interagissent de manière sélective avec FGFR1 activé. Dans le cas de ESyt2, cette interaction nécessite une courte séquence adjacente au TM et est indépendante de l'autophosphorylation du récepteur, mais dépendante de la conformation du récepteur. Les données montrent que ESyt2 reconnaît un site dans le lobe supérieur de la kinase de FGFR1 qui est révélé par le déplacement de la boucle d'activation du domaine kinase au cours de l'activation du récepteur.

Abstract

We previously demonstrated that ESyt2 interacts specifically with the activated FGF receptor and is required for a rapid phase of receptor internalization and for functional signaling via the ERK pathway in early Xenopus embryos. ESyt2 is one of the three-member family of Extended Synaptotagmins that were recently shown to be implicated in the formation of endoplasmic reticulum (ER)-plasma membrane (PM) junctions and in the Ca^{2+} dependent regulation of these junctions. Here we show that ESyt2 is directed to the ER by its putative transmembrane domain, that the ESyts hetero- and homodimerize, and that ESyt2 homodimerization in vivo requires a TM adjacent sequence but not the SMP domain. ESyt2 and ESyt3, but not ESyt1, selectively interact in vivo with activated FGFR1. In the case of ESyt2, this interaction requires a short TM adjacent sequence and is independent of receptor autophosphorylation, but dependent on receptor conformation. The data show that ESyt2 recognizes a site in the upper kinase lobe of FGFR1 that is revealed by displacement of the kinase domain activation loop during receptor activation.

2.1) Introduction

The Extended Synaptotagmin-like Proteins (ESyts) are similar in general structure to the Synaptotagmins, a C2 domain containing family of proteins involved in calcium mediated secretion and endocytosis (Moghadam and Jackson, 2013). So far, three proteins have been discovered that belong to the Extended Synaptotagmin family, ESyt1, ESyt2 and ESyt3. ESyt1 was originally discovered in vesicle preparations from rat adipocytes and named vp115 for 115kDa vesicular protein (Morris et al., 1999). However, it was not until 2007 that all three family members were initially studied and the name Extended Synaptotagmin first coined (Min et al., 2007). The domain architecture of the human ESyts revealed a putative N-terminal transmembrane domain (TM), an SMP (Synaptotagmin-like Mitochondrial lipid-Binding Protein) domain (Lee and Hong, 2006) followed C-terminally by multiple C2 domains. Human ESyt2 and ESyt3 each contain three C2 domains (C2A, C2B and C2C) while ESyt1 has five (C2A to C2E) (Figures 28A and 37), and this organisation is conserved in mouse (Herdman et al., 2014), Xenopus (Jean et al., 2010) and to a surprising extent in the yeast Tricalbins (Creutz et al., 2004).

Jean et al provided the first potential function for ESyt2 when they showed that it acted as an endocytic adapter specific for the activated FGF receptor and was required for functional signaling via the ERK MAP-kinase pathway during early Xenopus development (Jean et al., 2010). Xenopus ESyt2 was also later shown to recruit the p21-GTPase Activated Kinase PAK1 and to regulate the dynamics of the actin cytoskeleton (Jean et al., 2012). More recently the yeast Tricalbins were shown to be endoplasmic reticulum (ER) resident proteins that aid in the formation of ER to Plasma Membrane junction sites or bridges (Manford et al., 2012), and the human ESyts were shown to play a similar role (Chang et al., 2013; Giordano et al., 2013). The ESyts were also shown to associate with the ER membrane, probably via a TM hairpin, and to help tether the ER to the PM. Further, ESyt1 was shown to respond to cytosolic Ca^{2+} by translocating to the sites of ER-PM junctioning and to promote the

replenishment of PM associated phosphatidylinositol 4,5-bisphosphate (PIP2) (Chang et al., 2013).

Here we have investigated the molecular basis for the specificity of the ESyt-FGFR interaction. We have characterized the homologous and heterologous interactions between the human ESyts, the interactions of each with FGFR1, defined the homologous interaction and ER targeting domains of ESyt2 and used extensive deletion and point mutations to investigate the molecular specificity of the ESyt2-FGFR1 interaction. The data surprisingly reveal a mode of interaction that is independent of receptor autophosphorylation, or indeed catalytic activity, and is solely dependent on the active receptor conformation. The data show that ESyt2 recognizes a site in the upper kinase lobe of FGFR1 that is revealed when the activation loop is displaced into the active configuration.

2.2) Results

Given the general structural similarity to the Synaptotagmins, the ESyts were originally assumed to be plasma membrane (PM) proteins (Figure 28A and 37) (Jean et al., 2010; Min et al., 2007). However, at the time we were unable to detect these proteins on the PM via N-terminal FLAG epitope-tags (Figure 28B and 38), or HA-tags (data not shown) despite the same tags being fully available after cell permeabilization. A SNAP-tag™ fused to the N-terminus of ESyt2b was also not available before cell permeabilization, despite an N-terminal SNAP-tag fused to the Adrenergic Receptor β2 (ADRβ2) being easily detected with both the cell-impermeable SNAP-surface and cell permeable SNAP-Cell ligands (NEB) (Figure 28C). Recently it was found that rather than being inserted into the PM the ESyts are probably inserted into the membrane of the endoplasmic reticulum (ER) (Chang et al., 2013; Giordano et al., 2013). These data exclude the possibility that the ESyts traverse the PM and are consistent with an association with the ER, but also with a non-penetrating mode of membrane association such as recently proposed (Chang et al., 2013; Giordano et al., 2013).

2.2.1) ESyt2b is misdirected to the PM by fusion to the Syt1 transmembrane (TM) domain.

Exactly what directs the ESyts to insert exclusively into the ER membrane rather than into the PM, as does Syt1, is presently not known. To resolve this question we created a fusion between Syt1 and ESyt2b, such that the potential transmembrane/membrane-insertion (TM) domain and N-terminal sequences of ESyt2b were replaced by those of Syt1. This resulted in an ESyt that associated with and penetrated the PM much as did Syt1 (Figure 28D). Given that the ESyts and their splice variants display little if any homology preceding the potential membrane-associated domain, (Figure 37), this strongly suggests that the determinants for association with the ER membrane lie within the membrane-associated domain or the approximately 20 amino acids preceding it.

2.2.2) The ESyts homo- and hetero-dimerize.

Given their localization in the ER and to better understand the function of the ESyts in FGF signaling, we first wished to establish if they function as monomers or as hetero- or homodimers. Recent data demonstrated that the ESyts can probably heterodimerize and homodimerize (Giordano et al., 2013; Jean et al., 2010). Consistent with this, when differentially tagged versions of the three ESyts were expressed in homologous and heterologous pairs, it was evident that not only did all three heterodimerize, but also homodimerize (Figure 29). While ESyt1 interacted with itself and with ESyt3 relatively weakly, it appeared to interact strongly with the two N-terminal splice forms of ESyt2, (2a and 2b (Jean et al., 2010)), (Figure 29A). ESyt2a interacted both with itself and its N-terminal splice variant ESyt2b, as well as with ESyt1 and 3 (Figure 29B), and conversely ESyt3 interacted with both ESyt2a and 2b (Figure 29C). Since none of the three ESyts interacted with Syt1, clearly these interactions were highly specific.

2.2.3) ESyt2 dimerization maps to its N-terminal sequences and does not require the SMP domain.

We further investigated the domain of ESyt2 responsible for its dimerization. The N-terminal regions preceding the membrane domain of ESyt2a and 2b bear little homology, suggesting that these regions were probably not involved. However, when increasingly extensive C-terminal deletion mutants of FLAG-tagged ESyt2b were co-expressed with full length HA-tagged ESyt2b, interactions were observed with deletions mutants a.a.1 to 785, lacking C2C domain, a.a.1 to 510 lacking C2B and C2C, a.a. 1 to 359 lacking all three C2 domains, and even a.a. 1 to 139, lacking the SMP domain (Figure 30). Thus, the minimal homo-dimerization/oligomerization domain mapped between a.a. 1 and 139. This was somewhat surprising in the context of the recent crystal structure of two SMP domains that showed ß-barrel structures contacting end-to-end to form a dimer (Schauder et al., 2014). The data then suggest that either ESyt2 contains two or more redundant dimerization domains or that it predominantly dimerizes via sequences close to or within its putative transmembrane domain that were not present in the ESyt2 structure determination.

2.2.4) ESyt2 and 3, but not ESyt1 interact selectively with the activated FGF Receptor.

We had previously shown that both Xenopus and human ESyt2 interact in a highly selective manner with the activated forms of the FGF receptor family (FGFR1-4) (Jean et al., 2010). Extending these observations we found that this was a common property of the shorter two ESyts, the splice variants ESyt2a and -b and ESyt3 all displaying a strong selectivity for FGFR1 after bFGF stimulation and little or no interaction when the receptor was specifically inhibited using SU5402 (Figure 31A-C). By contrast, ESyt1 repeatedly displayed little or no interaction with FGFR1 in co-transfection assays as compared with ESyt2a (Figure 31D) or indeed ESyt2b or -3 (data not shown). At first sight this suggests a functional difference to the shorter ESyts. However, ESyt1 is predominantly associated with the cytosolic ER membrane and not with ER-PM junctions (Figure 28B) (Chang et al., 2013; Giordano et al.,

2013). Hence, the lack of interaction with FGFR may in part be a function of its different subcellular distribution.

2.2.5) ESyt2 is not internalized during endocytosis of activated FGFR.

The lack of an interaction of ESyt1 with the FGF receptor suggested that the interactions of the ESyts were at least in part determined by their subcellular distribution. We had previously shown that ESyt2 was implicated in determining receptor endocytosis and that it associate with Adaptin2 (AP-2) (Jean et al., 2010). This suggested that, consistent with its PM proximal distribution, its interaction with the activated FGF receptor initially occurs on the PM during the formation of clathrin-coated pits. We therefore asked if ESyt2b was internalized along with activated FGFR or if its interaction was limited to the PM-associated receptor fraction. When cells expressing N-terminally FLAG-tagged FGFR1 were subjected to FGF stimulation, as expected a significant level of initially PM-associated FGFR1 was observed to move into endocytic vesicles (Figure 31D and 39). In contrast, the distribution of ESyt2b remained unchanged and predominantly proximal to the PM. Thus, consistent with its presence in ER-PM junctions, ESyt2b interacts with the activated fraction of the PM-associated FGFR1.

2.2.6) Interaction of ESyt2b with FGFR1 is mediated by a TM adjacent domain.

To determine the structural determinants of the ESyt-FGFR interaction we used ESyt2b as a canonical model and investigated the interaction of truncation mutants with FGFR1. Co-transfection of FGFR1 with the series of ESyt2b C-terminal deletion mutants showed that loss of one, two or all of the C2 domains (ΔC2ABC) had no inhibitory effect on the interaction with FGFR1 (Figure 32A and B). However, deletion of the N-terminal, TM and adjacent sequences to a.a.136 (ΔTM) very strongly suppressed or eliminated the interaction (Figure 32B and C). Given that the sequences N-terminal of the TM show little or no homology between ESyt2a, 2b and 3 of (Figure 37), it was not surprising that their deletion from ESyt2b (a.a.1 to 87,

ΔNterm) did not eliminate the interaction with FGFR1. This interaction was clearly much weaker than for the WT, though significantly greater than for the ΔTM mutation at least in part because this mutant repeatedly expressed poorly (Figure 32B). Specific deletion of the SMP domain had no discernable effect on the interaction with FGFR1, and the interaction was suppressed by receptor inactivation (Figure 32C). Thus, the data show that the C2 and SMP domains of ESyt2b are not required for the interaction of ESyt2b with FGFR1. By contrast, this interaction does require the TM and sequences immediately flanking it (a.a. 88 to 138), though probably not the unconserved sequences further N-terminal, (Figure 32D). Hence, the domain required for ESyt2 dimerization (Figure 30) and its interaction with FGFR1 in greater part overlap.

2.2.7) Interaction of ESyt2 with activated FGFR1 is independent of receptor phosphorylation.

Interactions of signaling modules with activated tyrosine kinase receptors are often mediated by receptor autophosphorylation (Seet et al., 2006). To determine if this was the case for the ESyt-FGFR interaction we generated mutations of all seven phosphotyrosine sites on FGFR1 and determined if these affected the interaction with ESyt2b. Mutation of each site singly had no significant effect on the interaction (Figure 40), however as expected combined mutation of Y653 and 654, two activation loop phosphorylation sites essential for kinase activity, suppressed the interaction with ESyt2b (and ESyt3, data not shown) as strongly as did the kinase dead (KD) ATP-binding site mutation K514A (Figure 33A and B).

As expected, a combination of the five remaining non-catalytic phosphotyrosine site mutations (Y463,583,584,730,766F) very strongly reduced overall receptor phosphorylation and somewhat reduced interaction with ESyt2b, though to a much smaller extent than the activation loop mutations (Y653,654F) (Figure 33B). Thus, interaction of ESyt2b with FGFR1 was not mediated by any single phosphotyrosine and even combined elimination of 5 of the 7 sites had only moderate inhibitory

effects on the interaction. This left the possibility that a specific interaction with the activation loop phosphotyrosines might be involved. Thus, we replaced both the activation loop phospho-sites of FGFR1 by phosphomimics (Y653,654E). The resulting mutant interacted with Esyt2b only a little less efficiently than did the WT and certainly far better than the corresponding the Y653,654F mutant (Figure 33D). Further, the interactions of these three forms of FGFR1 with ESyt2b were roughly in proportion with their relative autophosphorylation levels (Figure 33D). This suggested that either ESyt2b was able to recognize the combined autophosphorylation state of all seven sites on FGFR1, or that it recognized a specific receptor conformation related to the receptor autophosphorylation state.

2.2.8) ESyt2 interaction depends on active receptor conformation but not catalytic activity.

The data from the FGFR1 phospho-site mutants suggested that phosphorylation did not play a direct role in the specificity of ESyt2 for the activated receptor, but that receptor activation did. This suggested that ESyt2 might recognize a specific change in receptor conformation occurring on activation. FGFR1 activation is brought about by a displacement of the activation loop that allows access to the active site of the kinase domain (Bae et al., 2009). Further, FGFR1 autophosphorylation was shown to occur via an asymmetric interaction between the kinase domains of adjacent receptors, one acting as enzyme and the other as substrate. Mutation of arginine a.a. 577 to glutamic acid (R577E) within the FGFR1 kinase domain was shown to prevent this asymmetric interaction and to lock the activation loop in the open "active" conformation while at the same time preventing catalytic activation of the receptor (Bae and Schlessinger, 2010) (Figure 34A). We therefore asked if ESyt2b would interact with FGFR1 carrying this mutation. ESyt2b did indeed interact with the FGFR1-R577E mutant, despite this mutant being clearly unable to autophosphorylate (Figure 34B) and also unable to recruit phospho-PLCγ (pY-PLCγ), as was the control Y766F mutant that eliminates the phospho-site bound by PLCγ (Mohammadi et al., 1992; Peters et al., 1992). FRS2 is constitutively recruited to the receptor and hence

for this reason was unlikely to be implicated in the ESyt2 interaction (Ong et al., 2000). However, to directly test this we also mutated the essential leucine 422 (L422A) within the FRS2 binding site on FGFR1, but found it had no effect on the ESyt2b interaction (Figure 34B).

We further investigated the interaction of ESyt2b with the FGFR1-R577E mutant in comparison with the inhibited and activated states of the wild type receptor and the kinase dead ATP binding site mutant K514A (Bellot et al., 1991). Both the wild type FGFR1 and the R577E inactive mutant interacted strongly with ESyt2b, while as should be expected, the K514A (KD) mutant did not (Figure 34C). Interestingly, the inhibitor SU5402 strongly suppressed the interaction of ESyt2b with wild type FGFR1, but had no effect on the interaction of ESyt2b with the R577E mutant. This is consistent with structural data suggesting that this mutant may also have a low affinity for ATP (Bae et al., 2010). Together these data show that ESyt2 specifically recognizes the open active conformation of FGFR1 independently of either catalytic activity or receptor autophosphorylation.

2.2.9) FGFR truncation reveals an interaction with ESyt2b independent of catalytic activity.

Since the data to this point indicated an ESyt2-FGFR1 interaction based solely on the recognition of the open receptor conformation, this suggested that displacement of the activation loop revealed an ESyt2 binding site that was otherwise hidden in the inactive receptor. Thus, we decided to ask if this surface would also be revealed in C-terminal receptor deletion mutants (Figure 35A). Deletion of the C-terminal tail, leaving the kinase domain intact, as expected, had no effect on the ESyt2b interaction, as did mutation of the transmembrane domain proximal Nedd4-1 ubiquitinylation site (Δ6) shown to be required for receptor internalization (Persaud et al., 2011) (Figure 35B). Surprisingly, deletion of the lower C-terminal kinase lobe and the activation loop also had no effect on the ESyt2b interaction, but deletion to a.a. 475, to remove most of the N-terminal kinase lobe, eliminated the interaction.

This supported the idea that ESyt2b recognized a binding site on FGFR1 contained within the N-terminal or upper C-terminal kinase lobes that was revealed on displacement of the activation loop during receptor activation.

To further delineate the ESyt2b binding site, we created three more C-terminal deletion mutants of FGFR1. Partial deletion of the upper part of the C-terminal kinase lobe to a.a. 600, or indeed its full deletion to a.a. 550, had no effect on the interaction of ESyt2b with the receptor. However, deletion to a.a. 500, also removing half the N-terminal kinase lobe, did eliminate the ESyt2b binding site. Together the data strongly suggest that the selectivity of ESyt2b for the active FGFR1 receptor depends on a binding site within the N-terminal kinase lobe of the receptor that is revealed when the activation loop is displaced to its position in the active receptor conformation. The probable structure of the N-terminal kinase lobe in the a.a. 550 deletion mutant can be seen in Figure 36A. Since we can fully delete the activation loop without affecting the ESyt2b-FGFR1 interaction, contact with the loop itself is clearly unnecessary for the interaction. However, within the context of the wild type FGFR1 the activation loop would prevent ESyt2 access to the underside of the N-terminal kinase lobe in its inactive configuration, but allow access in its active configuration (Figure 37B). This, in turn, suggests that the site of the ESyt2 interaction lies proximal to or corresponds with the ATP binding pocket.

2.3) Discussion

The interaction of ESyt2 with FGFR1 was previously shown to be dependent on receptor activation and to be required for a rapid phase of receptor internalization necessary for functional signaling via the ERK pathway during early Xenopus development and shown to be conserved in human (Jean et al., 2010). Here we have used the human system to investigate the molecular parameters of the ESyt-FGFR1 interaction in order to better understand its underlying specificity. However, ESyt2 is just one of the three member family of human Extended Synaptotagmins. These proteins were recently shown to be implicated in the formation of endoplasmic

reticulum (ER)-plasma membrane (PM) junctions and in the Ca^{++} dependent regulation of these junctions (Chang et al., 2013; Giordano et al., 2013; Manford et al., 2012). Here we provide evidence supporting the observations (Chang et al., 2013; Giordano et al., 2013) that the ESyts are not integral PM proteins, but rather are inserted into the ER membrane. We also show that in the case of ESyt2, this function is an intimate property of the putative transmembrane domain, since its replacement by the transmembrane domain of Syt1 redirects ESyt2 to the PM. We further show that all three ESyts hetero- and homodimerize to some degree, though ESyt1 displays a preference to heterodimerize with ESyt2 rather than to heterodimerize with ESyt3 or to homodimerize. Analysis of ESyt2b deletion mutants showed that neither the C2 domains nor the SMP domain are essential for its homodimerization in vivo. This suggests that the dimerization via the SMP domain observed in the ESyt2b crystal structure is not essential for its dimerization in vivo (Schauder et al., 2014).

We show that ESyt2 (both a and b splice variants) and ESyt3, but not ESyt1, selectively interact in vivo with the activated form of FGFR1. Interaction of ESyt2b with FGFR1 depends strongly, if not exclusively, on the TM and immediately adjacent sequences of ESyt2 (a.a. 88 to 138). This region is common to ESyt2a and 2b and shows 45% identity/ 71% similarity with the equivalent region of ESyt3 and 41% identity/ 61% similarity with the equivalent of ESyt1. Thus, the lack of an interaction of ESyt1 with FGFR may in part be due to the lower homology with ESyt2/3 or to its predominant localization to cytoplasmic ER membranes (Chang et al., 2013; Giordano et al., 2013), or both.

We further investigated the factors that determine the selective interaction of ESyt2b with activated FGFR1. We find that while receptor activation is a prerequisite for the interaction, none of the receptor autophosphorylation events are required. Indeed, even the activation loop phospho-sites Y653 and Y654 of FGFR1 can be replaced by phospho-mimics (Y653/654E) without affecting either the interaction with ESyt2 or its specificity. Most interestingly, we found that a R577E mutant FGFR1 was recognized by ESyt2. This mutant receptor has its activation loop locked in the open,

active position, but is catalytically inactive in vivo (Figure 34A) (Bae and Schlessinger, 2010). The ability of ESyt2 to interact with this mutant receptor, despite its catalytic inactivity strongly suggested that the interaction was based solely on receptor conformation and not activity. This finding was consistent with our data showing that the ESyt2-FGFR1 interaction was independent of receptor autophosphorylation, and suggested that ESyt2 recognized a surface of the FGFR1 catalytic domain revealed by displacement of the activation loop. Receptor deletion mapping confirmed this was the case and showed that the interaction site between ESyt2b and FGFR1 lay within the N-terminal kinase lobe of the receptor, probably close to the ATP binding fold. Together, the data strongly suggest that the conformation of the receptor activation loop defines access of ESyt2 to the lower surface of the N-terminal FGFR1 kinase lobe including the ATP binding pocket (Figure 36). This then explains the high degree of selectivity of ESyt2 and probably ESyt3 for the active form of the FGF receptor.

Our previous data showed that ESyt2 was required in very early Xenopus embryos for functional FGF signaling via the ERK but not the PI3-kinase pathways. The data further demonstrated a function of ESyt2 in a rapid phase of receptor endocytosis in these embryos. Recent data showing that ESyt2 and 3 localize to ER-PM junctions and may act in concert with other junctioning proteins (Manford et al., 2012) suggests that this function may be only one part of a more complex pathway regulating FGF signaling that involves the regulation of Ca^{2+} and phosphatidylinositol 4,5-bisphosphate (PIP2) levels (Chang et al., 2013). FGF signaling directly activates PLCγ, e.g. see Figure 34B, and hence stimulates the cleavage of PIP2 and the release of Ca^{2+} into the cytosol (Thisse and Thisse, 2005). This release of Ca^{2+} was shown to stimulate ESyt1 recruitment to, or the tightening of, ER-PM junctions and the replenishment of PIP2 on the PM (Chang et al., 2013). Such a feedback mechanism would effectively prolong or enhance signaling via PLCγ pathway and hence have an important modulating influence on intracellular signaling. Consistent with this, parallel mass spectrometric studies have shown that the interaction of ESyt2 with ESyt1 is dependent on FGFR activation (F. Guillou, unpublished data). Ca^{2+} has also

been shown in other systems to modulate clathrin-dependent endocytosis (Andersen and Moestrup, 2014; Yamashita, 2012). Thus, the response of the ESyts to Ca^{2+} release may explain their observed ability to modulate growth factor signaling in Xenopus by controlling the rate of endocytosis (Jean et al., 2010). Hence, further studies of the ESyts will certainly generate insight into the mechanisms underlying the cell-specific outcomes of growth factor signaling.

2.4) Materials and Methods

2.4.1) Plasmid constructs

Full-length human ESyt1, ESyt3 and Syt1 cDNAs were amplified from total MCF-7 cDNA and corresponded in coding sequence to FAM62A (NM_015292), FAM2C (NM_031913) and SYT1 (NM_005639). Construction of the human ESyt2b splice variant cDNA was previously described (Jean et al., 2010) and was equivalent in reading frame sequence to FAM62B (NM_020728). The open reading frame for the human ESyt2a splice variant was created from the ESyt2b cDNA by replacing the sequences 5' of the unique SacII site with a synthetic custom gene fragment (Integrated DNA Technologies, IDT) corresponding to the equivalent region of sequence DQ993201. All the ESyt mutants and epitope tagged constructs were created in these original cDNAs, subcloned in PCDNA3 and the full coding sequence of each was determined. The human FGFR1 was obtained from J. Wesche and E. M. Haugsten and was subcloned along with a FLAG N- or HA C-terminal epitope tag in the pCS^{2+} vector. FGFR1 mutants were created directly in this construct using the QuickChange strategy (Agilent Technologies) or by direct PCR amplification and the full coding sequence of each final mutant was determined.

2.4.2) Cell culture and transfections

HEK293T cells were cultured in Dulbecco's modified Eagle's medium supplemented with 10% fetal bovine serum (Wisent). 1.25 x 10^6 293T cells were seeded on poly-L-lysine (1mg/ml) (Sigma) treated 60mm petri dishes 24h prior to transfection.

Transfections were performed by polyethylenimine (PEI). Briefly, DNA was diluted in 400µl of Opti-MEM media (Invitrogen) followed by addition of 10µl PEI at 2mg/ml. After a 10sec vortex, the mixture is added dropwise to the cells. Where indicated, cells were treated with 25 mM SU-5402 (Symansis Cell Signaling Science) or with bFGF (Sigma), 20ng/ml, and Heparin (Sigma), 5µg/ml.

2.4.3) Coimmunoprecipitation

HEK293T cells were processed for co-immunoprecipitation as previously described (Jean et al., 2010). Briefly, 20µg of anti-HA (12CA5) and 20µl of a slurry of Protein A-Sepharose (GE Healthcare), or 20µl of anti-FLAG Agarose beads (Sigma), prepared following manufacturer instructions was added to the lysates and incubated at 4°C for 2h. Bound proteins were eluted with 2 x SDS-PAGE loading buffer, fractionated on Tris-glycine SDS-PAGE gels, transferred to Nitrocellulose membrane (Bio-Rad) and probed with the appropriate antibody. For Western blotting, antibodies were used at 1/1000 (anti-HA, Abcam), 1/1000 (anti-Myc, Cell Signaling), 1/400 (anti-FLAG, Sigma), 1/1000 (anti-Phospho-Tyr783-PLCγ, Cell Signaling), 1/1000 (anti-PLCγ, Abcam), and 1/5000 (anti-Phospho-Tyr (PY99), Santa-Cruz).

2.4.4) Immunofluorescence imaging

Cells were washed with PBS, fixed in 4% PFA for 15 minutes and permeabilized with 0.5 % Triton in PBS for 5 minutes. Incubation with the appropriate primary antibodies was performed for 1h in PBS, 5% BSA or goat serum and cells were then stained with AlexaFluor 488, 568 or 647 conjugated anti-rabbit or -mouse secondary antibodies (Molecular Probes) and counterstained with DAPI. After mounting in 50% glycerol, 50% glycine buffer (0.2 M Na-glycine, 0.3 M NaCl), 3D epifluorescent image stacks were acquired using a Leica SP5 II confocal microscope, equipped with a 63x immersion objective, running in standard scanning.

For FGFR1 uptake assays the above protocol was modified as follows; cells expressing N-terminally FLAG-tagged FGFR1 and HA-tagged ESyt2b were rinsed in

Opti-MEM (Invitrogen) and then incubated for 1h at 4 deg. C with rabbit anti-FLAG antibody diluted 1/500 in Opti-MEM. Subsequently cells were rinsed twice in Opti-MEM at 4 deg. C, incubated for 20 min. in Opti-MEM containing bFGF (Sigma), 20ng/ml, and Heparin (Sigma), 5µg/ml at either 37 deg. C or 4 deg. C (control), rinsed twice, and stained "live" with AlexaFluor 568 conjugated anti-rabbit antibody diluted 1/250 in Opti-MEM for 1h at 4 deg. C. Cells were then fixed and permeabilized before incubation with mouse anti-HA antibody (12CA5) and staining with AlexaFluor 488 conjugated anti-rabbit and AlexaFluor 647 conjugated anti-mouse antibodies, and counterstaining with DAPI.

The use of SNAP-tags (New England Bioloabs) followed the manufacturers recommendations. Briefly, cells were incubated for 30 min. in cell impermeable SNAP-Surface AlexaFluor 488 in culture medium. After 3 rinses in culture medium, cells were further incubated for 30 min. in cell permeable SNAP-Cell TMR-Star in culture medium. Cells were rinsed 3 times over 30 min. to permit unreacted SNAP-Cell ligand to diffuse out of cells, then fixed and observed as above.

2.5) Acknowledgements

We wished to thank Drs J. Wesche and E. M. Haugsten for providing a wild type human FGFR1 construct, and the Sequencing and Genotyping Service of the Quebec University Hospital Research Centre. This work was supported by an operating grant from the Cancer Research Society (CRS/SRC). The Quebec University Hospital Research Centre (CR-CHU de Québec) is supported by a grant from the FRSQ (Québec).

2.6) Competing Interests

The authors declare that there are no competing interests.

2.7) References

Andersen, C.B., and Moestrup, S.K. (2014). How calcium makes endocytic receptors attractive. Trends Biochem Sci *39*, 82-90.

Bae, J.H., Boggon, T.J., Tome, F., Mandiyan, V., Lax, I., and Schlessinger, J. (2010). Asymmetric receptor contact is required for tyrosine autophosphorylation of fibroblast growth factor receptor in living cells. Proc Natl Acad Sci U S A *107*, 2866-2871.

Bae, J.H., Lew, E.D., Yuzawa, S., Tome, F., Lax, I., and Schlessinger, J. (2009). The selectivity of receptor tyrosine kinase signaling is controlled by a secondary SH2 domain binding site. Cell *138*, 514-524.

Bae, J.H., and Schlessinger, J. (2010). Asymmetric tyrosine kinase arrangements in activation or autophosphorylation of receptor tyrosine kinases. Molecules and cells *29*, 443-448.

Bellot, F., Crumley, G., Kaplow, J.M., Schlessinger, J., Jaye, M., and Dionne, C.A. (1991). Ligand-induced transphosphorylation between different FGF receptors. EMBO J *10*, 2849-2854.

Chang, C.L., Hsieh, T.S., Yang, T.T., Rothberg, K.G., Azizoglu, D.B., Volk, E., Liao, J.C., and Liou, J. (2013). Feedback regulation of receptor-induced ca($^{2+}$) signaling mediated by ESyt1 and nir2 at endoplasmic reticulum-plasma membrane junctions. Cell Rep *5*, 813-825.

Creutz, C.E., Snyder, S.L., and Schulz, T.A. (2004). Characterization of the yeast tricalbins: membrane-bound multi-C2-domain proteins that form complexes involved in membrane trafficking. Cell Mol Life Sci *61*, 1208-1220.

Giordano, F., Saheki, Y., Idevall-Hagren, O., Colombo, S.F., Pirruccello, M., Milosevic, I., Gracheva, E.O., Bagriantsev, S.N., Borgese, N., and De Camilli, P. (2013).

PI(4,5)P(2)-dependent and Ca($^{2+}$)-regulated ER-PM interactions mediated by the extended synaptotagmins. Cell *153*, 1494-1509.

Guex, N., and Peitsch, M.C. (1997). SWISS-MODEL and the Swiss-PdbViewer: an environment for comparative protein modeling. Electrophoresis *18*, 2714-2723.

Jean, S., Mikryukov, A., Tremblay, M.G., Baril, J., Guillou, F., Bellenfant, S., and Moss, T. (2010). Extended-synaptotagmin-2 mediates FGF receptor endocytosis and ERK activation in vivo. Dev Cell *19*, 426-439.

Jean, S., Tremblay, M.G., Herdman, C., Guillou, F., and Moss, T. (2012). The endocytic adapter ESyt2 recruits the p21 GTPase activated kinase PAK1 to mediate actin dynamics and FGF signaling. Biol Open *1*, 731-738.

Lee, I., and Hong, W. (2006). Diverse membrane-associated proteins contain a novel SMP domain. Faseb J *20*, 202-206.

Manford, A.G., Stefan, C.J., Yuan, H.L., Macgurn, J.A., and Emr, S.D. (2012). ER-to-plasma membrane tethering proteins regulate cell signaling and ER morphology. Dev Cell *23*, 1129-1140.

Min, S.W., Chang, W.P., and Sudhof, T.C. (2007). ESyts, a family of membranous Ca^{2+}-sensor proteins with multiple C2 domains. Proc Natl Acad Sci U S A *104*, 3823-3828.

Moghadam, P.K., and Jackson, M.B. (2013). The functional significance of synaptotagmin diversity in neuroendocrine secretion. Frontiers in endocrinology *4*, 124.

Mohammadi, M., Dionne, C.A., Li, W., Li, N., Spivak, T., Honegger, A.M., Jaye, M., and Schlessinger, J. (1992). Point mutation in FGF receptor eliminates phosphatidylinositol hydrolysis without affecting mitogenesis. Nature *358*, 681-684.

Mohammadi, M., Schlessinger, J., and Hubbard, S.R. (1996). Structure of the FGF receptor tyrosine kinase domain reveals a novel autoinhibitory mechanism. Cell *86*, 577-587.

Morris, N.J., Ross, S.A., Neveu, J.M., Lane, W.S., and Lienhard, G.E. (1999). Cloning and preliminary characterization of a 121 kDa protein with multiple predicted C2 domains. Biochimica et Biophysica Acta (BBA) - Protein Structure and Molecular Enzymology *1431*, 525-530.

Ong, S.H., Guy, G.R., Hadari, Y.R., Laks, S., Gotoh, N., Schlessinger, J., and Lax, I. (2000). FRS2 proteins recruit intracellular signaling pathways by binding to diverse targets on fibroblast growth factor and nerve growth factor receptors. Mol Cell Biol *20*, 979-989.

Persaud, A., Alberts, P., Hayes, M., Guettler, S., Clarke, I., Sicheri, F., Dirks, P., Ciruna, B., and Rotin, D. (2011). Nedd4-1 binds and ubiquitylates activated FGFR1 to control its endocytosis and function. EMBO J *30*, 3259-3273.

Peters, K.G., Marie, J., Wilson, E., Ives, H.E., Escobedo, J., Del Rosario, M., Mirda, D., and Williams, L.T. (1992). Point mutation of an FGF receptor abolishes phosphatidylinositol turnover and Ca^{2+} flux but not mitogenesis. Nature *358*, 678-681.

Schauder, C.M., Wu, X., Saheki, Y., Narayanaswamy, P., Torta, F., Wenk, M.R., De Camilli, P., and Reinisch, K.M. (2014). Structure of a lipid-bound extended synaptotagmin indicates a role in lipid transfer. Nature *510*, 552-555.

Seet, B.T., Dikic, I., Zhou, M.M., and Pawson, T. (2006). Reading protein modifications with interaction domains. Nat Rev Mol Cell Biol *7*, 473-483.

Thisse, B., and Thisse, C. (2005). Functions and regulations of fibroblast growth factor signaling during embryonic development. Developmental Biology *287*, 390-402.

Yamashita, T. (2012). Ca^{2+}-dependent regulation of synaptic vesicle endocytosis. Neuroscience research *73*, 1-7.

2.8) Figure Legends

Figure 28. ESyt1, 2 and 3 do not penetrate the plasma membrane. A) Diagrammatic structure of the human ESyt family members, including the two studied splice variants of ESyt2, in comparison with human Syt1. B) Sequential anti-FLAG immunofluorescence (IF) labeling of N-terminally FLAG-tagged Syt1, ESyt1, 2 and 3 and the human FGFR1 receptor. The tagged proteins were transiently expressed in HEK293T cells and then labeled before (green) and after (red) membrane permeabilisation. C) N-terminally SNAP™-tagged human and Xenopus ESyt2, and the Adrenergic Receptor β2 (ADRβ2) were expressed in HEK293T and labeled using the SNAP-Surface and SNAP-Cell ligands following the manufacturers instructions (New England Biolabs). D) N-terminally HA-tagged Syt1, ESyt2b and Syt1/ESyt2b fusion proteins were expressed and subjected to anti-HA IF labeling before (green) and after (red) cell permeabilisation as in B). The scale bar in A) to C) indicates 6mm.

Figure 29. All three ESyt proteins and splice variants homo- and hetero-dimerize in vivo. A) N-terminally FLAG-tagged human ESyt1 was co-expressed in HEK293T cells with each of the other N-terminally HA-tagged human ESyt forms and human Syt1. Subsequently, co-immunoprecipitation of FLAG-tagged ESyt1 was determined by Western blot. B) and C) The same analysis was performed respectively for N-terminally FLAG-tagged ESyt2a and ESyt3.

Figure 30. Neither the C2 domains nor the SMP domain are essential for ESyt2b dimerization in vivo. A) Diagrammatic structure of ESyt2b and corresponding deletion mutants. B) and C) Analysis of co-immunoprecipitation of N-terminally HA-tagged full length ESyt2b with the corresponding N-terminally FLAG-tagged deletion mutants co-expressed in HEK293T cells.

Figure 31. Both ESyt2 and 3, but not ESyt1, interact selectively with activated FGFR1. A) to C) co-immunoprecitation of N-terminally FLAG-tagged FGFR1

respectively with N-terminally HA-tagged ESyt2b and 3, ESyt2a and ESyt1 co-expressed in HEK293T cells after receptor activation with bFGF or inhibition with SU5402. FGFR1 activation was monitored by tyrosine auto-phosphorylation (pY). D) ESyt2b is not internalized with FGFR1 on stimulation with FGF. FLAG-FGFR1 and HA-ESyt2b were coexpressed in HEK293T cells and PM associated FGFR1 was labeled in live cell with a primary anti-FLAG. After FGF stimulation (20min.) cells were labeled before fixation and permeabilisation with an Alexa568 conjugated secondary (FGFR1 PM associated, red) then after fixation and permeabilisation with an Alexa488 conjugated secondary (FGFR1 Total, green) and with an HA primary, Alexa693 secondary to display HA-ESyt2b (magenta). The merged panels show overlap of ESyt2b and FGFR1 (indicated by white) is limited to the PM (white arrows) and does not occur after FGFR1 internalization (yellow arrows)

Figure 32. ESyt2b interacts with FGFR1 via TM adjacent sequences. A) Diagrammatic structure of ESyt2b and corresponding deletion mutants. B) and C) Analysis of co-immunoprecipitation of C-terminally HA-tagged FGFR1 with N-terminally FLAG-tagged full-length ESyt2b and corresponding deletion mutants co-expressed in HEK293T cells. D) Diagrammatic summary of the ESyt2b dimerization and FGFR1 interaction domain.

Figure 33. The ESyt2b interaction with FGFR1 depends on receptor activation but not its autophosphorylation. A) Diagrammatic structure of the cytoplasmic region of FGFR1 showing the trans-membrane sequence (TM), the N-terminal and upper and lower C-terminal lobes of the kinase domain, and the autophosphorylation sites. B) Co-immunoprecipitation of C-terminally Myc-tagged ESyt2b with N-terminally FLAG-tagged wild type (WT), kinase dead (KD) and activation loop mutant (Y653 and/or 654F) FGFR1 forms co-expressed in HEK293T cells. In the cases of wild type and kinase dead forms of FGFR1, receptor inhibition with SU5402 demonstrates the high degree of selectivity of ESyt2b for the active form of the receptor. C) Co-immunoprecpitation of ESyt2b with FGFR1 auto-phosphorylation site mutants as in B). D) Co-immunoprecipitation of N-terminally HA-tagged ESyt2b with N-

terminally FLAG tagged wild type FGFR1 (WT) and constitutively active Y653,654E and inactive Y653,654F activation loop mutants as in B), but after receptor activation with bFGF or inhibition with SU5402. In B) to D) receptor activation was monitored by its level of autophosphorylation (pY).

Figure 34. ESyt2b recognizes the activated conformation of FGFR1 independently of catalytic activity. A) Path of the activation loops, respectively from left to right, top to bottom, for the inactive (white) (Mohammadi et al., 1996) (PDB code: 3KY2), activated (Y653/654-phosphorylated, green) (Bae et al., 2009) (PDB code: 3QGI), R577E mutant (blue) (Bae et al., 2010) (PDB code: 3KXX) and overlayed "active" and R577E mutant FGFR1 configurations. The dot surface of the active site aspartic acid (D623) is indicated, as are tyrosine 653 and 654 (Y653/654) side chains and the position of the AMP-PCP non-hydrolysable ATP analog within the inactive configuration. B) Co-immunoprecipitation of N-terminally HA-tagged ESyt2b and N-terminally FLAG tagged wild type FGFR1 (WT), or the corresponding R577E, L422A and Y766F receptor mutants after co-expression of ESyt2b and receptors in HEK293T cells and receptor activation with bFGF. Endogenous PLCg and phospho-PLCg (pY-PLCg) were monitored using specific antibodies. C) Co-immunoprecipitation of N-terminally HA-tagged ESyt2b with N-terminally FLAG tagged wild type FGFR1 (WT), or the corresponding kinase dead K514A (KD) and R577E receptor mutants as in B), but after receptor activation with bFGF or inhibition with SU5402. In B) and C) receptor activation levels were monitored by the level of receptor tyrosine auto-phosphorylation (pY).

Figure 35. C-terminal deletions of FGFR1 reveal that ESyt2b interacts with the N-terminal lobe of the receptor kinase domain. A) Extent of deletion mutants of FGFR1 as compared to the organization of the cytoplasmic domain of the receptor. B) and C) Co-immunoprecipitation of N-terminally HA-tagged ESyt2b with N-terminally FLAG-tagged full length (WT) FGFR1 and corresponding receptor deletion mutants. The Nedd4-1 ubiquitinylation site mutant (FGFR1 Δ6) (Persaud et al., 2011), independently generated in our laboratory, was included in B) and showed that this

modification did not play a part in the ESyt2b interaction. Despite this, other analyses confirmed the role of the Nedd4-1 site in receptor internalization (data not shown).

Figure 36. The conformation of the activation loop may control access to the ESyt2b binding site. A) Left panel: the structure of the activated FGFR1 kinase domain with the ATP analog AMP-PCP bound, the N-terminal kinase lobe is shown boxed. Right panels: the probable structure of a.a. 464 to 550 in the corresponding C-terminal FGFR1 deletion mutant a.a. 1-550, in the presence and absence of the ATP analog. B) Probable structure of the N-terminal kinase lobe in the C-terminal FGFR1 deletion mutant a.a. 1-550 superimposed on the left with the active and on the right the inactive conformations of the activation loop. The N-terminal lobes in A) and B) are taken from the activated catalytic domain FGFR1 structure (Bae et al., 2009) (PDB code: 3QGI), while the superimposed activation loop structures in B) are taken from the activated (red) (Bae et al., 2009) (PDB code: 3QGI) and inactive (white) (Mohammadi et al., 1996) (PDB ID: 3KY2) catalytic domain structures. Images were generated using Swiss-PdbViewer http://www.expasy.org/spdbv/ (Guex and Peitsch, 1997)

2.9) Supplementary Figure Legends

Figure 37. Alignment of the predicted amino acid sequences of the human ESyts 1, 2a, 2b and 3 (Acc. No. NP_056107, ABJ97706.1, NP_065779.1 and NP_114119.2. The putative transmembrane domains are shown in red, the SMP domain in green and the C2 domains in yellow, cyan, magenta, orange and blue.

Figure 38. Anti-FLAG immunofluorescence (IF) labeling of N-terminally FLAG-tagged Syt1, ESyt1, 2 and 3 and the human FGFR1 receptor. The tagged proteins were transiently expressed in HEK293T cells and then labeled before (green, External) and after (red, Total) cell permeabilisation and counter-stained with DAPI. The scale bar in the XY plane indicates 6mm and in the Z plane 5mm.

Figure 39. ESyt2b is not internalized with FGFR1 on stimulation with FGF. FLAG-FGFR1 and HA-ESyt2b were coexpressed in HEK293T cells and PM associated FGFR1 was labeled at 4^{o}C in live cell with a primary anti-FLAG antibody. Cells were then either held at 4^{o}C or subjected to FGF stimulation at 37^{o}C (20min.), and subsequently labeled before fixation and permeabilisation with an Alexa568 conjugated secondary (FGFR1 PM associated, red), then after fixation and permeabilisation with an Alexa488 conjugated secondary (FGFR1 Total, green) and with an HA primary, Alexa693 secondary to display HA-ESyt2b (magenta). The merged panels show overlap of ESyt2b and FGFR1 (indicated by white) is limited to the PM (white arrows) and does not occur after FGFR1 internalization (yellow arrows).

Figure 40. Co-immunoprecipitation of N-terminally HA-tagged ESyt2b with N-terminally FLAG-tagged wild type (WT) and point mutant phospho-site FGFR1 forms after co-expressed in HEK293T cells.

Figure 28. ESyt1, 2 and 3 do not penetrate the plasma membrane.

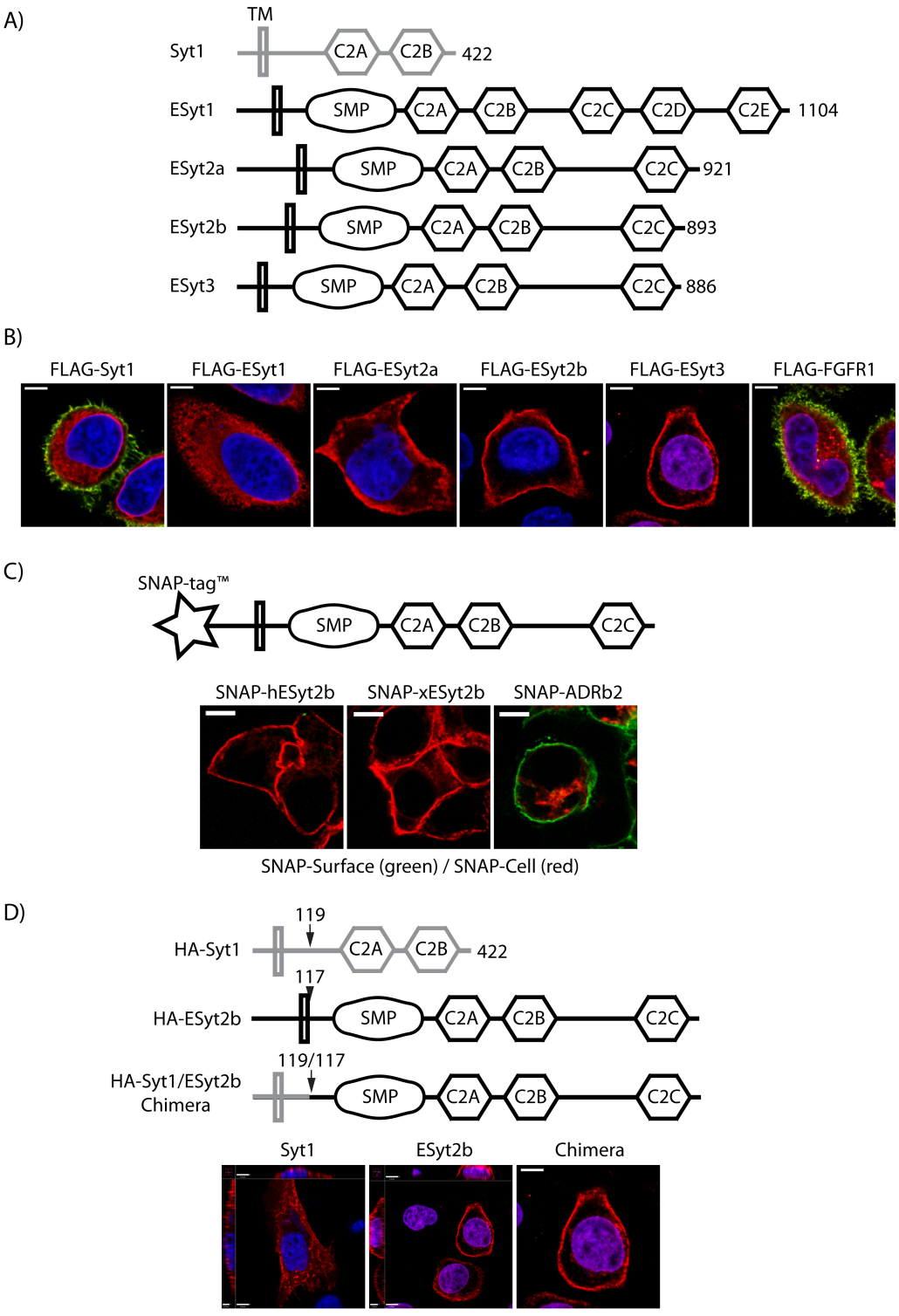

Figure 29. All three ESyt proteins and splice variants homo- and hetero-dimerize in vivo.

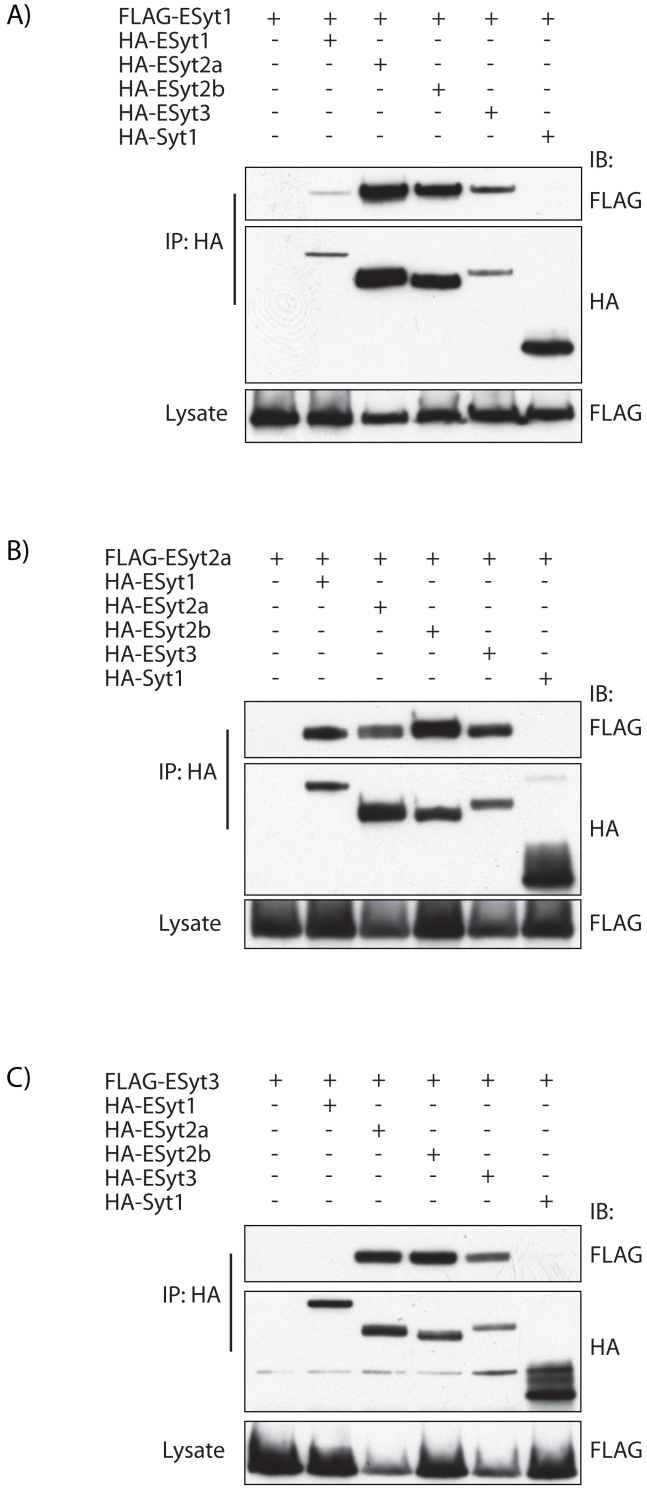

Figure 30. Neither the C2 domains nor the SMP domain are essential for ESyt2b dimerization in vivo.

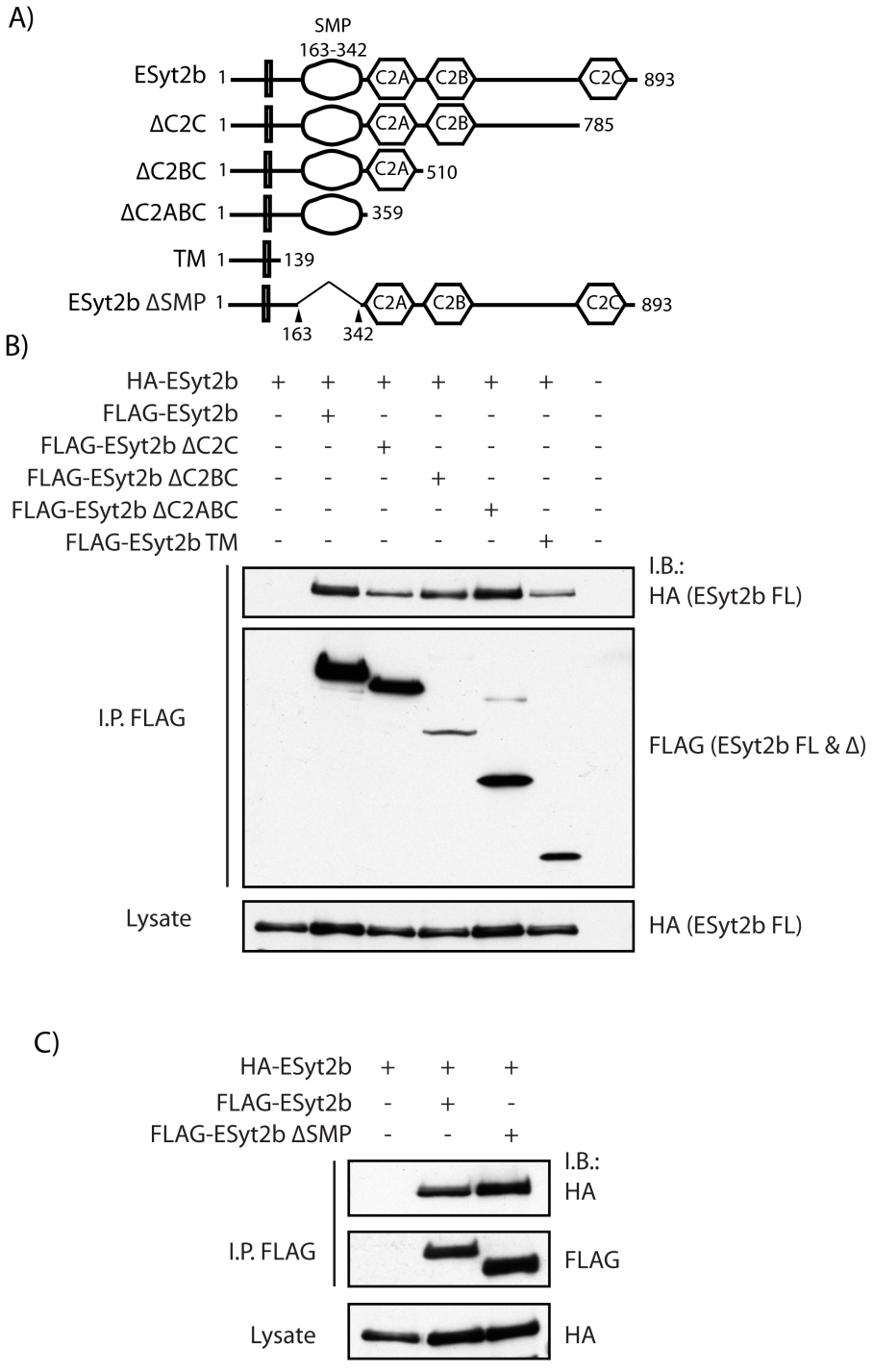

Figure 31. Both ESyt2 and 3, but not ESyt1, interact selectively with activated FGFR1.

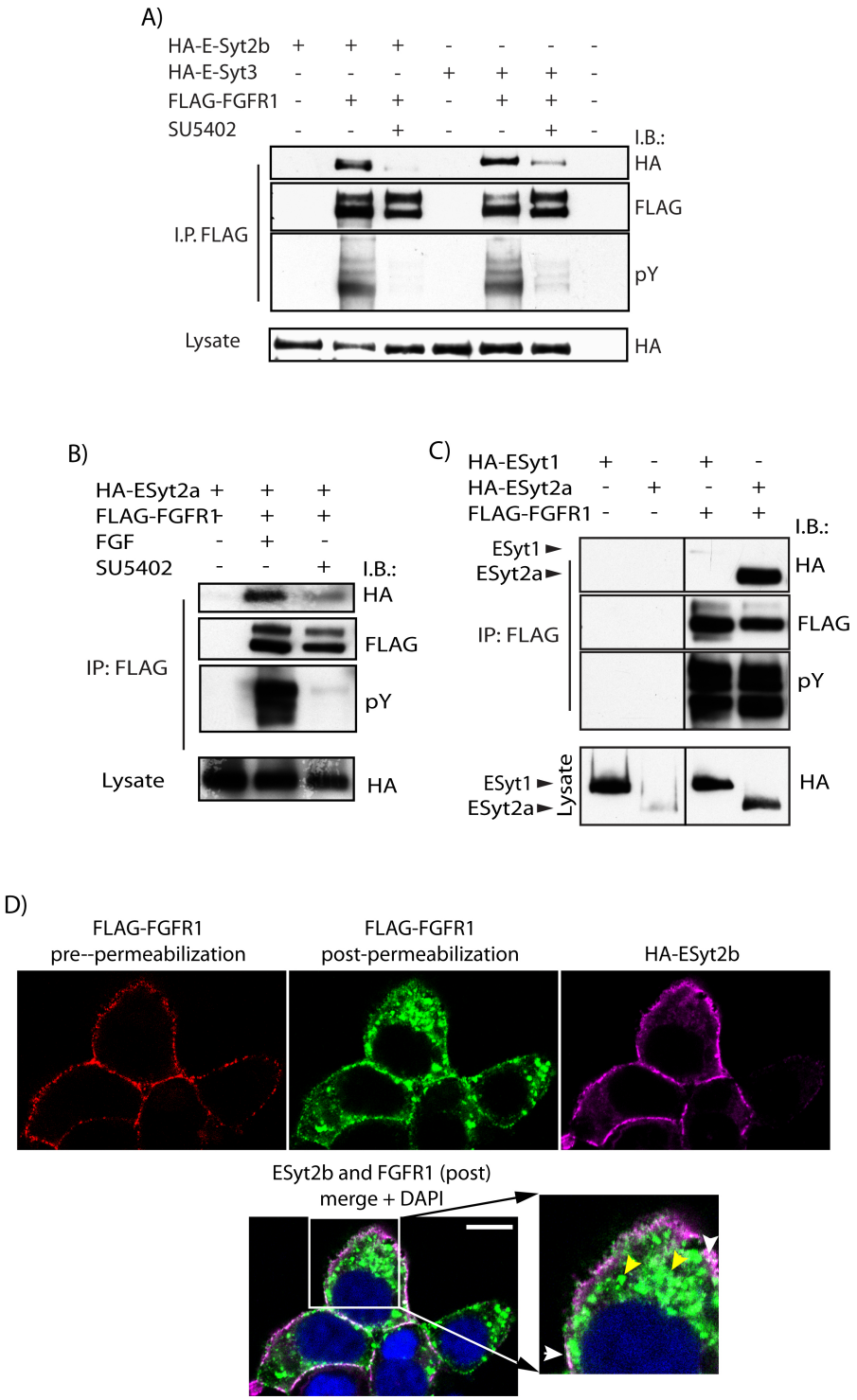

Figure 32. ESyt2b interacts with FGFR1 via TM adjacent sequences.

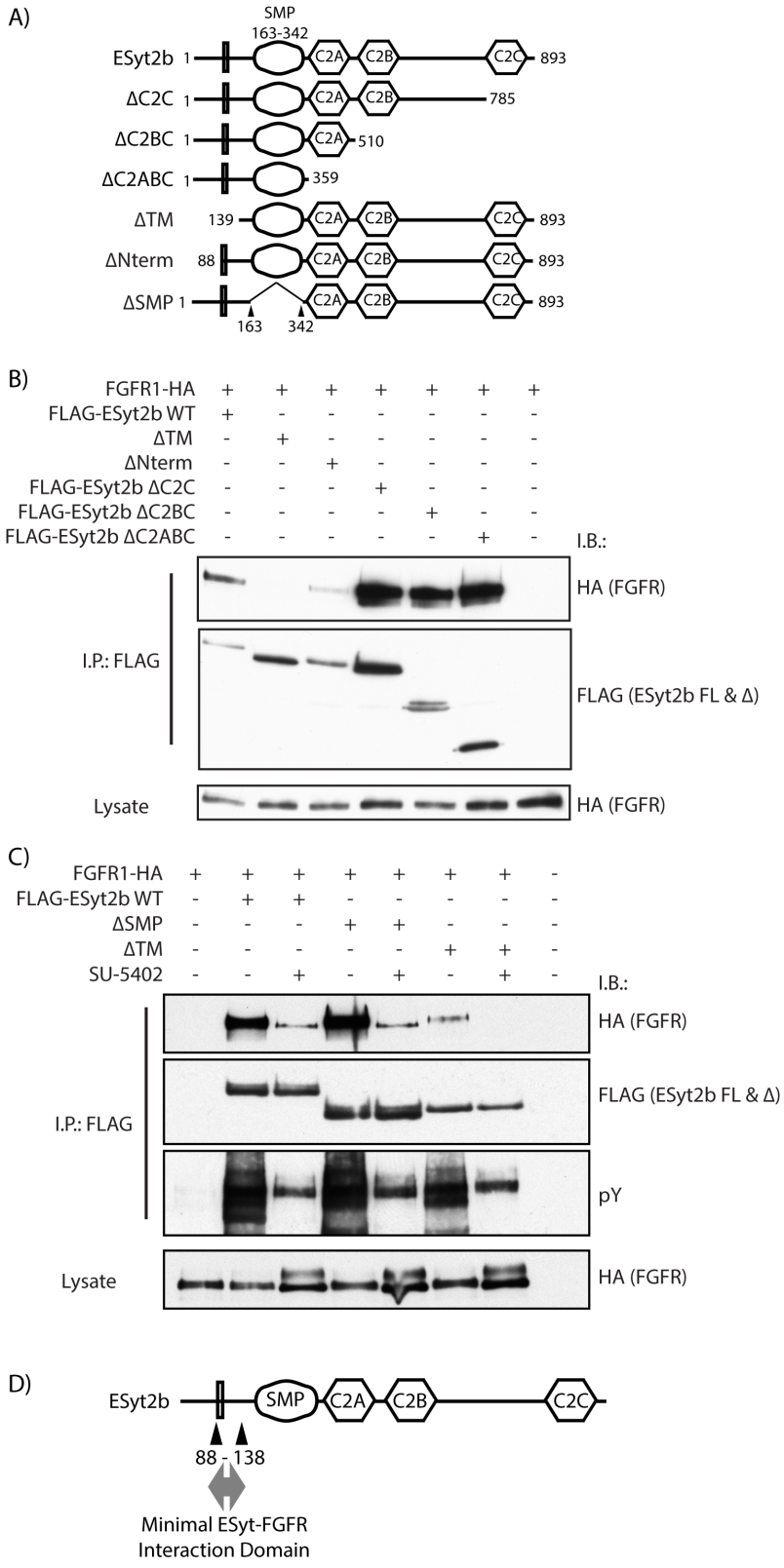

Figure 33. The ESyt2b interaction with FGFR1 depends on receptor activation but not its autophosphorylation.

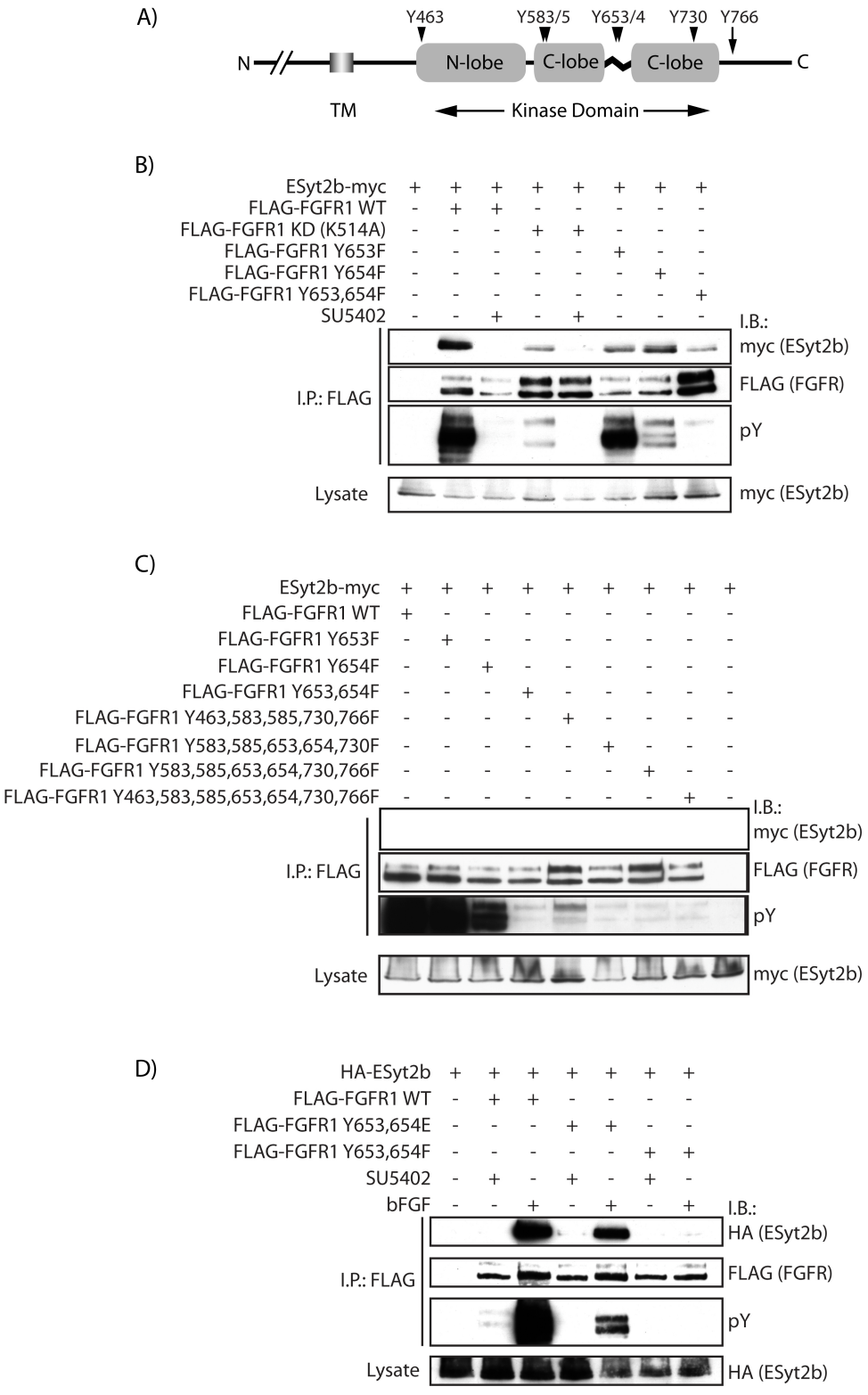

Figure 34. ESyt2b recognizes the activated conformation of FGFR1 independently of catalytic activity.

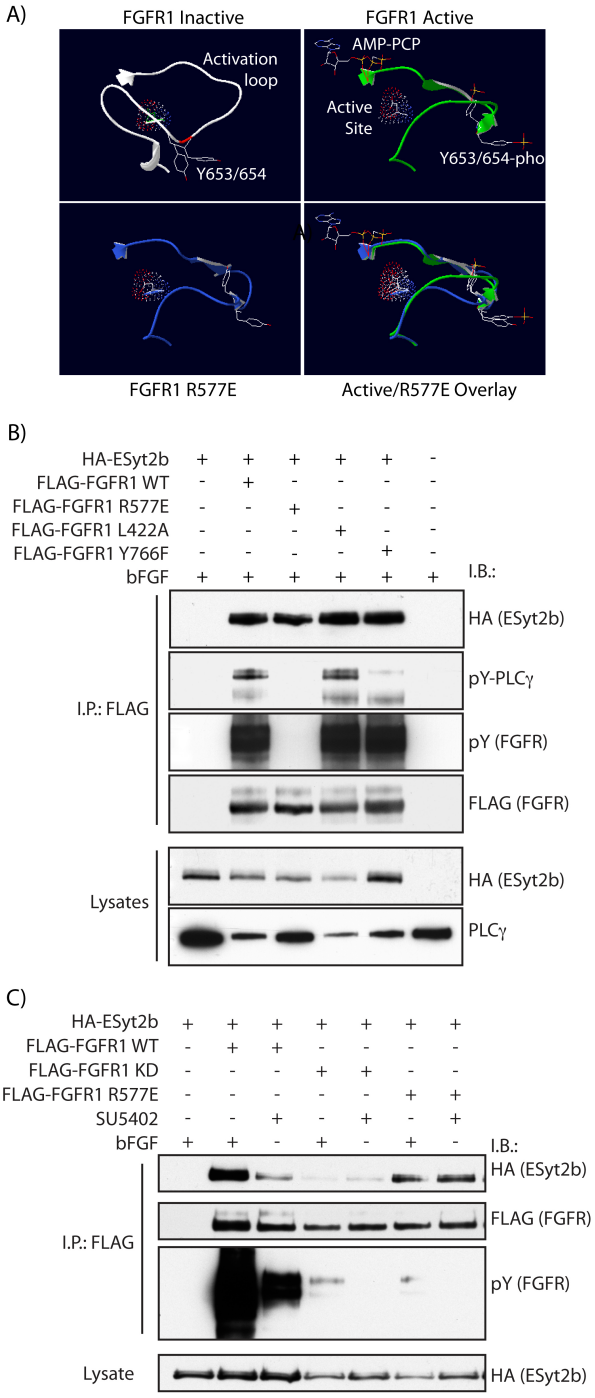

Figure 35. C-terminal deletions of FGFR1 reveal that ESyt2b interacts with the N-terminal lobe of the receptor kinase domain.

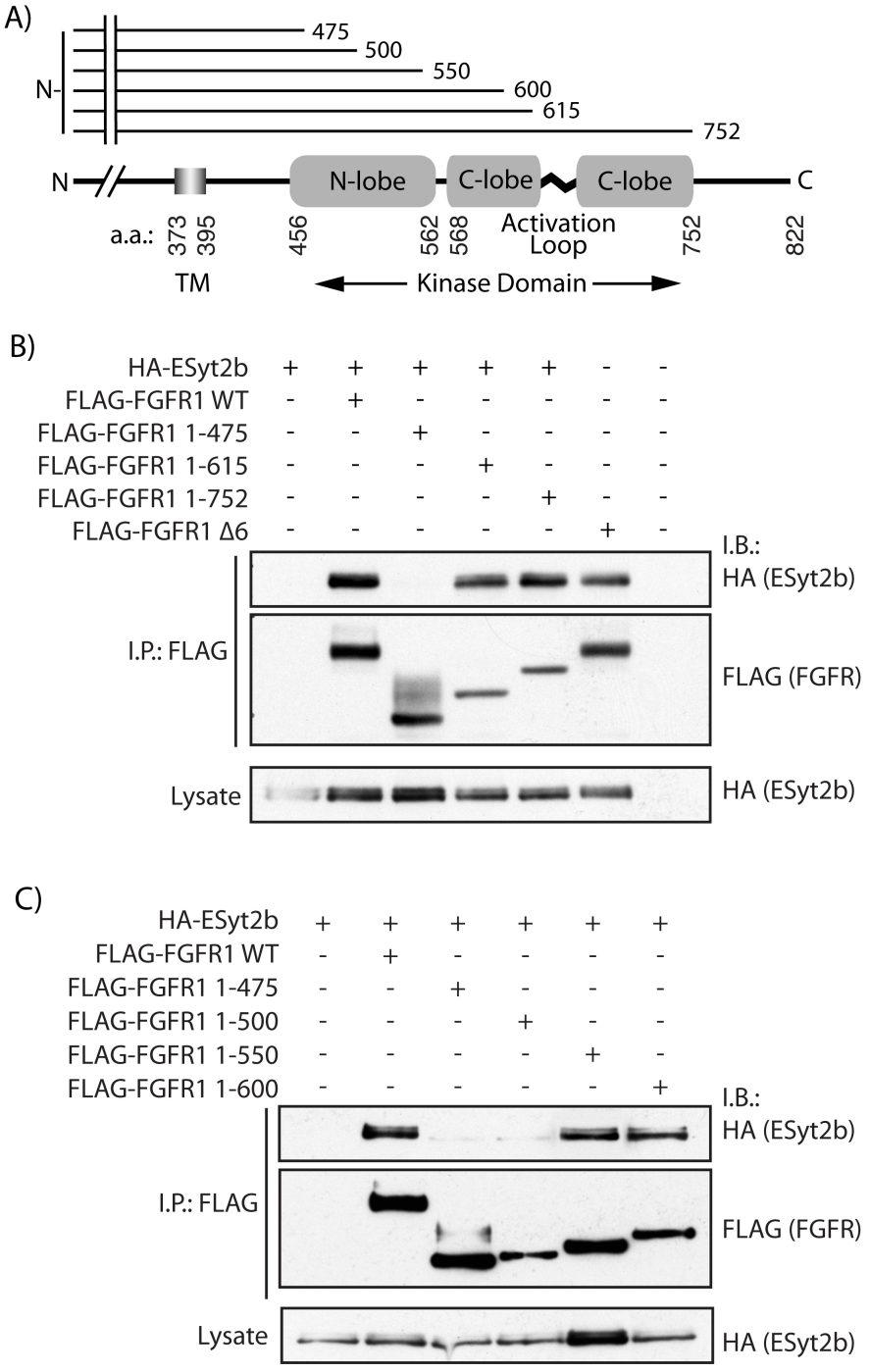

Figure 36. The conformation of the activation loop may control access to the ESyt2b binding site.

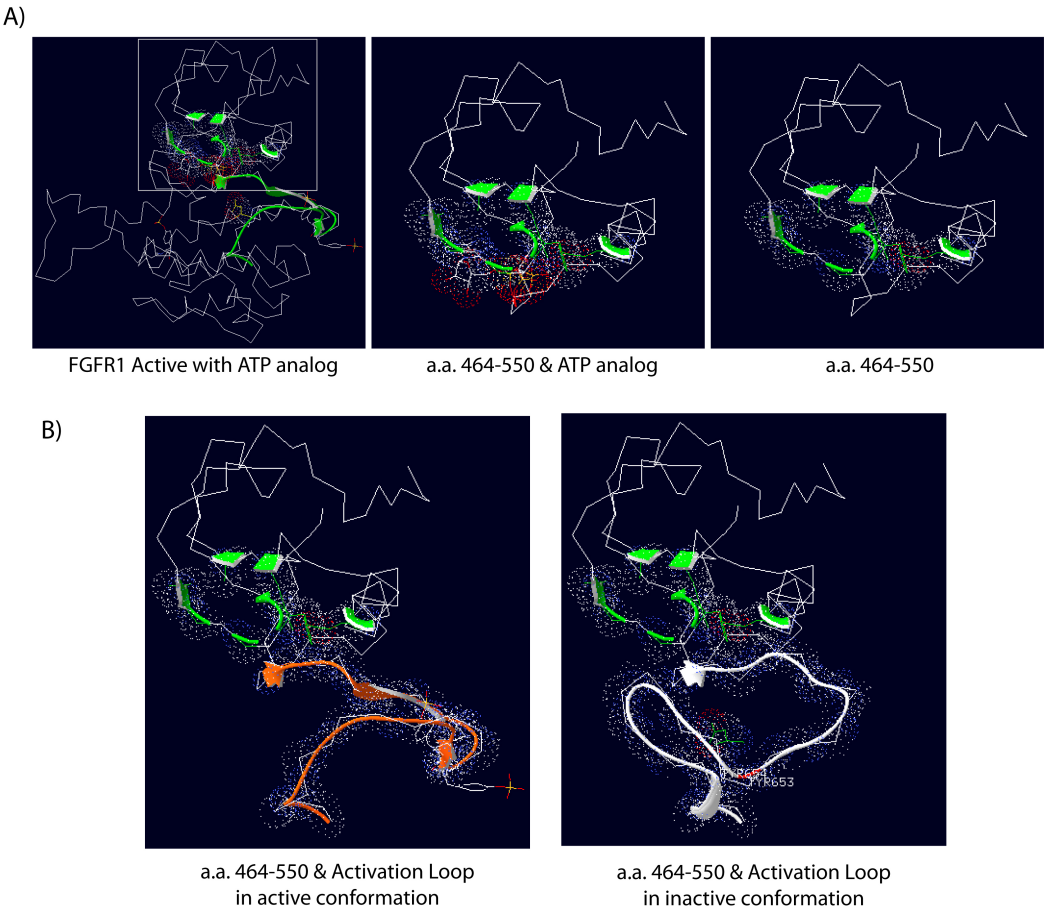

Figure 37 (Supplementary). Alignment of the predicted amino acid sequences of the human ESyts 1, 2a, 2b and 3 (Acc. No. NP_056107, ABJ97706.1, NP_065779.1 and NP_114119.2.

A)

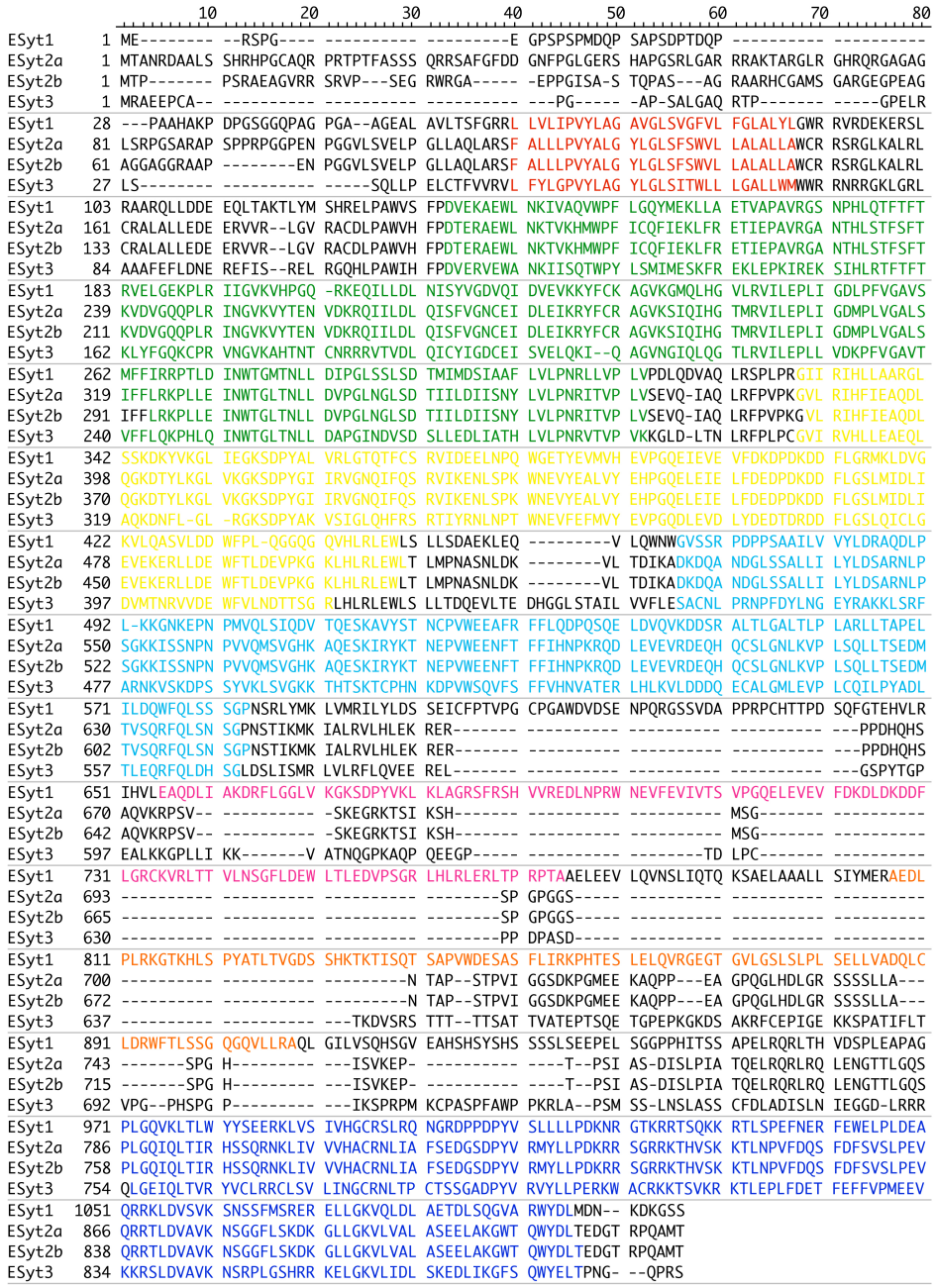

Figure 38 (Supplementary). Anti-FLAG immunofluorescence (IF) labeling of N-terminally FLAG-tagged Syt1, ESyt1, 2 and 3 and the human FGFR1 receptor.

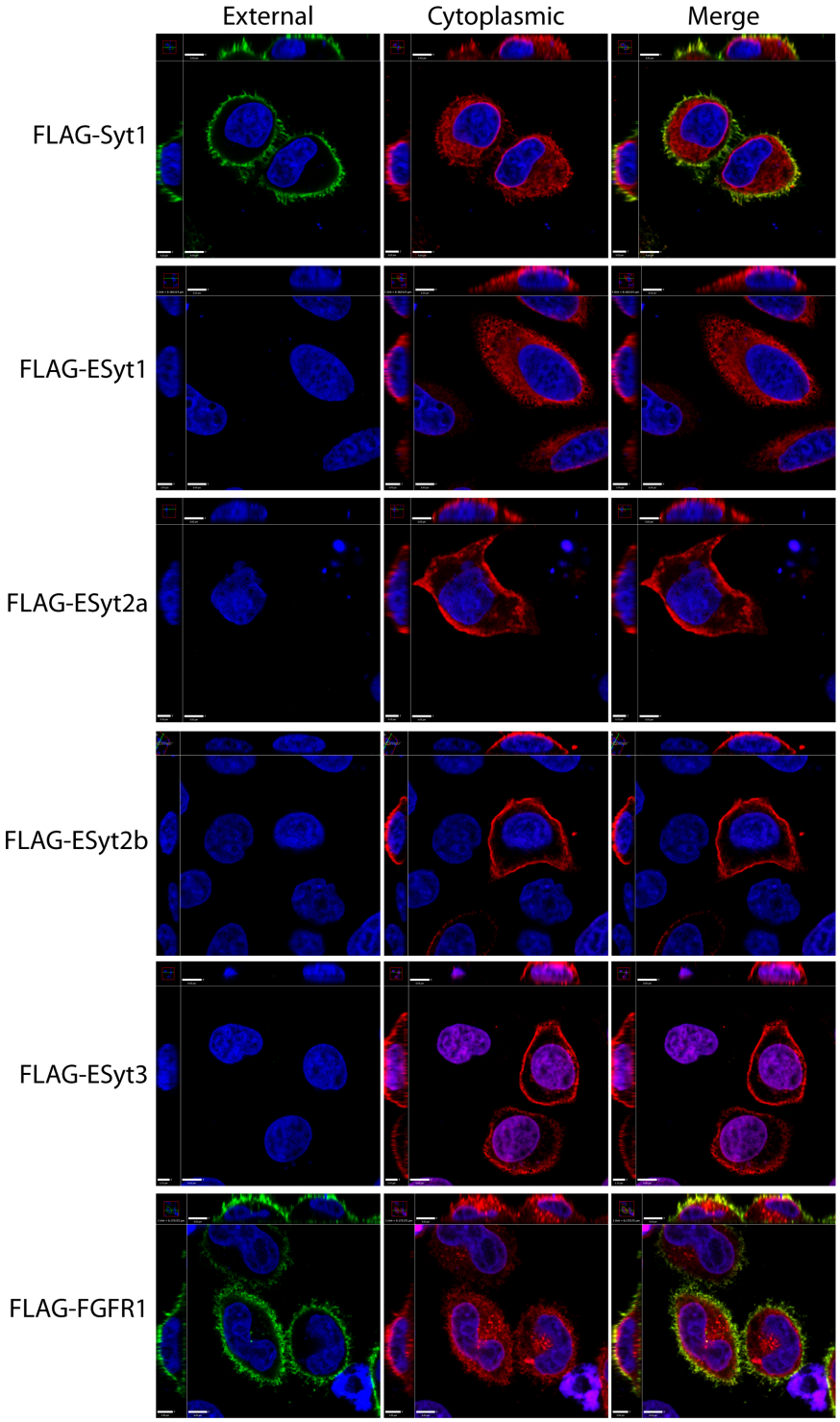

Figure 39 (Supplementary). ESyt2b is not internalized with FGFR1 on stimulation with FGF.

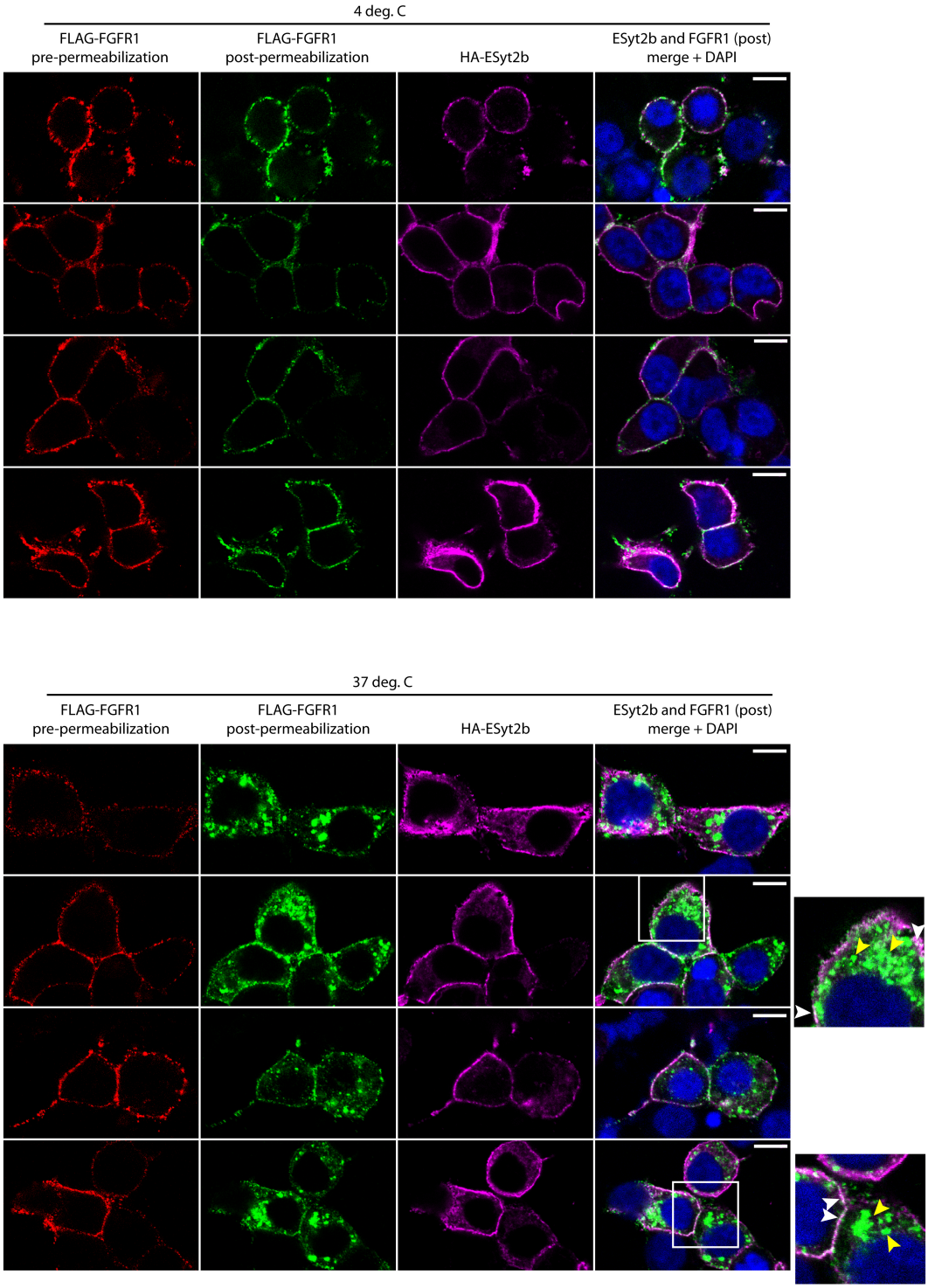

Figure 40 (Supplementary). Co-immunoprecipitation of N-terminally HA-tagged ESyt2b with N-terminally FLAG-tagged wild type (WT) and point mutant phospho-site FGFR1 forms after co-expressed in HEK293T cells.

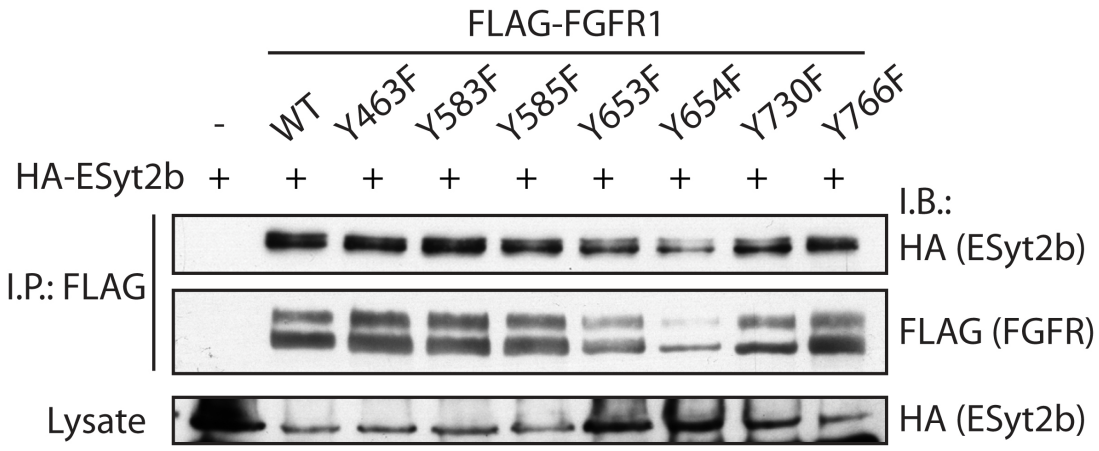

Chapter 3

ESyt 2/3 loss affects the viability of the Mouse Embryonic Fibroblast cells under stress.

Prakash K. Mishra and Tom Moss

Foreword

The study presented in this chapter was undertaken to compare the growth characteristics of cells lacking ESyt2 and ESyt3. As such, it formed part of the larger laboratory study of the effects of ESyt2/3 loss in mouse. Part of the work presented in this chapter was included in the publication "Loss of Extended Synaptotagmins ESyt2 and ESyt3 does not affect mouse development or viability, but in vitro cell migration and survival under stress are affected." (Herdman et al., 2014).

Résumé

La famille des « Extended Synaptotagmins » est connue pour son implication dans de multiples fonctions cellulaires, cependant le rôle de ces protéines *in vivo* demeure largement inconnu. Elles ont été impliquées dans plusieurs fonctions tissulaires et cellulaires chez les mammifères incluant la signalisation récepteur dépendante, l'endocytose, la formation des jonctions entre le reticulum endoplasmique et la membrane plasmique (RE-MP), la sensibilité au calcium. Ils ont été impliqués également dans l'induction de la formation du mésoderme et l'embriogénèse chez *Xenopus* ainsi que chez *C.elegans*. Etonnamment, l'élimination de 2 des 3 membres de cette famille protéique, ESyt2 et ESyt3, n'affecte pas le développement des souris, leur viabilité et n'induit aucun changement phénotypique particulier. Cependant, l'analyse des fibroblastes embryonnaire de souris (FESs) en culture cellulaire montre des défauts de migration ainsi qu'une sensibilité accrue à des conditions de culture stringentes ou aux stress oxydatif. La perte de ESyt2 ou celle de Esyt2 et 3 dans des FESs immortalisées par l'antigène T du virus SV40 réduit leur viabilité dans un milieu sans sérum comparé à des FESs de type sauvage possédant le même contexte génétique. De plus, la perte de ESyt2/3 rend les FESs plus sensibles aux stress oxydatifs. Et donc, malgré l'absence de phénotype dans les études sur l'animal, la perte de ESyt2 et 3 affecte certaines réponses cellulaires résultants probablement de défauts dans la transduction du signal en général.

Abstract

Extended Synaptotagmins have been reported to be involved in multiple cellular functions, but the in vivo requirements for these proteins remains largely unknown. They have been implicated in several cell and tissue functions in mammals including receptor signaling, endocytosis, endoplasmic reticulum-plasma membrane (ER-PM) junction formation, calcium sensing, as well as mesoderm induction and embryogenesis in *Xenopus* and *C. elegans*. It was therefore surprising to find that the elimination of two of the three members of this family of proteins, i.e. ESyt 2 and ESyt3, did not affect mouse development or viability, nor did it induce any detected change in phenotype. This said, by analysing mouse embryonic fibroblast (MEFs) in culture both defects in migration and susceptibilities to stringent culture conditions and oxidative stress were observed. Loss of ESyt 2 or loss of ESyt2 and 3 in SV40 T-antigen immortalized MEFs reduce their viability in serum free media as compared to wild type MEFs from the same genetic background. Further, ESyt2/3 loss renders the MEFs prone to oxidative stress. Thus, despite a lack of phenotype in whole animal studies, loss of ESyt2 and 3 does indeed affect certain cellular responses that are probably the result of defects in signal transduction.

3.1) Introduction

The Extended Synaptotagmins (ESyts) have been implicated in receptor signaling, and receptor endocytosis, as well as being required for mesoderm induction in *Xenopus* and cell division in *C. elegans*. The recent discovery that the ESyts are ER-resident protein and help in the formation of ER-PM contact site has yet further increased the possible number of roles they play (Giordano et al., 2013). But even after more than a decade of research we still do not know the in vivo requirements for the ESyts in mammals. The importance of membrane contact sites (MCS) in maintaining normal homeostasis in cells is well known (Voelker, 2009; Lewis, 2007). The C2 domains of the ESyts may play a direct role in calcium signaling, while the SMP domain could be responsible for lipid transport and either domain could also be an interaction site for protein partners. Xenopus ESyt2 has been shown to serve as an endocytic adapter that determines the timing of ERK activation in blastula embryos by binding both Fibroblast Growth Factor Receptor (FGFR) and Adaptin 2 (AP-2) to catalyze rapid receptor endocytosis via the Clathrin pathway (Jean et al., 2010). Also, ESyt2 recruits the cytoskeleton regulator p21-Activated-Kinase-1 (PAK1) to modulate the cortical actin de-polymerization logically required for endocytosis (Jean et al., 2012; McMahon et al., 2011). ESyt2 and ESyt3 are present in the ER-PM junction and strongly bind to the plasma membrane. In comparison, ESyt1 only localizes to ER-PM junctions in in response to enhanced Ca^{2+}.

However, we have failed to observe any significant phenotype in ESyt2$^{-/-}$/3$^{-/-}$ double knock out mice (see Annexe) (Herdman et al., 2014). Hence, we undertook several lines of study to determine whether a phenotype could be identified under defined conditions in cell culture.

In this chapter I present the growth response of Mouse Embryonic Fibroblasts (MEFs) isolated from ESyt2/3$^{-/-}$ mice to various stringencies of in vitro culture and to the oxidative stress. Part of this work was included in our published studies of ESyt2/3 loss (Herdman et al., 2014).

3.2) Results

In order to study the difference in growth pattern and in viability of cells lacking ESyt2 and 3, we generated MEFs from E14.5 ESyt 2/3 null and from ESyt2/3$^{+/+}$ mouse embryos (Giroux et al., 1999; Bisson et al., 2008). These cells were then immortalized by transfection with pBSV0.3T/t, which expresses both SV40 large T and small t antigens (*SvTt*).

3.2.1) ESyt 2/3 deficient MEFs are more susceptible to serum withdrawal than their wild type counterparts.

Initially the immortalized MEFs were cultured for 7.5 days in serum-free and antibiotic-free medium (SFM) with or without fetal bovine serum (FBS) or fibroblast growth factor (FGF). As shown in Figure 41 A and B the ESyt 2/3$^{-/-}$ (DKO) MEFs grew in media containing FBS similarly to the ESyt2/3$^{+/+}$ (WT) MEFs. Both DKO and WT MEFs also grew in SFM supplemented with FGF, however, their proliferation was somewhat reduced as compared with MEFs grown in FBS supplemented SFM. WT MEFs also continued to proliferate in SFM lacking both FBS and FGF albeit more slowly than in the presence of FBS or FGF (Figure 41A). In contrast, the DKO MEFs grown in the absence of both FBS and FGF underwent extensive cell death (Figure 41B).

3.2.2) Serum withdrawal differentially affects immortalized MEFs.

Before immortalization, primary MEFs grow relatively slowly and after a certain number of cell divisions become quiescent, and when subjected to serum free conditions show a similar behavior. Figure 42 shows a comparison of the effects of serum withdrawal over 2 weeks on WT and DKO primary and immortalized MEFs. As observed in Figure 41, immortalized WT MEFs continue to proliferate in the

serum free media while the immortalized DKO MEFs die. On the other hand, though WT and DKO primary MEFs arrest division, they survive and their cell bodies appear to grow in size. This suggests that enhanced cell division driven by oncogenic immortalization renders the DKO cells differentially sensitive to serum withdrawal.

3.2.3) Inhibition of FGF signaling affects the initial phase of growth of WT and DKO MEFs equally.

Since *Xenopus* ESyt2 has been implicated in FGF signaling (Jean et al., 2010), I first determined the effect of short-term treatment of both WT and DKO immortalized MEFs with the FGFR1 specific inhibitor SU5402 on their initial rate of growth (Figure 43). When MEFs were cultured for 2 days in serum-free medium to which SU5402 was added, both WT and DKO MEFs suffered roughly equal levels of cell death, while the addition of FGF improved survival of both cell types. These observations were consistent with short-term assays of MAP-kinase (ERK) activation by FGF, which was unaffected by deletion of ESyt2 and 3 (Herdman et al., 2014).

3.2.4) Long-term SU5402 treatment causes cell death in both immortalized DKO and WT MEFs.

Figure 44A and B show comparisons of DKO and WT immortalized MEFs grown under different conditions over a period of 5 days. Both cell types respond similarly in most of the conditions studied, except those in which only serum free media available. The DKO MEFs show extensive cell death both in SFM and in SFM plus SU5402, while the WT MEFs clearly continue to grow in SFM but rapidly die when grown in SFM plus SU5402. Thus, autocrine signaling through the FGF receptor appears to be sufficient to maintain viability and proliferation of the WT MEFs but not of the DKO MEFs. The data therefore suggest that the DKO MEFs are partially

defective in FGF signaling and that this effect can be overcome by addition of exogenous FGF to the medium.

In order to better quantify these data, I also performed cell proliferation/viability assays on WT and DKO MEFs cultured under the different conditions. Cells were plated at a fixed density and then allowed to grow in different medium condition for 4 days before determining relative viable cell counts using Resazurin, a nonfluorescent substrate which is converted to fluorescent resofurin in viable cells. These data (Figure 44C) quantitatively confirm that both WT and DKO MEFs respond similarly to serum, FGF and FGF receptor inhibition (SU), but differently to serum withdrawal. It is clear from the data that a residual autocrine signal passing via the FGF receptor is sufficient to maintain WT MEFs viable and that inhibition with SU5402 block this signal, reducing their proliferation/survival to that of the DKO MEFs. Consistent with this, SU5402 has no negative effect on the proliferation/survival of DKO MEFs beyond that of serum withdrawal.

3.2.5) Esyt 2/3 deficient MEFs are highly prone to oxidative stress.

DKO MEFs were found to be highly prone to the oxidative stress. DKO and WT MEFs were treated overnight (ON) with 0.2 mM or 0.4mM H_2O_2 in SFM with or without addition of FGF, then transferred to SFM plus 10% FBS and cultured overnight. Only around 10% of the DKO cells survived this treatment (Figure 45A). In contrast, more than 50% of the WT MEFs survived the same treatment. The addition of FGF to the medium did not visibly confer much protection to DKO MEFs, whereas it obviously confered some protection to WT MEFs (Figure 45B). These effects were also quantified using the Resazurin cell viability assay as in section 3.2.4. For the cell viability assay, MEFs were treated for only 2h with 0.2 mM or 0.4mM H_2O_2 in SFM. As can be seen from Figure 45C, the DKO MEFs were far more sensitive to H_2O_2 than the WT, but in both cases survival was quantitatively

improved by FGF. Thus, here again the DKO MEFs did appear to respond to FGF, but were clearly exceptionally sensitive to oxidative stress.

3.3) Discussion

During our studies of ESyt "knockout" mice, we found that loss of both ESyt2 and ESyt3 had no detectable effect on mouse development, viability or fertility (Herdman et al., 2014). This was very surprising given that our lab had shown experimentally that ESyt2 was necessary for mesoderm induction during early *Xenopus* embryogenesis (Jean et al., 2010). In *Xenopus*, ESyt2 was found to be required for FGF signaling, a function that was correlated with a direct interaction with the activated FGF receptor, and in the absence of ESyt2 with a delay in endocytosis of the receptor that prevented normal activation of the ERK MAP-kinase pathway. A subsequent manuscript from our group showed that ESyt2 recruited PAK1 to suppress cortical actin polymerization, possibly explaining how ESyt2 facilitates receptor endocytosis (Jean et al., 2012).

However, by studying MEFs from mice lacking both ESyt2 and 3 I was able to show that indeed loss of these proteins causes a defect in FGF signaling. Comparison of immortalized ESyt2/3$^{-/-}$ (DKO) MEFs with their wild type (WT) counterparts showed that both cell types grew equivalently in standard medium containing fetal serum (FBS). The WT MEFs continued to grow and showed good survival even when serum was withdrawn. However, specific inhibition of the FGF receptor in the absence of serum caused the WT MEFs to arrest growth and to rapidly succumb to cell death. In contrast, the DKO MEFs already grew extremely poorly in serum-free medium and inbition of the FGF receptor had little or no further effect. This strongly suggested that a level of autocrine signaling via the FGF receptor was sufficient for growth and survival of the WT MEFs and that this FGF pathway was either defective or the autocrine signal was lacking in the DKO MEFs. Thus, the data strongly suggest that loss of ESyt2 and 3 indeed causes a defect in FGF signaling, at least in immortalized MEFs. Thus said, both WT and DKO MEFs responded similarly to

FGF when grown in serum-free medium. This tends to suggest that the DKO MEFs retain a functional FGF signaling pathway, but lack the residual endocrine signal that enables the WT MEFs to survive. Further sudies will be necessary to discern which scenario is correct, that is the DKO MEFs either suffer from a partial defect in FGF signaling or the lack of an autocrine FGF signal. This may explain the observation that ESyt2/3 loss affects in vitro FGF stimulated cell migation (Herdman et al., 2014).

The enhanced sensitivity of the DKO MEFs might also be related to a partial deficit in cell signal transduction. Wang et al. (2001) reported that PLCγ1 null MEFs are also more susceptible to the H_2O_2 treatment than WT MEFs and that ectopic expression of PLCγ1 restored the WT level of resistance. One major target of FGF signaling is of course PLCγ activation. The sensitivity of the DKO MEFs to oxidative stress may also reveal a partial deficit in signaling through the FGF receptor. Figure 46 shows an overview of the possible Esyt functions and the known effects of Esyt 2/3 loss.

3.4) Materials and Methods

3.4.1) Reagents and chemicals.

Dulbecco's Modified Eagle Medium (DMEM), Penicillin/Streptomycin/Antimycotic (Anti-Anti), heparin and basic FGF (bFGF) were from Invitrogen. SU5402 was from EMD/Merck and resazurin from Sigma-Aldrich.

3.4.2) Cell culture.

Mouse embryo fibroblasts (MEFs) from E14.5 embryos were prepared as described and routinely cultured in Dulbecco's modified Eagle medium (DMEM) – high glucose (Invitrogen), supplemented with 10% fetal bovine serum (FBS, Wisent) and Penicillin/Streptomycin/Antimycotic (Anti-Anti, Invitrogen).

3.4.3) Cell viability asays.

On day 0, cells were seeded at a density of 75,000/well in 6-well plates. On day 1, cells were rinsed twice with serum-free and antibiotic-free medium (SFM) and then cultured for 6h in the same medium. Culture medium was replaced with SFM alone or supplemented by either 10% FBS, by bFGF (5 µg/ml heparin, 20ng/ml bFGF (Invitrogen)), by 25 mM SU5402 (EMD/Merck), or by bFGF plus SU5402. On day 3 cells were briefly rinsed twice in SFM and cultured until day 5 in fresh aliquots of the respective media.

To determine cell viability, media were replaced with PBS containing 0.001% Resazurin (Sigma-Aldrich) and incubated for a further 2h before estimating the viable cell count using the relative fluorescence units (RFU) of resofurin in the cell supernatant (ex. 544nm, em. 590nm, Fluoroskan Ascent, Thermo Biolabs) (Ahmed et al., 1994). The effects of oxidative stress on viability were measured in a similar way, except that on day 1, cells were treated for 2h with the indicated concentrations of H_2O_2 or H_2O_2 plus bFGF in SFM. Cells were then briefly rinsed twice in SFM before addition of medium containing 10% FBS. At day 3, cells were then subjected to the resazurin assay as above.

3.4.4) Isolation and culture of mouse embryonic fibroblast (MEFs):

Preparation and culturing of MEFs were done based on standard procedures, as described in Herdman et al., 2014 (Annexe).

3.4.5) Serum starvation and oxidative stress assay:

The method for serum starvation and oxidative stress is described in Herdman et al., 2014 (Annexe).

3.4.6) Cell imaging and resazurin cell viability assay:

Images were taken by widefield flurorescense microscope. The protocol for resazurin cell viability assay was done as recommended by the manufacturer, described in Herdman et al., 2014 (Annexe).

3.5) References

Bisson, N., et al. (2008). "Mice lacking both mixed-lineage kinase genes Mlk1 and Mlk2 retain a wild type phenotype." Cell Cycle **7**(7): 909-916.

Bowes, J. B., et al. (2010). "Xenbase: gene expression and improved integration." Nucleic Acids Res **38**(Database issue): D607-612.

Giordano, F., et al. (2013). "PI(4,5)P(2)-dependent and Ca($^{2+}$)-regulated ER-PM interactions mediated by the extended synaptotagmins." Cell **153**(7): 1494-1509.

Giroux, S., et al. (1999). "Embryonic death of Mek1-deficient mice reveals a role for this kinase in angiogenesis in the labyrinthine region of the placenta." Curr Biol **9**(7): 369-372.

Jean, S., et al. (2010). "Extended-synaptotagmin-2 mediates FGF receptor endocytosis and ERK activation in vivo." Dev Cell **19**(3): 426-439.

Jean, S., et al. (2012). "The endocytic adapter E-Syt2 recruits the p21 GTPase activated kinase PAK1 to mediate actin dynamics and FGF signaling." Biol Open **1**(8): 731-738.

Lewis, R. S. (2007). "The molecular choreography of a store-operated calcium channel." Nature **446**(7133): 284-287.

Manford, A. G., et al. (2012). "ER-to-plasma membrane tethering proteins regulate cell signaling and ER morphology." Dev Cell **23**(6): 1129-1140.

Voelker, D. R. (2009). "Genetic and biochemical analysis of non-vesicular lipid traffic." Annu Rev Biochem **78**: 827-856.

Wang, X. T., et al. (2001). "Oxidative stress-induced phospholipase C-gamma 1 activation enhances cell survival." J Biol Chem **276**(30): 28364-28371.

3.6) Figure legends

Figure 41: Effect of serum withdrawal on ESyt 2/3 deficient and wild type mouse embryonic fibroblasts (MEFS). MEFs were cultured for 7.5 days in serum-free and antibiotic-free medium (SFM) with or without addition of fetal bovine serum (FBS) or fibroblast growth factor (FGF). Images were taken using wide-field fluorescence microscope at the respective time point as indicated in the figure. The withdrawal of both FBS and FGF resulted in limited proliferation and extensive cell death in the double knock out (DKO) MEFs (Figure 41B) as compared to the wild type (WT) MEFs (Figure 41A).

Figure 42: Comparison of immortalized vs. primary WT and ESyt 2/3 DKO MEFs. MEFs were cultured for a period of 2 weeks in serum-free and antibiotic-free medium before taking the images using wide-field fluorescence microscope.

Figure 43: Effect of inhibition of FGF signaling on the ESyt 2/3 DKO and WT MEFs. MEFs were cultured for 2 days in serum-free and antibiotic-free medium with or without FBS /FGF/ or FGFR1 specific inhibitor SU5402 either alone or in combination with FGF. Images were taken using wide-field fluorescence microscope at the respective time point as indicated in the figure.

Figure 44: Effect of serum withdrawal or inhibition of FGF signaling in ESyt 2/3 DKO and WT MEFs. Cells were cultured for 5 days in serum-free and antibiotic-free medium (SFM) containing FBS, FGF, SU5402 (SU), SU5402 plus FGF or no addition. Figure 44A shows the effect in DKO MEFs while Figure 44B shows the effect in WT MEFs. Figure 44C: Cell viability assay. Cell viability assay was done via enzymatic reduction of resazurin to resorufin. Results are given in arbitrary relative fluorescence units (RFU). The control condition (with FBS) was assumed as 100% and the graph was plotted as relative % change.

Figure 45: Response of ESyt 2/3 DKO and WT MEFs when subjected to the oxidative stress. Cells were subjected to the overnight (ON) treatment with the indicated concentrations of H_2O_2 in serum free medium in the presence (Figure 45A) or absence of bFGF (Figure 45B). Subsequently cells were grown in FBS supplemented serum for another day before taking the images using wide-field fluorescence microscope. Figure 45C: A graphical representation of number of viable cells remained after 2Hrs of H_2O_2 treatment. Cells were treated for 2 h with the indicated concentrations of H_2O_2 in serum free medium in the presence or absence of bFGF. Subsequently cells were grown in FBS supplemented serum for 2 days before determining viable cells via resazurin conversion. Results are given in arbitrary relative fluorescence units (RFU). The graph represents the percentage change compared to the control conditions (with serum) assuming it to be 100%.

Figure 46: Overview of ESyt function.

3.7) Figures

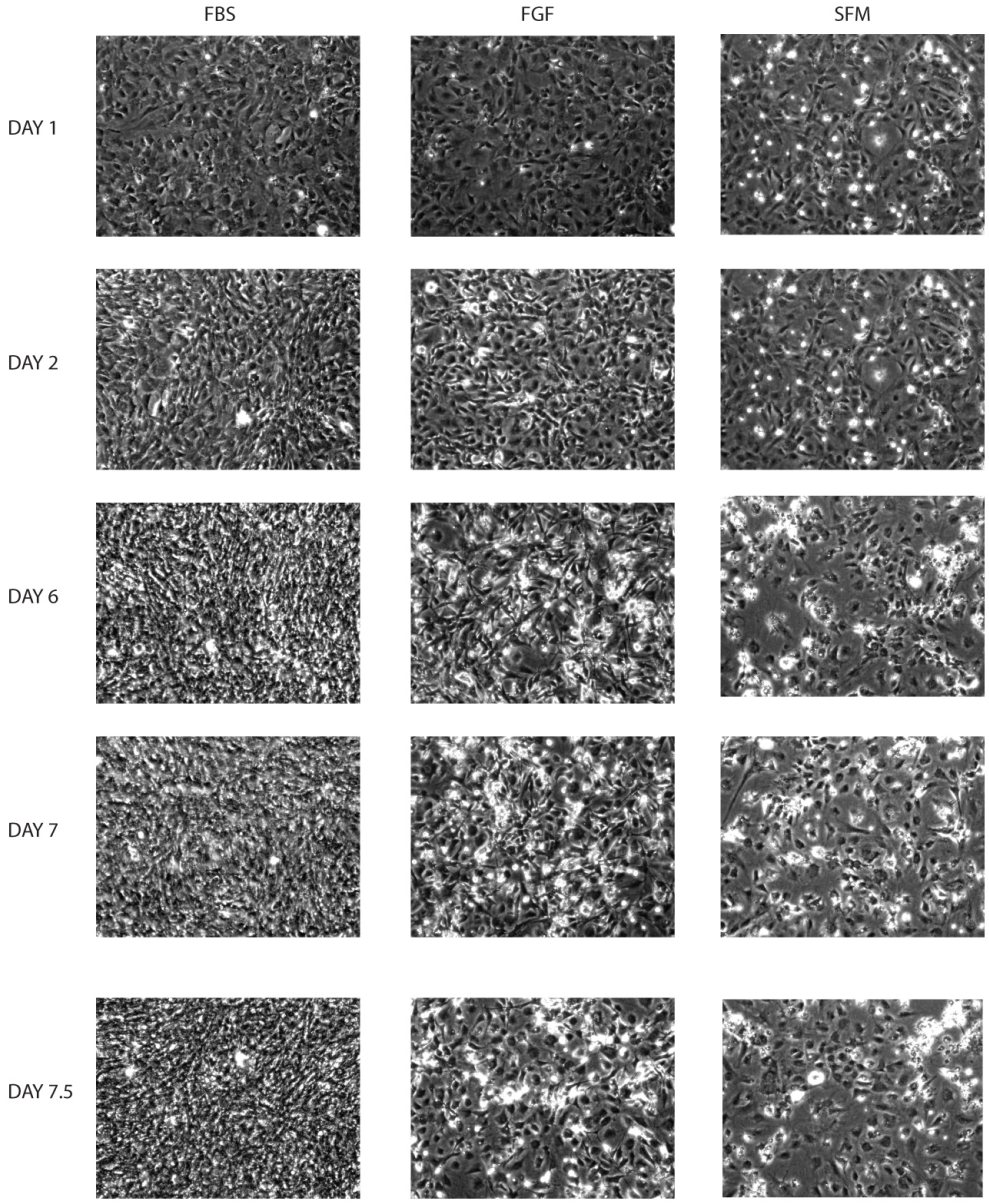

Figure 41A. Effect of serum withdrawal on ESyt 2/3 WT MEFs.

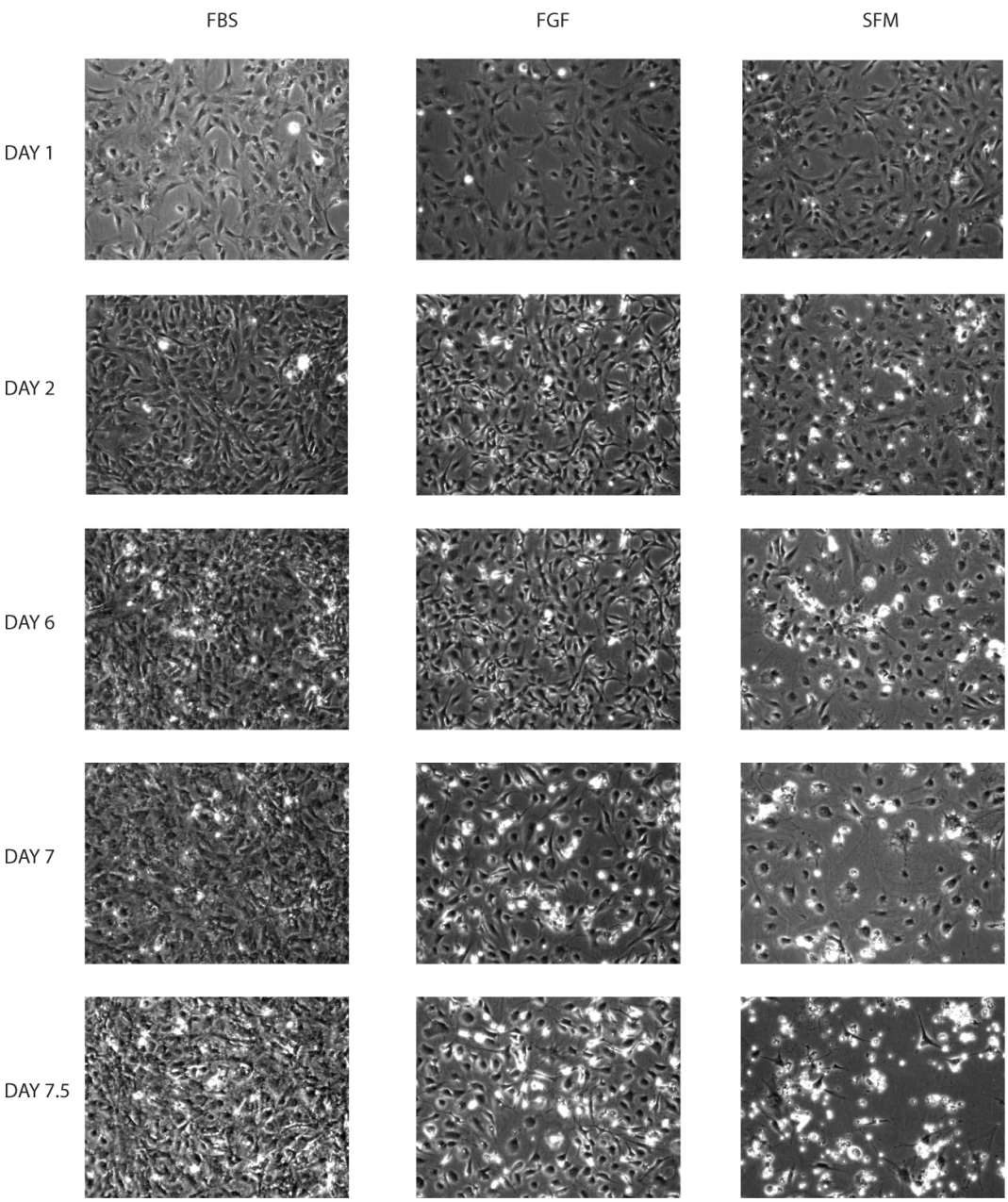

Figure 41B. Effect of serum withdrawal on ESyt 2/3 DKO MEFs.

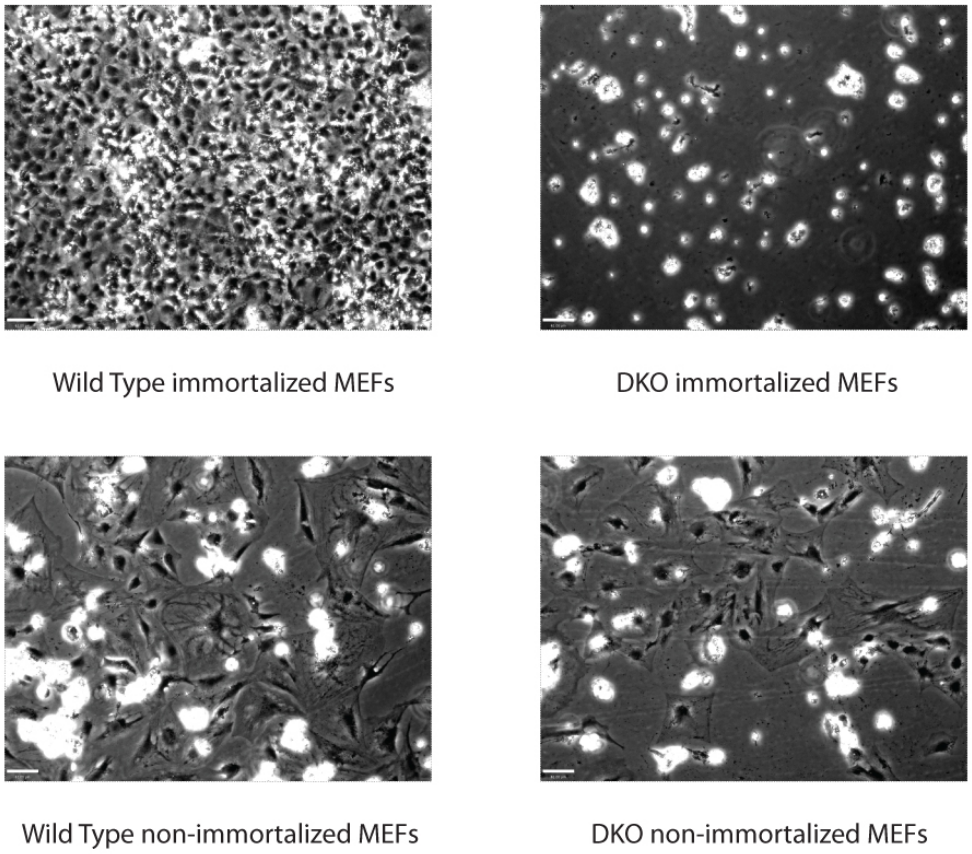

Figure 42. Comparison of immortalized vs. non-immortalized WT and ESyt 2/3 DKO MEFs after 2 weeks in culture.

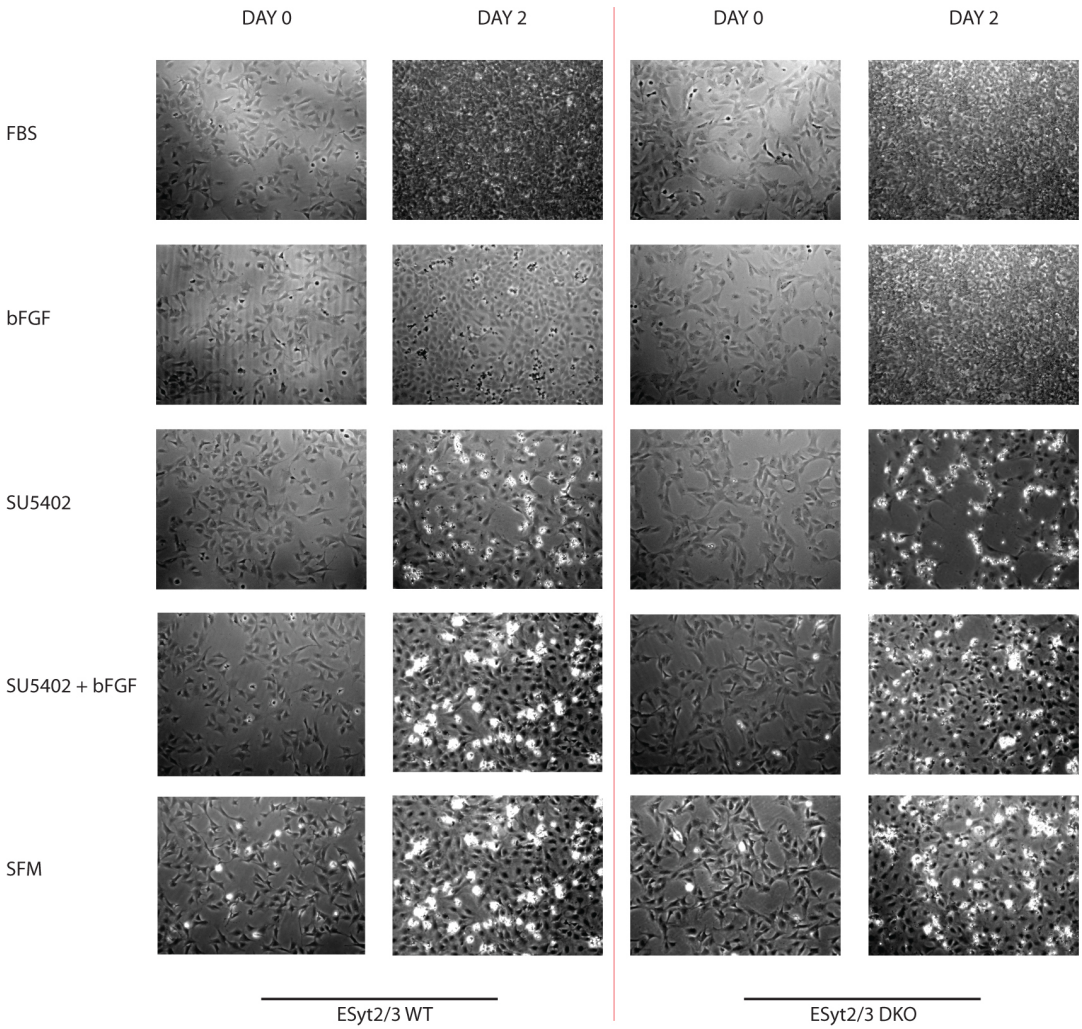

Figure 43. Effect of inhibition of FGF signaling on the WT and DKO MEFs.

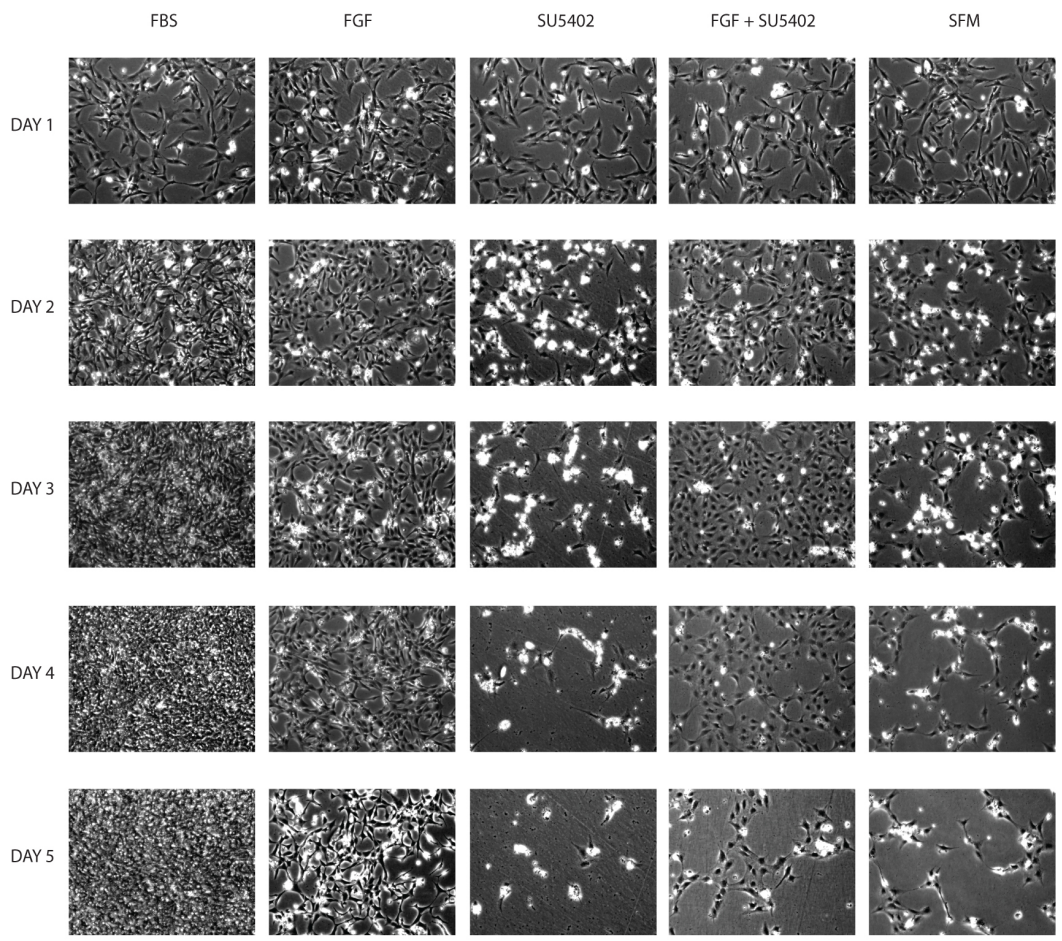

Figure 44A. Effect of serum withdrawal or inhibition of FGF signaling in DKO MEFs.

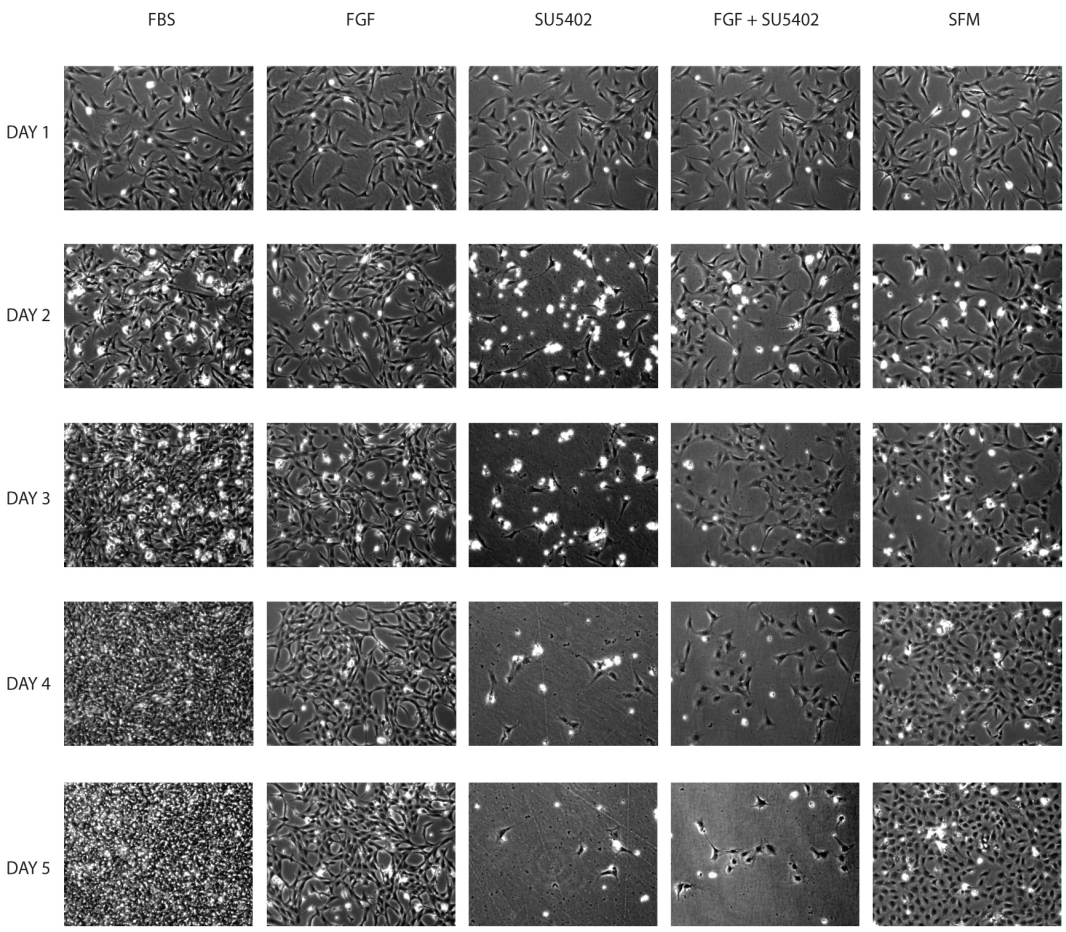

Figure 44B. Effect of serum withdrawal or inhibition of FGF signaling in WT MEFs.

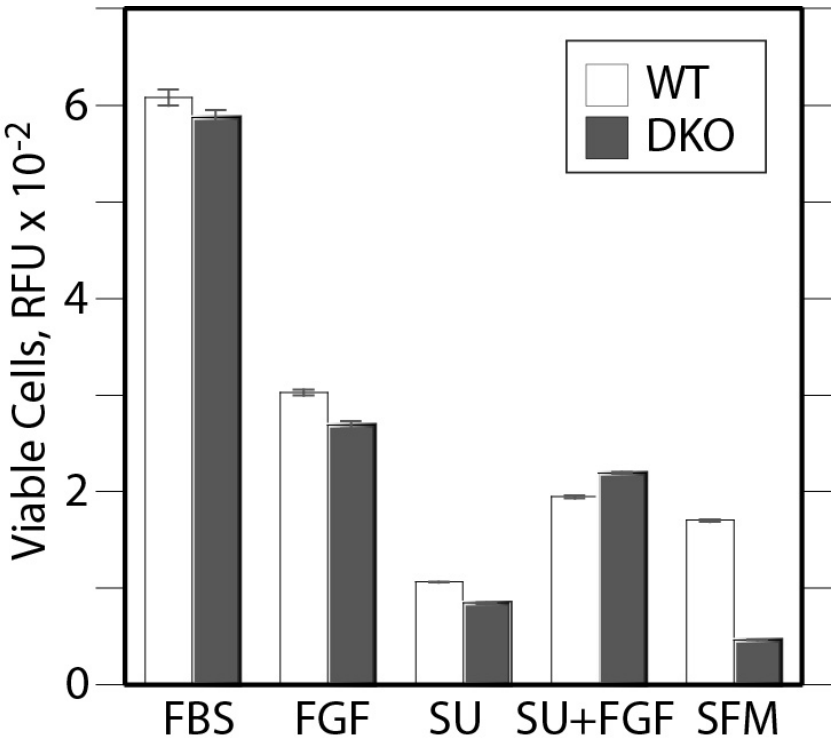

Figure 44C. Cell viability assay.

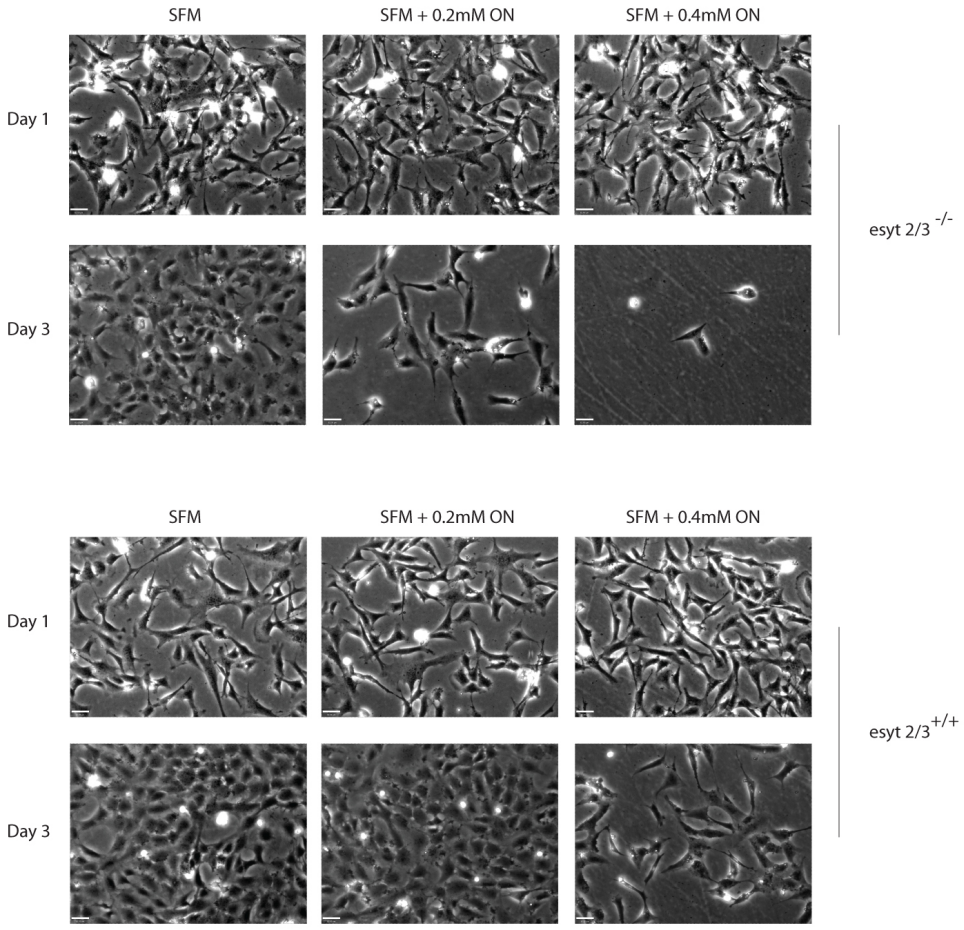

Figure 45A. Response of ESyt 2/3 DKO and WT MEFs subjected to an overnight (ON) oxidative stress (H_2O_2) in the absence of serum or FGF.

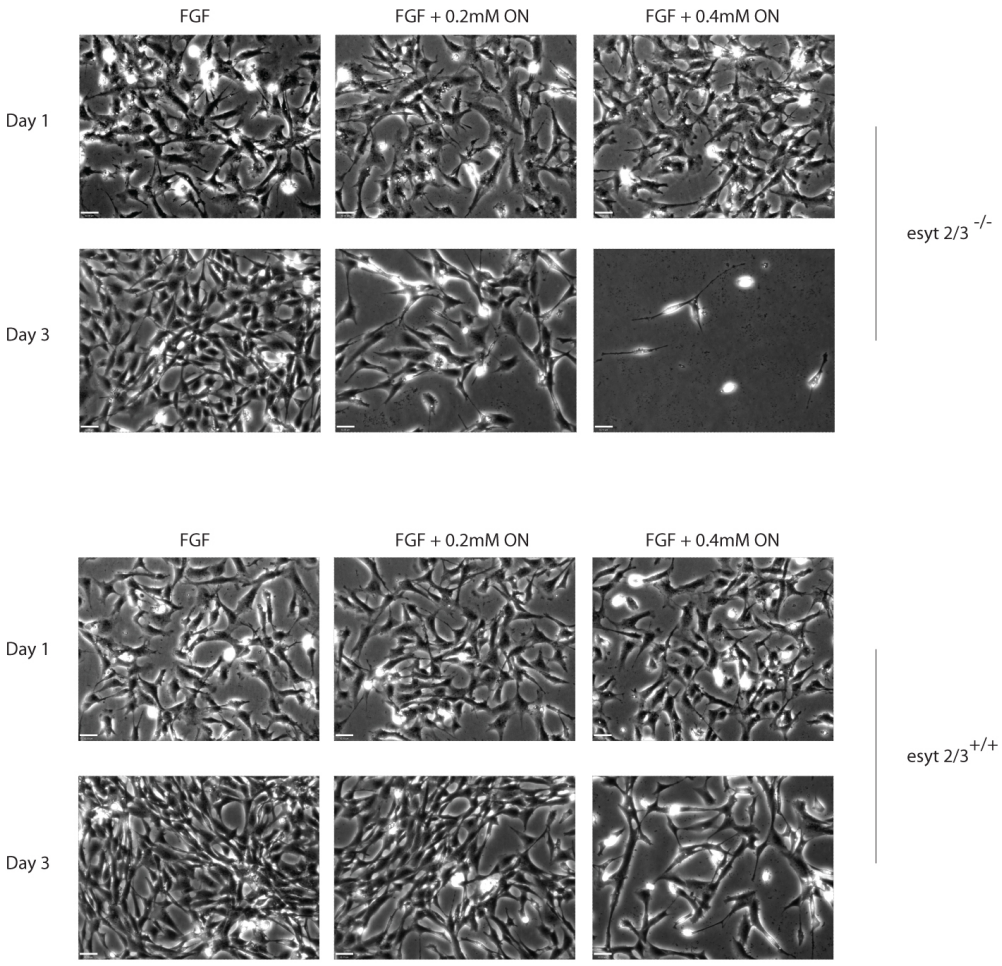

Figure 45B. Response of ESyt 2/3 DKO and WT MEFs subjected to an overnight (ON) oxidative stress (H_2O_2) in the absence of serum but presence 20ng/ml FGF.

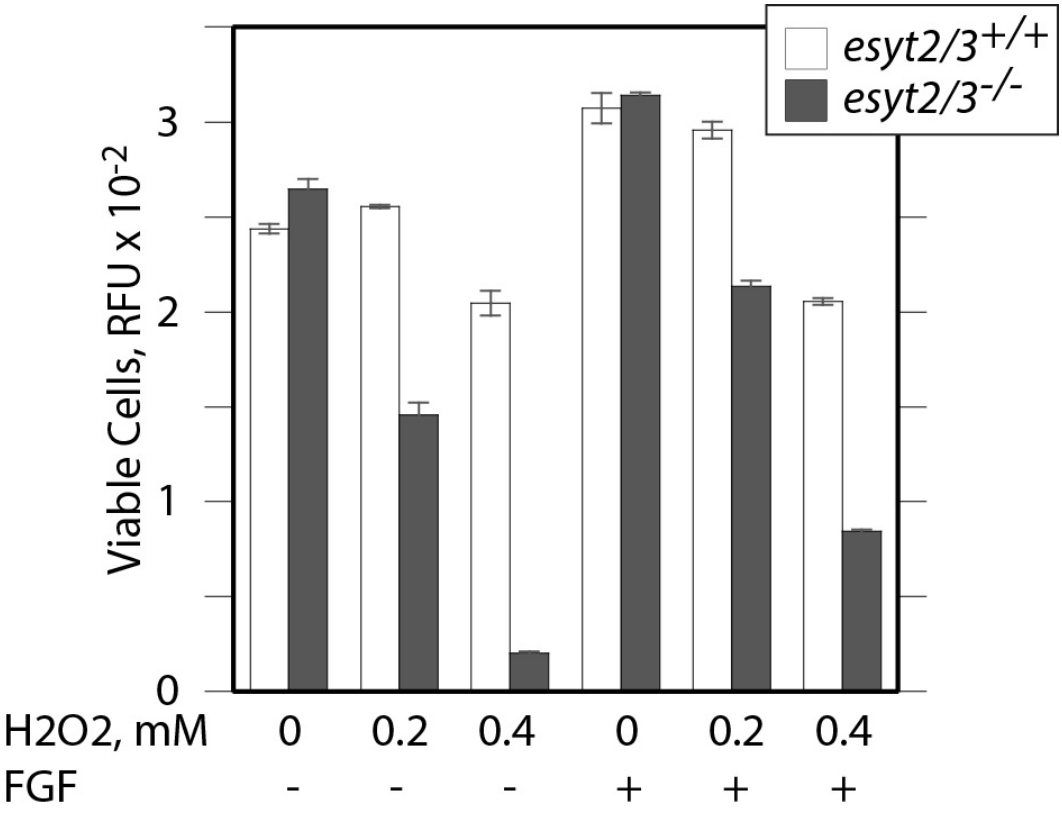

Figure 45C. Cell viability assay.

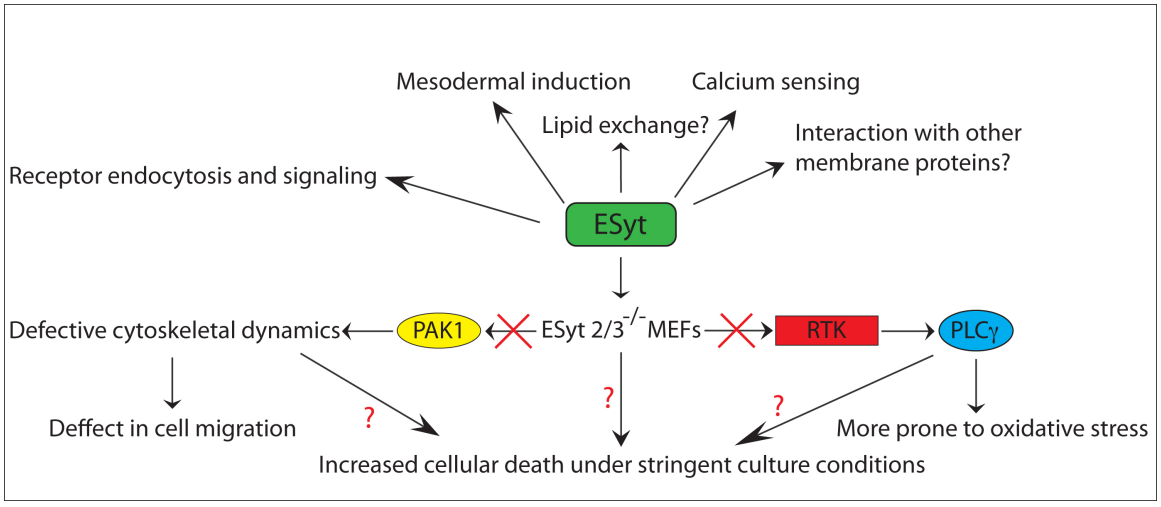

Figure 46. Overview of ESyt function.

Chapter 4: Discussion and Conclusion

4.1) Discussion

Cellular signaling plays an important role in the normal development and maintainance of homeostasis in multicellular organisms. Specialized inter- and intra-cellular signaling networks govern such functions. While a single signaling event may diverge to activate multiple pathways and generate complexity in signaling network, multiple pathways may also converge to activate a single cellular event. The sum of all the positive and negative stimuli may then result in a single cellular outcome. But how these multiple signaling transduction routes work as a whole and how they are regulated in a spatio-temporal way, still remains to be fully understood.

I started my PhD by studying the timing of onset of ERK activation upon FGF stimulation of *Xenopus* embryo Animal Caps (AC) dissected from blastula embryos injected at the 4 cell stage with FGFR1 mRNAs and/or antisense Morpholino™ against xESyt2. A previous study published from our lab. (Jean et al., 2010) had shown that the antisense Morpholino™ depletion of *Xenopus* Extended Synaptotagmin 2 (ESyt2) blocked FGF-dependent induction of the early mesodermal marker Xbra in *Xenopus*, and that the loss of xESyt2 prevented a rapid phase of FGFR1 internalization that occurred within 5 min. of FGF treatment and was essential for significant activation of the ERK MAP-kinase pathway and for subsequent Xbra induction. Previously it had been shown that FGF receptor activation was necessary for both the onset and maintenance of Xbra expression (Fletcher and Harland 2008). However, the onset of Xbra expression occurs at least 40 min. after activation of the ERK cascade. Thus, the requirement for a rapid phase of ERK activation suggested that Xbra activation depended on the prior establishment of an unknown factor. Based upon these results, I attempted to use this system to understand the precise relationship between the rapid phase of receptor internalization, ERK activation and Xbra induction. This required a highly reproducible depletion of ESyt2, followed by the demanding task of AC isolation, treatment and biochemical analysis. Unforthunately, despite a concerted effort I failed to obtain the sufficiently consistent results required for the planned detailed study

(data not shown). Although there are few reports of transient activation of ERK due to injury or cell stress during Animal Cap dissection (Christen and Slack, 1999; Kuroda et al., 2005; LaBonne and Whitman, 1997), that may last >40 minutes, it was difficult to infer any relative change in the amount of ERK activation in mRNA/morpholino injected embryos versus control morpholino injected embryos. Thereafter I shifted my focus to the functional properties of ESyts in RTK signaling in mouse and human cells.

Inter-organelle communication plays a crucial role in maintaining homeostasis in cells. Membrane contact sites (MCS), a region where two organelles come in close proximity, within ≈20nm (Toulmay and Prinz, 2012) plays a role in functions such as lipid exchange (Volker, 2009) and exchange of calcium (Lewis, 2007). Thus, the recent discovery that the Extended Synaptotagmins (ESyts) are endoplasmic reticulum (ER) - resident proteins that help in the formation of endoplasmic reticulum – plasma membrane (ER-PM) junctions has further increased the possible number of functions played by ESyts. The Ca^{2+}- dependent functions of the C2 domains and the recent data that ESyt1 is actively recruited to ER-PM jnctions suggest roles in calcium signaling, while the SMP domain present in each ESyt may be responsible for lipid transport and/or interaction with other proteins.

4.1.1) Localization and Oligomerization of ESyts

4.1.1.1) Localization of ESyts

The ESyts, due to their structural resemblance to Synaptotagmins were assumed to be plasma membrane (PM) proteins (Figure 28 Chapter 2) (Jean et al., 2010; Min et al., 2007). However, studies from our lab failed to detect these proteins on the PM without permeabilizing the cells (Figure 28 and 38 Chapter 2). Further a SNAP-tag™ fused to the N-terminus of ESyt2b was also not detected before cell permeabilization, whereas an N-terminal SNAP-tag fused to the Adrenergic Receptor β2 (ADRβ2) was easily detected with both the cell-impermeable SNAP-surface and cell-permeable SNAP-Cell ligands (NEB) (Figure 28 Chapter 2). These results strongly support the recent findings that rather than being inserted into the PM, the ESyts are probably inserted into the membrane of the endoplasmic reticulum (ER) (Chang et al., 2013; Giordano et al., 2013). Data from our lab clearly exclude the possibility that the ESyts traverse the PM. Additional studies from our lab show that the ESyt2b is misdirected to the PM by fusion to the Syt1 transmembrane (TM) domain (Figure 28 Chapter 2). A fusion protein between Syt1 and ESyt2b, in which the potential transmembrane/ membrane-insertion (TM) domain and the N-terminal sequences of ESyt2b were replaced by those of Syt1, resulted in a ESyt that associated with and penetrated the PM similar to Syt1 (Figure 28 Chapter 2). As ESyts and their splice variants show very little homology preceding the potential membrane-associated domain (Figure 37 Chapter 2), suggest that the membrane-domain and/or at best 20 amino acids preceding it determine association with the ER rather than the PM.

4.1.1.2) Homo and Hetero-dimerization of ESyts.

In order to study the function of ESyts in RTK signaling, we tried to establish whether the ESyts function as monomers or form homo- or hetero-dimers. When I started the work, preliminary dimerization data for ESyt2a, ESyt2b (spliced variant forms of ESyt2) and ESyt3 had been obtained and ESyt1 was thought not to interact

with any other ESyt or the FGF receptor. We found out that ESyt1 does indeed interact with ESyt2 and ESyt3 (Figure 29 Chapter 2). However, the interaction of ESyt1 is slightly weaker with ESyt3 than with ESyt2a or ESyt2b, and it forms also homo-dimers poorly. ESyt2a, ESyt2b and ESyt3, form homo-dimers as well as hetero-dimers. Our results are also consistent with a recent report (Giordano et al., 2013). It remains unclear why ESyt2 and ESyt3 form strong homo-dimers whereas ESyt1 does not.

Recently, the SMP domain of ESyt2 has been shown to form end-to-end dimers when crystallized (Schauder et al., 2014), suggesting that this might explain the ability of the ESyts to dimerize in vivo. This idea was further supported when we showed that Syt1, which is structurally similar to ESyt2 but lacks SMP domain, does not interact with any of the ESyts (Figure 29 Chapter 2). These data strongly suggested that the SMP domain might be involved in the oligomerization of ESyts. However, our recent results show that deletion of the SMP does not affect dimerization of ESyt2 and that the minimal homo-dimerization/oligomerization domain lies between a.a. 1 and 139 (Figure 30 Chapter 2), and hence lies N-terminal to the SMP domain. Although, structural data presented by Schauder et al. (2014) showed ß-barrel structures of two SMP domains contacting end-to-end, this may turn-out to be an interaction induced by crystallization.

The exact function of ESyt is still poorly understood. Nevertheless, there are few studies that indicate some of the possible function of ESyts. A study published in 2009 by Laliot et al. had reported that the Cdk5 phosphorylates ESyt1, which then associates with the GLUT4 and modulates glucose transport in 3T3-L1 adipocytes. Yet, another study published in 2012 by Jun et al., highlights the role of ESyt1 phosphorylation in a novel invasiveness pathway activated by the Oncogenic Lung Cancer Fusion Kinase CD74-ROS. Other reports have also suggested the role of ESyt1 phosphorylation in various cancers (see, Jun et al., 2012).

4.1.2) ESyt and Receptor Tyrosine Kinase.

4.1.2.1) ESyt as an interacting partner with a broader range of RTKs?

A previous report published from our lab had shown that the ESyt2 selectively interacts with FGFR1 (Jean et al., 2010). However, my results show that the ESyts may interact with a broader range of RTKs, possibly expanding the overall possible functional role of ESyts in RTKs signaling.

Interaction of ESyt2 with the MET receptor was compared with that with FGFR1. HEK293T cells were transfected with MET wild type receptor (MET wt) or MET kinase dead (MET kd) mutant and ESyt2b, and the results compared with a parallel analysis of the interaction of ESyt2b with wild type and kinase dead FGFR1 (FGFR1-wt and FGFR1-kd). As shown in Figure 47A, in this experiment interaction with FGFR1-kd there was only slightly less than with FGFR1-wt. (In our hands the interaction of ESyt2b with FGFR1-kd is variable, sometimes showing a slight decrease and other times a complete loss. The interaction studies done by co-immunoprecipitation from transient transfection depends upon several factors such as the type of cells used, the passage number and the batch of cells used, cells condition, density, transfection method used, amount of transfection reagent used, transfection time etc.) Despite this proviso, Figure 47A indicates that ESyt2b does interact with the MET receptor, though no difference in the interaction was observed between MET-wt and MET-kd forms.

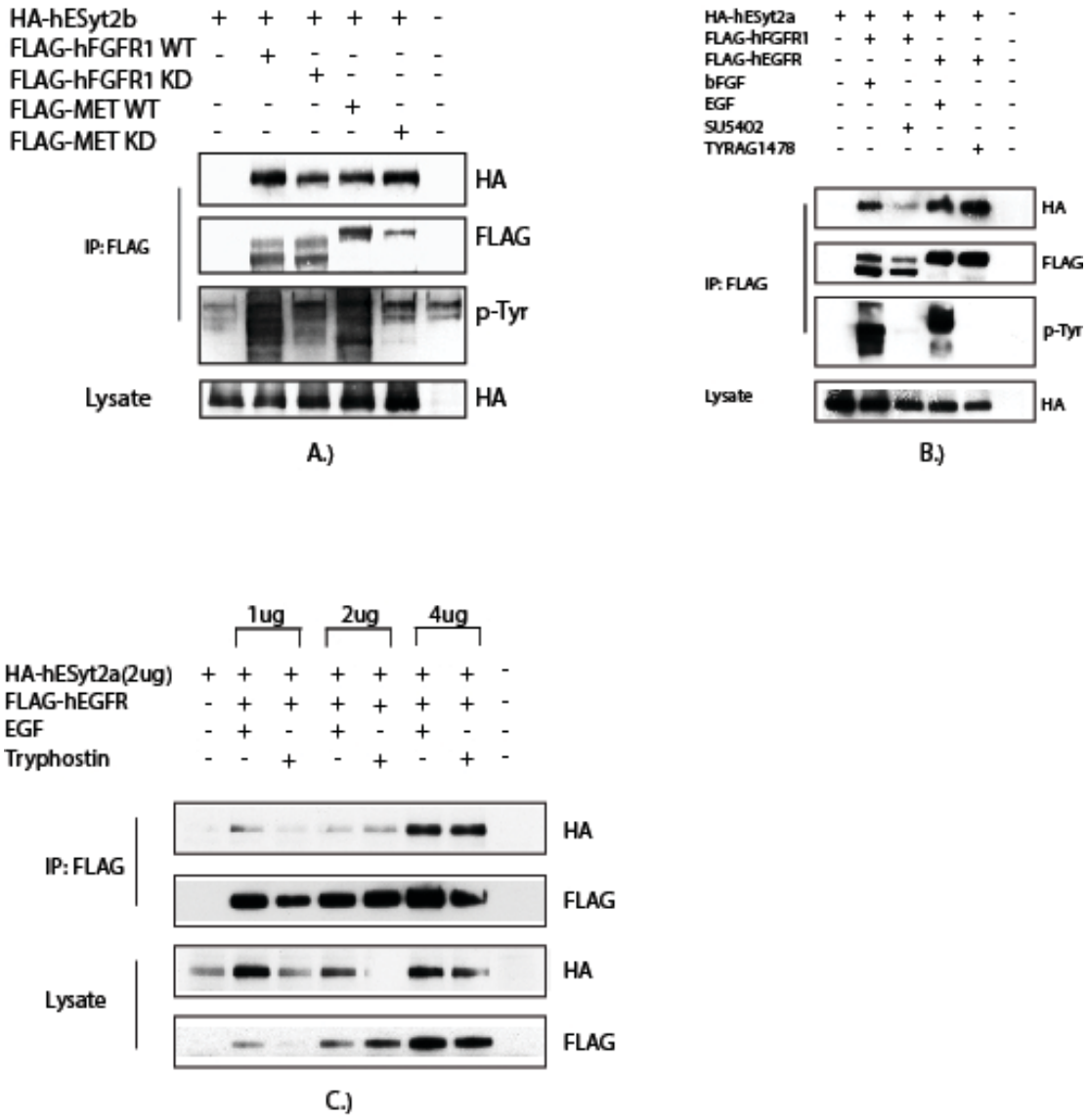

Figure 47. A.) Interaction of hESyt2b with hFGFR1 and MET recceptor. B.) Interaction of hESyt2a with hFGFR1 and hEGFR upon activation or inhibition. C.) Interaction of hESyt2b with different concentration of hEGFR with activation by EGF or inhibition by TYRAG1478.

I also verified the interaction between ESyt2 and EGF Receptor. As shown in Figure 47B, I used the wild type FLAG-tagged human FGFR1 (FLAG-hFGFR1), FLAG-tagged human EGFR (FLAG-hEGFR) and HA-hESyt2b to transfect HEK293T cells. Cells transfected with FLAG-FGFR1 were either stimulated by FGF or inhibited by FGFR specific inhibitor SU5402. Similarly, cells transfected with FLAG-hEGFR were stimulated by EGF or inhibited by EGFR specific inhibitor Tyrphostin AG1478.

As can be seen in Figure 47B, FGFR1 shows the expected result with a gain of interaction upon FGF stimulation and loss of interaction upon overnight inhibition with SU5402. On the other hand, the interaction of ESyt2b with EGFR is unaffected by the EGF receptor specific (TYR) AG1478. The active state of the receptor was determined via its phospho-tyrosine levels as shown in Figure 47B. Considering the possibility that overexpression of either ESyt2b or EGFR may lead to artifactual results, I also used different amounts of hEGFR plasmid in co-transfections with Esyt2b, but as shown in the Figure 47C, the result was the same.

Based upon these observations, it can be concluded that the ESyt2, and probably by analogy ESyt3, does bind other RTKs and that the receptor activation may or may not be required for the interaction. As we argue in Chapter 2, in the case of FGFR1 interaction with ESyt2b depends on a conformational change in the receptor, but this could clearly be a highly receptor-specific effect. The role of ESyt2 interaction with RTKs other than FGFR therefore needs further investigation.

4.1.2.2) Interaction of ESyt's and FGFRs

ESyt2 was previously shown to interact highly selectively with the active form of the FGF receptors. All the ESyts interact to varying degrees with all four FGF receptors FGFR1-4, although as was the case for ESyt oligomerization, ESyt1 appeared to interact poorly as compared to ESyt2 and ESyt3. This said, it is easily possible to observe an interaction between ESyt1 and all four FGF receptors (Figure 48). A possible explanation for the weaker interaction of ESyt1 could be that it alone displays a Ca^{2+}-dependent PM recruitment (Giordano et al., 2013). While ESyt2 and ESyt3 bind strongly to the PM at basal cellular levels of Ca^{2+}, ESyt1 is localized to the PM only upon an increase in intracellular Ca^{2+} levels. Thus, the cellular localization of ESyt1 might play a role in the observation of a weaker interaction with other ESyts or RTKs.

It was previously shown from our lab that ESyt2 was implicated in determining receptor endocytosis and that it associates with Adaptin2 (AP-2) (Jean et al., 2010), suggesting that the interaction of ESyt2 with the activated FGFR initially occurs during the formation of clathrin-coated pits. So, we further asked if ESyt2b was internalized along with activated FGFR or if its interaction was limited to the PM-associated receptor fraction. The data strongly suggested that ESyt2 is not internalized during endocytosis of activated FGFR (Figure 39, Chapter 2). Further, we investigated the interaction of truncation mutants of ESyt2b with FGFR1 in order to determine the structural determinants of the ESyt-FGFR interaction using ESyt2b as a canonical model (Figure 32, Chapter 2). Our data clearly show that the C2 and SMP domains of ESyt2b are not required for the interaction between ESyt2b and FGFR1. Instead, the interaction requires the TM and/or sequences immediately flanking it (a.a. 88 to 138), suggesting that the domain required for ESyt2 dimerization (Figure 30 Chapter 2) and its interaction with FGFR1 in greater part overlaps.

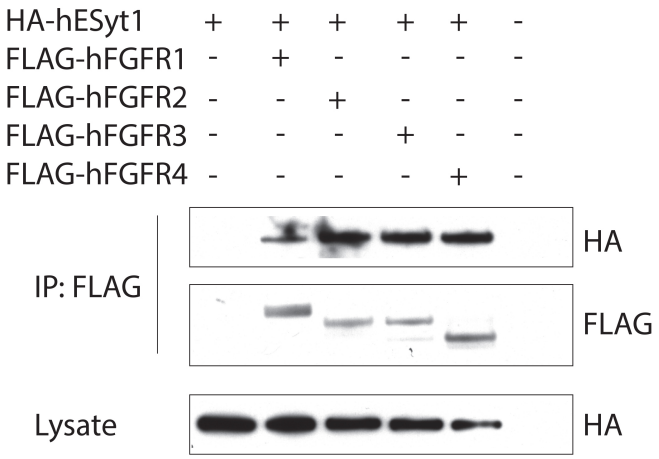

Figure 48. Interaction of hESyt1 with FGFR1, FGFR2, FGFR3 and FGFR4.

4.1.2.3) ESyt2-FGFR1 interaction is independent of receptor activation and phosphorylation.

Since the activation or inhibition does not have any impact on the interaction of ESyt2 with MET and EGF receptors while the interaction is lost in the case of FGFR1 when inhibited overnight, it became important to ask when during receptor inhibition the bulk interaction is lost. I, therefore, performed a time course study of receptor inhibition (Figure 49). As can be seen, the interaction of ESyt2b and FGFR1 is very strong with or without activation of the receptor. There is no difference in the interaction with or without exogenous FGF, presumably due to activation of the receptor by the endogenous FGF secretion by HEK293T cells, compare p-Tyr tracks in Figure 49. Treatment of cells with SU5402 for 1hour strongly inactivated FGFR1 (as seen by p-Tyr status), but did not affect the bulk interaction with ESyt2b. However, after 3 hours of receptor inhibition we clearly see that the interaction of ESyt2b is almost completely eliminated while after 15 hours of inhibition there is a complete loss of interaction. Thus the shorter duration of inhibitor use confirms that the interaction is not simply due to receptor activation, and is potentially consistent with an interaction dependent on receptor conformation.

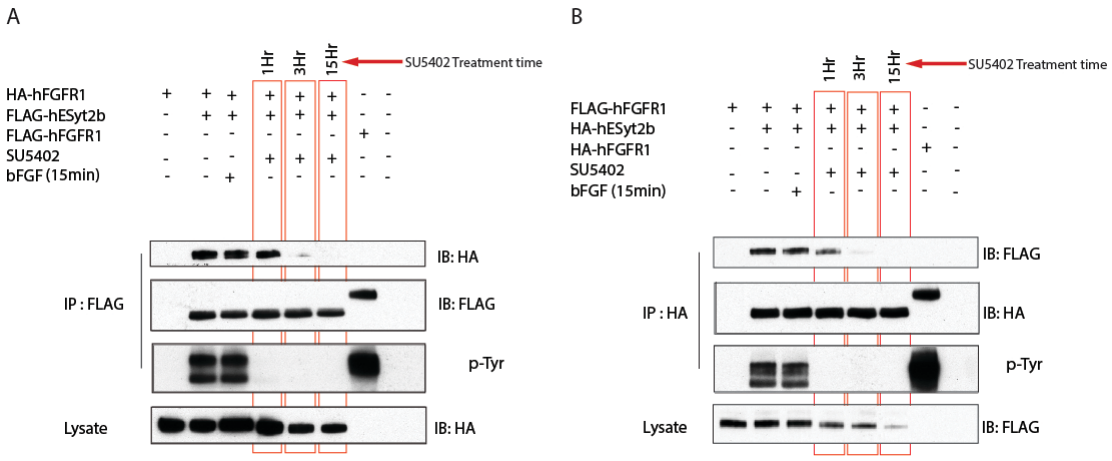

Figure 49. SU5402 inhibitor time course study for the interaction of hESyt2b with the hFGFR1.

To further evaluate the role of receptor phosphorylation in the interaction of FGFR1 with ESyt2, we mutated all the 7 Tyrosine residues important for receptor activation and autophosphorylation. While the single site mutation had no effect (Figure 33 Chapter 2), the combined mutation of Y653 and Y654 (two activation loop phosphorylation sites essential for kinase activity) strongly suppressed the interaction with ESyt2b. The kinase dead (KD) ATP-binding site mutation had similar effect (Figure 33 Chapter 2). The combined mutation of the five remaining non-catalytic phosphotyrosine sites (Y463,583,584,730,766F) strongly reduced receptor autophosphorylation and did somewhat suppress interaction with ESyt2b but to a much smaller extent than F-mutation at Y653 and Y654, which essentially eliminates catalytic activation. We, thus, concluded that the 5 non-catalytic phosphotyrosine sites were not required for the interaction with ESyt2b. We further replaced the activation loop phosphosite of FGFR1 by phosphomimics (Y653/654 to E), and this mutant interacted with the ESyt2b significantly, when compared to wild type (Figure 33 Chapter 2). Thus, either the ESyt2b recognizes the combined autophosphorylation state of all the seven sites on FGFR1 or it recognizes a specific receptor conformation related to the receptor autophosphorylation state.

4.1.2.4) The curious case of FGFR1-R577E Mutant!

The FGFR1-R577E mutant (explained on page no. 64 Section 1.6.5) gave us a better picture of the interaction of ESyt2 with the FGFR1. This mutation is very unusual since it prevents the receptor activation and autophosphorylation in vivo, but incongruously forces the catalytic domain activation loop into the activated conformation. Thus, while the receptor is inactive in vivo, in vitro it is perfectly able to phosphorylate a normal substrate *in trans* (Bae et al., 2010). I verified whether the FGFR1-R577E mutant receptor interacts with ESyt2b or not (Figure 34 Chapter 2). Surprisingly, even though the receptor was unable to autophosphorylate (confirmed by p-Tyr levels), it still interacted with ESyt2b. In addition, to the p-Tyr levels, further confirmation of the receptor being inactive in vivo came from the fact that it failed to recruit and phosphorylate PLC-γ, as was the case for FGFR1-Y766F mutant (FGFR1 PLC-γ binding site mutation). These data strongly indicated that the interaction of ESyt with FGFR1 depends upon the conformational state of the receptor rather than on its catalytic activity.

In another study done in our lab, we investigated the interaction of ESyt2b with FGF activated and SU5402 inhibited FGFR1-R577E mutant and compared with the wild type receptor and the kinase dead ATP binding site mutant K514A. In the FGF stimulated condition, both the wild type FGFR1 and the R577E mutant interacted strongly with ESyt2b while the K514A mutant did not (Figure 34 Chapter 2). The interesting observation was that the inhibitor SU5402 strongly suppressed the interaction of ESyt2b with the wild type FGFR1 but had no effect on the interaction of the ESyt2b with the R577E mutant. This observation is in accordance with the structural data by Bae et al in 2010, suggesting that this mutant may have low affinity for ATP. This further confirmed that ESyt2b specifically recognizes the open active conformation of FGFR1 independently of either catalytic activity or receptor autophosphorylation.

4.1.2.5) FGFR truncation reveals an interaction with ESyt2b independent of catalytic activity.

The results obtained from the FGFR1 inhibitor studies, phosphotyrosine mutants and the FGFR1 R577E mutant suggested the ESyt2-FGFR1 interaction is solely based on the recognition of the open receptor conformation and that the displacement of the activation loop is required in order for ESyt2 to gain access to a binding site that is hidden in the inactive receptor. Based upon this, we decided to ask whether this binding site could be revealed in C-terminal deletion mutants of the receptor. The previous results from our lab had suggested that a deletion of the C-terminal form of the receptor extending up to amino acid 475 eliminates the ESyt2 interaction. So, I reconfirmed the interaction of FGFR1 1-475, and determined if C-terminal deletions 1-615 and 1-752 would or would not interact with ESyt2b (Figure 34 B Chapter 2). The deletion of just the C-terminal tail (aa. 715 to end), but leaving the kinase domain intact, had no effect on the ESyt2b interaction. Complete deletion of the C-terminal kinase lobe including the activation loop also had no effect on the ESyt2b interaction, but the deletion extending up to amino acid 475, to remove a large part of the N-terminal kinase lobe, eliminated the interaction. This supported the idea that ESyt2b recognized a binding site on FGFR1 contained within its N-terminal kinase lobe. In passing, mutation of the transmembrane domain proximal Nedd4-1 binding site (Δ6 mutation) shown to be required for receptor internalization (Persaud et al., 2011), also had no effect on the interaction of ESyt2b with FGFR1.

To further localize the ESyt2 binding site, I created three additional FGFR1 C-terminal mutants i.e. FGFR1 1-500, FGFR1 1-550, and FGFR1 1-600 (Figure 34 C Chapter 2). The partial deletion to amino acid 600 of the C-terminal kinase lobe, or its full deletion to amino acid 550 had no effect on the interaction of ESyt2b with the receptor. However, deletion to amino acid 500, removing the first part of the N-terminal kinase lobe, eliminated ESyt2b binding. Together these data strongly supporting the proposition that selectivity of ESyt2b for the active FGFR1 receptor

depends on access to a binding site within the N-terminal kinase lobe of the receptor that is afforded when the receptor takes up its active conformation.

4.1.4) Loss of Extended Synaptotagmins ESyt2 and ESyt3 does not affect mouse development or viability, but in vitro cell migration and survival under stress are affected (Herdman et al., 2014, Annexe)

Since ESyt2 or ESyt3 are present at the ER-PM junction and that they strongly bind to the plasma membrane in comparison of ESyt1 that localizes to the ER-PM junction in a Ca^{2+} dependent manner, a lack of any significant phenotype in ESyt2/3$^{-/-}$ double knockout mice was really surprising and totally unexpected (chapter 2). Why very early *Xenopus* development was found to be sensitive to ESyt2 depletion (Jean et al. 2010) while mouse is not, remains unclear. The expression profiles of the Xenopus ESyts suggest that ESyt1, 2 and 3 mRNAs are present maternally (Bowes et al., 2010), however whether or not they are all translated at this stage is still unknown. Cultured ESyt2$^{-/-}$ and ESyt2$^{-/-}$ ESyt3$^{-/-}$ mouse embryonic cells (MEFs) showed defects in FGF-stimulated migration and were found to be more susceptible to the stringent culture conditions and to the oxidative stress as compared to the wild type MEFs. At least in part these defects appear to be related to an inability to respond to an autocrine FGF signal, though the response of the ERK pathway to exogenous FGF was found to be normal. Possibly, some effects may be attributed to the fact that PAK1 recruitment to ESyt2 would be affected, potentially affecting cytoskeletal dynamics. Yet another possibility is suggested by data from PLCγ1 null MEFs, which display high sensitivity to H_2O_2 treatment (Wang et al., 2001). Potentially ESyt2/3 loss could affect signaling through PLCγ and thus Ca^{2+} signaling.

4.2) Conclusion and perspectives.

Given the surprising result that ESyt1/2 inactivation in mouse displayed no phenotype, it is imperative to inactivate the third ESyt and determine whether loss of all three ESyts will affect mouse viability. The lab has already shown that ESyt1-null mice are viable and fertile, and we await the generation of ESyt1/2/3-null mice.

Signaling events occurring at membrane contact sites (MCS) represent a complex mechanism of regulation of cellular homeostasis that has increased the curiosity of researchers in recent times. The discovery that the ESyts are ER resident proteins has also greatly increased the possible number of ESyt function. Yet, there are many unanswered questions and some of them can be explained based upon the recent findings. Our result shows that among all ESyts, ESyt1 poorly dimerizes with itself and with other ESyts and also that the ESyt1-FGFR1 interaction is poor when compared to ESyt2 and ESyt3. A possible explanation for that observation might be the cellular localization and Ca^{2+} dependent functions of ESyt1. ESyt2 and ESyt3 localize at the ER-PM contact site and bind strongly to the PM at basal cellular Ca^{2+} levels. On the other hand, ESyt1 mostly resides in ER away from the PM and only upon increase in intracellular Ca^{2+} levels does it localize to ER-PM contact sites and binds the PM. Also, data presented by Schauder et al (2014) showed ß-barrel structures of two SMP domains contacting end-to-end to form dimers. But our results suggests that neither C2 domain and nor SMP domain is essential for homo- and heterodimerization of ESyts and its interaction with the receptor. This is quite possible that there might be more than one binding site and/ or the SMP domain might be somehow stabilizing the dimerization of ESyts or interaction with the receptor.

Based upon our studies and recent reports on ESyts (explained in Section 1.1), a hypothetical model of ESyt function is shown in the Figure 50.

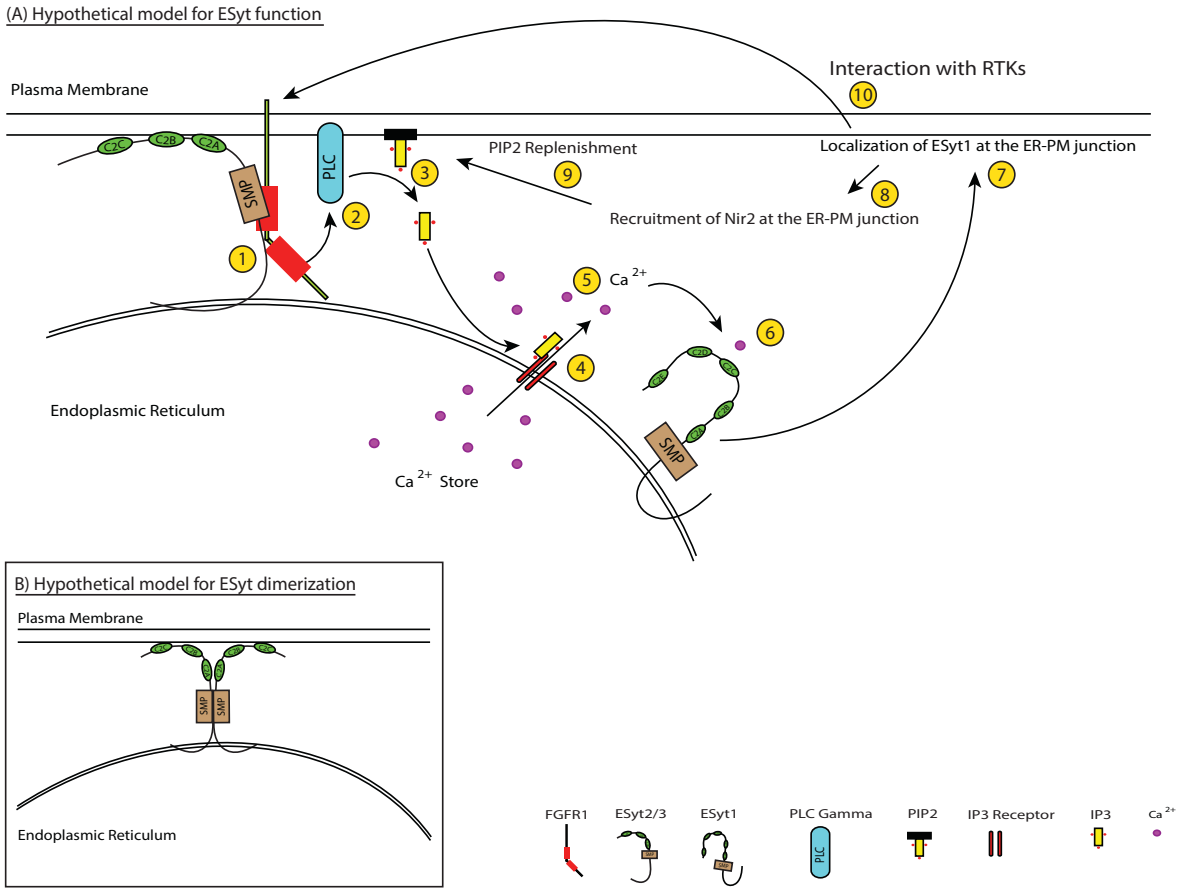

Figure 50. A hypothetical model of ESyt function

(A) Hypothetical model of ESyt function. ESyt2 and ESyt3 bind to the plasma membrane via its C2C domain. Further, C2A domain might bind to the phospholipids on the plasma membrane in a Ca^{2+} dependent manner and thereby bringing SMP domain close to plasma membrane. ESyt2 and ESyt3 then interact with RTK's (with active conformation of FGFR1 as shown in Figure 50A step 1) via the transmembrane region (TM) and sequences immediately flanking it (a.a. 88 to 138) of the ESyt2. The SMP domain then may (or may not) stabilize this interaction. Upon stimulation the receptor becomes autophosphorylated and activated and this results in the phosphorylation and activation of PLC (step 2). The activated PLC then hydrolyzes the PIP2 and converts it into IP3 and DAG (step 3). The IP3 thus formed binds to the IP3 receptor (step 4) and triggers the release of Ca^{2+} into cytosol (step 5). The elevation of cytosolic Ca^{2+} level results in the binding of Ca^{2+} to the C2C domain of ESyt1 (step 6). Upon Ca^{2+} binding ESyt1 then relocalizes to the ER-PM junction (step 7). The newly formed ER-PM junction helps to reduce the gap distance between

ER and plasma membrane and recruits Nir2 protein at the ER-PM junction (step 8). Nir2 protein then helps in the transfer of IP to the plasma membrane where it is converted back to PIP2 (step 9), which then further helps in the receptor induced Ca^{2+} signaling. The ESyt1 localized to ER-PM junction can also interact with other RTK's, thereby resulting in the regulation of further cellular functions (step 10). **(B) Hypothetical model of ESyt2 and ESyt3 dimerization.** ESyt2 and ESyt3 bind to the plasma membrane via its C2C domain and forms homo- and hetrodimers via the transmembrane region (TM) and sequences immediately flanking it (a.a. 88 to 138) and SMP domain then can (or can not) stabilize this interaction. Further the C2A domain can bind to phospholipids on the plasma membrane in Ca^{2+} dependent manner, thereby bringing the SMP domain closer to the plasma membrane for the transfer of lipids and to stimulate cellular signaling.

This model is fully consistent with our ESyt2b C-terminal deletion experiments, C-terminal FGFR1 deletion mutants and lower preference of ESyt1 to form homo- and heterodimers and to interact with FGFR1.

Given the mild phenotypes our studies disclosed in cultured MEFs lacking ESyt2 and 3, the lab initiated a collaboration with the group of Dr Jen Liou (UT Southwestern Medical Center). This has already revealed that loss of ESyt2 and 3 significantly reduces the number or ER-PM junction sites in these cells and regeneration of PIP2 is also significantly slowed. Further, ESyt1-null MEFs do not display the normal junction tightening in response to Store-Operated Calcium Entry (SOCE). These studies will be taken further using mutant ESyts and if possible the ESyt1/2/3-null MEFs and should provide an alternative approach to understanding how and in which pathways these proteins function.

Since ESyt1 is localized to the ER-PM junction in a Ca^{2+} dependent manner and both ESyt2 and ESyt3 binds to Ca^{2+} via its C2A domain, it will be interesting to see whether a transient increase or decrease of Ca^{2+} levels in the cytosol has any effect on the interaction of ESyt1 (or ESyt2 and ESyt3) with the FGFR1 and whether it somehow affects the dimerization and localization of ESyts in a spatio-temporal way? Phosphorylation of ESyt has been observed in some diseases (Jun et al., 2012), so, it will be really important to check whether the phosphorylation of ESyts has any role

in binding to the RTKs or forming dimers. This will require the mapping of phosphorylation sites and the generation of phospho-specific antibodies. Also, does the phosphophorylation event some how controls the binding of Ca^{2+} ions or phopholipids? The collaboration with the group of Dr Jen Liou should provide the techniques necessary to pursue these questions.

References

Achanzar, W.E., and S. Ward. 1997. A nematode gene required for sperm vesicle fusion. Journal of cell science. 110 (Pt 9): 1073-1081.

Baass, P.C., G.M. Di Guglielmo, F. Authier, B.I. Posner, and J.J. Bergeron. 1995. Compartmentalized signal transduction by receptor tyrosine kinases. Trends in cell biology. 5:465-470.

Bae, J.H., T.J. Boggon, F. Tome, V. Mandiyan, I. Lax, and J. Schlessinger. 2010. Asymmetric receptor contact is required for tyrosine autophosphorylation of fibroblast growth factor receptor in living cells. Proceedings of the National Academy of Sciences of the United States of America. 107:2866-2871.

Bisson, N., N. Islam, L. Poitras, S. Jean, A. Bresnick, and T. Moss. 2003. The catalytic domain of xPAK1 is sufficient to induce myosin II dependent in vivo cell fragmentation independently of other apoptotic events. Developmental biology. 263:264-281.

Bisson, N., L. Poitras, A. Mikryukov, M. Tremblay, and T. Moss. 2007. EphA4 signaling regulates blastomere adhesion in the Xenopus embryo by recruiting Pak1 to suppress Cdc42 function. Molecular biology of the cell. 18:1030-1043.

Boesze-Battaglia, K., and R. Schimmel. 1997. Cell membrane lipid composition and distribution: implications for cell function and lessons learned from photoreceptors and platelets. The Journal of experimental biology. 200:2927-2936.

Bokoch, G.M. 2003. Biology of the p21-activated kinases. Annual review of biochemistry. 72:743-781.

Cargnello, M., and P.P. Roux. 2011. Activation and function of the MAPKs and their substrates, the MAPK-activated protein kinases. Microbiology and molecular biology reviews: MMBR. 75:50-83.

Carpenter, G., and Q. Ji. 1999. Phospholipase C-gamma as a signal-transducing element. Experimental cell research. 253:15-24.

Chaffer, C.L., B. Dopheide, P. Savagner, E.W. Thompson, and E.D. Williams. 2007. Aberrant fibroblast growth factor receptor signaling in bladder and other cancers. Differentiation; research in biological diversity. 75:831-842.

Chang, C.L., T.S. Hsieh, T.T. Yang, K.G. Rothberg, D.B. Azizoglu, E. Volk, J.C. Liao, and J. Liou. 2013. Feedback regulation of receptor-induced Ca^{2+} signaling mediated by ESyt1 and Nir2 at endoplasmic reticulum-plasma membrane junctions. Cell reports. 5:813-825.

Chapman, E.R. 2002. Synaptotagmin: a Ca^{2+} sensor that triggers exocytosis? Nature reviews. Molecular cell biology. 3:498-508.

Citores, L., D. Khnykin, V. Sorensen, J. Wesche, O. Klingenberg, A. Wiedlocha, and S. Olsnes. 2001. Modulation of intracellular transport of acidic fibroblast growth factor by mutations in the cytoplasmic receptor domain. Journal of cell science. 114:1677-1689.

Cooper, C.S., M. Park, D.G. Blair, M.A. Tainsky, K. Huebner, C.M. Croce, and G.F. Vande Woude. 1984. Molecular cloning of a new transforming gene from a chemically transformed human cell line. Nature. 311:29-33.

Cortesina, G., T. Martone, E. Galeazzi, M. Olivero, A. De Stefani, M. Bussi, G. Valente, P.M. Comoglio, and M.F. Di Renzo. 2000. Staging of head and neck squamous cell carcinoma using the MET oncogene product as marker of tumor

cells in lymph node metastases. International journal of cancer. Journal international du cancer. 89:286-292.

Craxton, M. 2007. Evolutionary genomics of plant genes encoding N-terminal-TM-C2 domain proteins and the similar FAM62 genes and synaptotagmin genes of metazoans. BMC genomics. 8:259.

Creutz, C.E., S.L. Snyder, and T.A. Schulz. 2004. Characterization of the yeast tricalbins: membrane-bound multi-C2-domain proteins that form complexes involved in membrane trafficking. Cellular and molecular life sciences : CMLS. 61:1208-1220.

Domchek, S.M., K.R. Auger, S. Chatterjee, T.R. Burke, Jr., and S.E. Shoelson. 1992. Inhibition of SH2 domain/phosphoprotein association by a nonhydrolyzable phosphonopeptide. Biochemistry. 31:9865-9870.

Dvorak, P., D. Dvorakova, and A. Hampl. 2006. Fibroblast growth factor signaling in embryonic and cancer stem cells. FEBS letters. 580:2869-2874.

Edwards, D.C., L.C. Sanders, G.M. Bokoch, and G.N. Gill. 1999. Activation of LIM-kinase by Pak1 couples Rac/Cdc42 GTPase signaling to actin cytoskeletal dynamics. Nature cell biology. 1:253-259.

Eswarakumar, V.P., I. Lax, and J. Schlessinger. 2005. Cellular signaling by fibroblast growth factor receptors. Cytokine & growth factor reviews. 16:139-149.

Eyster, K.M. 2007. The membrane and lipids as integral participants in signal transduction: lipid signal transduction for the non-lipid biochemist. Advances in physiology education. 31:5-16.

Furdui, C.M., E.D. Lew, J. Schlessinger, and K.S. Anderson. 2006. Autophosphorylation of FGFR1 kinase is mediated by a sequential and precisely ordered reaction. Molecular cell. 21:711-717.

Furge, K.A., Y.W. Zhang, and G.F. Vande Woude. 2000. Met receptor tyrosine kinase: enhanced signaling through adapter proteins. Oncogene. 19:5582-5589.

Geppert, M., Y. Goda, R.E. Hammer, C. Li, T.W. Rosahl, C.F. Stevens, and T.C. Sudhof. 1994. Synaptotagmin I: a major Ca^{2+} sensor for transmitter release at a central synapse. Cell. 79:717-727.

Giordano, F., Y. Saheki, O. Idevall-Hagren, S.F. Colombo, M. Pirruccello, I. Milosevic, E.O. Gracheva, S.N. Bagriantsev, N. Borgese, and P. De Camilli. 2013. PI(4,5)P(2)-dependent and Ca^{2+}-regulated ER-PM interactions mediated by the extended synaptotagmins. Cell. 153:1494-1509.

Groer, G.J., M. Haslbeck, M. Roessle, and A. Gessner. 2008. Structural characterization of soluble ESyt2. FEBS letters. 582:3941-3947.

Harduf, H., E. Halperin, R. Reshef, and D. Ron. 2005. Sef is synexpressed with FGFs during chick embryogenesis and its expression is differentially regulated by FGFs in the developing limb. Developmental dynamics: an official publication of the American Association of Anatomists. 233:301-312.

Ho, H.K., S. Pok, S. Streit, J.E. Ruhe, S. Hart, K.S. Lim, H.L. Loo, M.O. Aung, S.G. Lim, and A. Ullrich. 2009. Fibroblast growth factor receptor 4 regulates proliferation, anti-apoptosis and alpha-fetoprotein secretion during hepatocellular carcinoma progression and represents a potential target for therapeutic intervention. Journal of hepatology. 50:118-127.

Huang, X., C. Yang, C. Jin, Y. Luo, F. Wang, and W.L. McKeehan. 2009. Resident hepatocyte fibroblast growth factor receptor 4 limits hepatocarcinogenesis. Molecular carcinogenesis. 48:553-562.

Jean, S., A. Mikryukov, M.G. Tremblay, J. Baril, F. Guillou, S. Bellenfant, and T. Moss. 2010. Extended-synaptotagmin-2 mediates FGF receptor endocytosis and ERK activation in vivo. Developmental cell. 19:426-439.

Jean, S., M.G. Tremblay, C. Herdman, F. Guillou, and T. Moss. 2012. The endocytic adapter ESyt2 recruits the p21 GTPase activated kinase PAK1 to mediate actin dynamics and FGF signaling. Biology open. 1:731-738.

Jeffers, M., M.S. Rao, S. Rulong, J.K. Reddy, V. Subbarao, E. Hudson, G.F. Vande Woude, and J.H. Resau. 1996. Hepatocyte growth factor/scatter factor-Met signaling induces proliferation, migration, and morphogenesis of pancreatic oval cells. Cell growth & differentiation: the molecular biology journal of the American Association for Cancer Research. 7:1805-1813.

Jun, H.J., H. Johnson, R.T. Bronson, S. de Feraudy, F. White, and A. Charest. 2012. The oncogenic lung cancer fusion kinase CD74-ROS activates a novel invasiveness pathway through ESyt1 phosphorylation. Cancer research. 72:3764-3774.

Kawakami, Y., J. Rodriguez-Leon, C.M. Koth, D. Buscher, T. Itoh, A. Raya, J.K. Ng, C.R. Esteban, S. Takahashi, D. Henrique, M.F. Schwarz, H. Asahara, and J.C. Izpisua Belmonte. 2003. MKP3 mediates the cellular response to FGF8 signaling in the vertebrate limb. Nature cell biology. 5:513-519.

Kikkawa, U., A. Kishimoto, and Y. Nishizuka. 1989. The protein kinase C family: heterogeneity and its implications. Annual review of biochemistry. 58:31-44.

Kopec, K.O., V. Alva, and A.N. Lupas. 2010. Homology of SMP domains to the TULIP superfamily of lipid-binding proteins provides a structural basis for lipid exchange between ER and mitochondria. Bioinformatics. 26:1927-1931.

Kornmann, B., E. Currie, S.R. Collins, M. Schuldiner, J. Nunnari, J.S. Weissman, and P. Walter. 2009. An ER-mitochondria tethering complex revealed by a synthetic biology screen. Science. 325:477-481.

Kovalenko, D., X. Yang, R.J. Nadeau, L.K. Harkins, and R. Friesel. 2003. Sef inhibits fibroblast growth factor signaling by inhibiting FGFR1 tyrosine phosphorylation and subsequent ERK activation. The Journal of biological chemistry. 278:14087-14091.

Lebiedzinska, M., G. Szabadkai, A.W. Jones, J. Duszynski, and M.R. Wieckowski. 2009. Interactions between the endoplasmic reticulum, mitochondria, plasma membrane and other subcellular organelles. The international journal of biochemistry & cell biology. 41:1805-1816.

Lee, I., and W. Hong. 2006. Diverse membrane-associated proteins contain a novel SMP domain. FASEB journal : official publication of the Federation of American Societies for Experimental Biology. 20:202-206.

Lek, A., F.J. Evesson, R.B. Sutton, K.N. North, and S.T. Cooper. 2012. Ferlins: regulators of vesicle fusion for auditory neurotransmission, receptor trafficking and membrane repair. Traffic. 13:185-194.

Lek, A., F.J. Evesson, R.B. Sutton, K.N. North, and S.T. Cooper. 2012. Ferlins: regulators of vesicle fusion for auditory neurotransmission, receptor trafficking and membrane repair. Traffic. 13:185-194.

Lemmon, M.A., and J. Schlessinger. 2010. Cell signaling by receptor tyrosine kinases. Cell. 141:1117-1134.

Lemmon, M.A., and J. Schlessinger. 2010. Cell signaling by receptor tyrosine kinases. Cell. 141:1117-1134.

Levine, T., and C. Loewen. 2006. Inter-organelle membrane contact sites: through a glass, darkly. Current opinion in cell biology. 18:371-378.

Lewis, R.S. 2007. The molecular choreography of a store-operated calcium channel. Nature. 446:284-287.

Lin, W., M. Furthauer, B. Thisse, C. Thisse, N. Jing, and S.L. Ang. 2002. Cloning of the mouse Sef gene and comparative analysis of its expression with Fgf8 and Spry2 during embryogenesis. Mechanisms of development. 113:163-168.

Luo, Y., C. Yang, W. Lu, R. Xie, C. Jin, P. Huang, F. Wang, and W.L. McKeehan. 2010. Metabolic regulator betaKlotho interacts with fibroblast growth factor receptor 4 (FGFR4) to induce apoptosis and inhibit tumor cell proliferation. The Journal of biological chemistry. 285:30069-30078.

Manford, A.G., C.J. Stefan, H.L. Yuan, J.A. Macgurn, and S.D. Emr. 2012. ER-to-plasma membrane tethering proteins regulate cell signaling and ER morphology. Developmental cell. 23:1129-1140.

Miaczynska, M., L. Pelkmans, and M. Zerial. 2004. Not just a sink: endosomes in control of signal transduction. Current opinion in cell biology. 16:400-406.

Min, S.W., W.P. Chang, and T.C. Sudhof. 2007. ESyts, a family of membranous Ca^{2+}-sensor proteins with multiple C2 domains. Proceedings of the National Academy of Sciences of the United States of America. 104:3823-3828.

Morris, N.J., S.A. Ross, J.M. Neveu, W.S. Lane, and G.E. Lienhard. 1999. Cloning and preliminary characterization of a 121 kDa protein with multiple predicted C2 domains. Biochimica et biophysica acta. 1431:525-530.

Murakami, M., and M. Simons. 2008. Fibroblast growth factor regulation of neovascularization. Current opinion in hematology. 15:215-220.

Niehrs, C., and H. Meinhardt. 2002. Modular feedback. Nature. 417:35-36.

Nishizuka, Y. 1988. The molecular heterogeneity of protein kinase C and its implications for cellular regulation. Nature. 334:661-665.

Olivero, M., G. Valente, A. Bardelli, P. Longati, N. Ferrero, C. Cracco, C. Terrone, S. Rocca-Rossetti, P.M. Comoglio, and M.F. Di Renzo. 1999. Novel mutation in the ATP-binding site of the MET oncogene tyrosine kinase in a HPRCC family. International journal of cancer. Journal international du cancer. 82:640-643.

Ong, S.H., Y.R. Hadari, N. Gotoh, G.R. Guy, J. Schlessinger, and I. Lax. 2001. Stimulation of phosphatidylinositol 3-kinase by fibroblast growth factor receptors is mediated by coordinated recruitment of multiple docking proteins. Proceedings of the National Academy of Sciences of the United States of America. 98:6074-6079.

Pang, Z.P., and T.C. Sudhof. 2010. Cell biology of Ca^{2+}-triggered exocytosis. Current opinion in cell biology. 22:496-505.

Park, M., M. Dean, C.S. Cooper, M. Schmidt, S.J. O'Brien, D.G. Blair, and G.F. Vande Woude. 1986. Mechanism of met oncogene activation. Cell. 45:895-904.

Park, W.S., S.M. Dong, S.Y. Kim, E.Y. Na, M.S. Shin, J.H. Pi, B.J. Kim, J.H. Bae, Y.K. Hong, K.S. Lee, S.H. Lee, N.J. Yoo, J.J. Jang, S. Pack, Z. Zhuang, L. Schmidt, B. Zbar, and J.Y. Lee. 1999. Somatic mutations in the kinase domain of the Met/hepatocyte growth factor receptor gene in childhood hepatocellular carcinomas. Cancer research. 59:307-310.

Pawson, T. 2004. Specificity in signal transduction: from phosphotyrosine-SH2 domain interactions to complex cellular systems. Cell. 116:191-203.

Pawson, T., and G.D. Gish. 1992. SH2 and SH3 domains: from structure to function. Cell. 71:359-362.

Pawson, T., and P. Nash. 2000. Protein-protein interactions define specificity in signal transduction. Genes & development. 14:1027-1047.

Preger, E., I. Ziv, A. Shabtay, I. Sher, M. Tsang, I.B. Dawid, Y. Altuvia, and D. Ron. 2004. Alternative splicing generates an isoform of the human Sef gene with altered subcellular localization and specificity. Proceedings of the National Academy of Sciences of the United States of America. 101:1229-1234.

Ren, Y., L. Cheng, Z. Rong, Z. Li, Y. Li, X. Zhang, S. Xiong, J. Hu, X.Y. Fu, and Z. Chang. 2008. hSef potentiates EGF-mediated MAPK signaling through affecting EGFR trafficking and degradation. Cellular signaling. 20:518-533.

Ren, Y., Z. Li, Z. Rong, L. Cheng, Y. Li, Z. Wang, and Z. Chang. 2007. Tyrosine 330 in hSef is critical for the localization and the inhibitory effect on FGF signaling. Biochemical and biophysical research communications. 354:741-746.

Ron, D., Y. Fuchs, and D.S. Chorev. 2008. Know thy Sef: a novel class of feedback antagonists of receptor tyrosine kinase signaling. The international journal of biochemistry & cell biology. 40:2040-2052.

Rong, S., S. Segal, M. Anver, J.H. Resau, and G.F. Vande Woude. 1994. Invasiveness and metastasis of NIH 3T3 cells induced by Met-hepatocyte growth factor/scatter factor autocrine stimulation. Proceedings of the National Academy of Sciences of the United States of America. 91:4731-4735.

Sanders, L.C., F. Matsumura, G.M. Bokoch, and P. de Lanerolle. 1999. Inhibition of myosin light chain kinase by p21-activated kinase. Science. 283:2083-2085.

Schmidt, L., F.M. Duh, F. Chen, T. Kishida, G. Glenn, P. Choyke, S.W. Scherer, Z. Zhuang, I. Lubensky, M. Dean, R. Allikmets, A. Chidambaram, U.R. Bergerheim, J.T. Feltis, C. Casadevall, A. Zamarron, M. Bernues, S. Richard, C.J. Lips, M.M. Walther, L.C. Tsui, L. Geil, M.L. Orcutt, T. Stackhouse, J. Lipan, L. Slife, H. Brauch, J. Decker, G. Niehans, M.D. Hughson, H. Moch, S. Storkel, M.I. Lerman, W.M. Linehan, and B. Zbar. 1997. Germline and somatic mutations in the tyrosine kinase domain of the MET proto-oncogene in papillary renal carcinomas. Nature genetics. 16:68-73.

Schmidt, L., K. Junker, G. Weirich, G. Glenn, P. Choyke, I. Lubensky, Z. Zhuang, M. Jeffers, G. Vande Woude, H. Neumann, M. Walther, W.M. Linehan, and B. Zbar. 1998. Two North American families with hereditary papillary renal carcinoma and identical novel mutations in the MET proto-oncogene. Cancer research. 58:1719-1722.

Shin, O.H., W. Han, Y. Wang, and T.C. Sudhof. 2005. Evolutionarily conserved multiple C2 domain proteins with two transmembrane regions (MCTPs) and unusual Ca^{2+} binding properties. The Journal of biological chemistry. 280:1641-1651.

Sigismund, S., E. Argenzio, D. Tosoni, E. Cavallaro, S. Polo, and P.P. Di Fiore. 2008. Clathrin-mediated internalization is essential for sustained EGFR signaling but dispensable for degradation. Developmental cell. 15:209-219.

Sivak, J.M., L.F. Petersen, and E. Amaya. 2005. FGF signal interpretation is directed by Sprouty and Spred proteins during mesoderm formation. Developmental cell. 8:689-701.

Sorokin, A., M. Mohammadi, J. Huang, and J. Schlessinger. 1994. Internalization of fibroblast growth factor receptor is inhibited by a point mutation at tyrosine 766. The Journal of biological chemistry. 269:17056-17061.

Sudhof, T.C. 2004. The synaptic vesicle cycle. Annual review of neuroscience. 27:509-547.

Sutton, R.B., B.A. Davletov, A.M. Berghuis, T.C. Sudhof, and S.R. Sprang. 1995. Structure of the first C2 domain of synaptotagmin I: a novel Ca^{2+}/phospholipid-binding fold. Cell. 80:929-938.

Tanyi, J., K. Tory, J. Rigo, Jr., B. Nagy, and Z. Papp. 1999. Evaluation of the tyrosine kinase domain of the Met proto-oncogene in sporadic ovarian carcinomas*. Pathology oncology research : POR. 5:187-191.

Torii, S., M. Kusakabe, T. Yamamoto, M. Maekawa, and E. Nishida. 2004. Sef is a spatial regulator for Ras/MAP kinase signaling. Developmental cell. 7:33-44.

Toulmay, A., and W.A. Prinz. 2012. A conserved membrane-binding domain targets proteins to organelle contact sites. Journal of Cell Science. 125:49-58.

Tsang, M., R. Friesel, T. Kudoh, and I.B. Dawid. 2002. Identification of Sef, a novel modulator of FGF signaling. Nature Cell biology. 4:165-169.

Tvorogov, D., and G. Carpenter. 2002. EGF-dependent association of phospholipase C-gamma1 with c-Cbl. Experimental Cell Research. 277:86-94.

Umbhauer, M., C.J. Marshall, C.S. Mason, R.W. Old, and J.C. Smith. 1995. Mesoderm induction in Xenopus caused by activation of MAP kinase. Nature. 376:58-62.

van der Geer, P., and T. Hunter. 1994. Phosphopeptide mapping and phosphoamino acid analysis by electrophoresis and chromatography on thin-layer cellulose plates. Electrophoresis. 15:544-554.

van der Geer, P., T. Hunter, and R.A. Lindberg. 1994. Receptor protein-tyrosine kinases and their signal transduction pathways. Annual review of cell biology. 10:251-337.

van der Geer, P., T. Hunter, and R.A. Lindberg. 1994. Receptor protein-tyrosine kinases and their signal transduction pathways. Annual review of cell biology. 10:251-337.

van Meer, G., D.R. Voelker, and G.W. Feigenson. 2008. Membrane lipids: where they are and how they behave. Nature reviews. Molecular cell biology. 9:112-124.

Voelker, D.R. 2009. Genetic and biochemical analysis of non-vesicular lipid traffic. Annual review of biochemistry. 78:827-856.

Whitman, M., C.P. Downes, M. Keeler, T. Keller, and L. Cantley. 1988. Type I phosphatidylinositol kinase makes a novel inositol phospholipid, phosphatidylinositol-3-phosphate. Nature. 332:644-646.

Wiedlocha, A., and V. Sorensen. 2004. Signaling, internalization, and intracellular activity of fibroblast growth factor. Current topics in microbiology and immunology. 286:45-79.

Xiong, S., Q. Zhao, Z. Rong, G. Huang, Y. Huang, P. Chen, S. Zhang, L. Liu, and Z. Chang. 2003. hSef inhibits PC-12 cell differentiation by interfering with Ras-mitogen-activated protein kinase MAPK signaling. The Journal of biological chemistry. 278:50273-50282.

Xu, J., T. Bacaj, A. Zhou, D.R. Tomchick, T.C. Sudhof, and J. Rizo. 2014. Structure and Ca(2)(+)-binding properties of the tandem C(2) domains of ESyt2. Structure. 22:269-280.

Yang, R.B., C.K. Ng, S.M. Wasserman, L.G. Komuves, M.E. Gerritsen, and J.N. Topper. 2003. A novel interleukin-17 receptor-like protein identified in human umbilical vein endothelial cells antagonizes basic fibroblast growth factor-induced signaling. The Journal of biological chemistry. 278:33232-33238.

Ziv, I., Y. Fuchs, E. Preger, A. Shabtay, H. Harduf, T. Zilpa, N. Dym, and D. Ron. 2006. The human sef-a isoform utilizes different mechanisms to regulate receptor tyrosine kinase signaling pathways and subsequent cell fate. The Journal of biological chemistry. 281:39225-39235.

Zwick, E., J. Bange, and A. Ullrich. 2001. Receptor tyrosine kinase signaling as a target for cancer intervention strategies. Endocrine-related cancer. 8:161-173.

Annexe

Loss of Extended Synaptotagmins ESyt2 and ESyt3 does not affect mouse development or viability, but in vitro cell migration and survival under stress are affected.

[#]Chelsea Herdman, [#]Michel G. Tremblay, Prakash K. Mishra and Tom Moss*.

Laboratory of Growth and Development, St-Patrick Research Group in Basic Oncology, Cancer Division of the Quebec University Hospital Research Centre. Department of Molecular Biology, Medical Biochemistry and Pathology, Faculty of Medicine, Laval University, Edifice St Patrick, 9 rue McMahon, Québec, QC, G1R 3S3, Canada.

Joint first authors

*To whom correspondence should be addressed,

E-mail. Tom.Moss@crhdq.ulaval.ca

Tel. 1 418 691 5281

FAX 1 418 691 5439

Keywords: Extended-Synaptotagmin, Esyt1, Esyt2, Esyt3, Expression Analysis, Genetic Deletion, Phenotypic Analysis, Cell Migration Defects, Cell Survival Defects, Signal Transduction.

Abstract

The Extended Synaptotagmins (Esyts) are a family of multi-C2 domain membrane proteins with orthologs in organisms from yeast to human. Three Esyt genes exist in mouse and human and they have most recently been implicated in the formation of junctions between endoplasmic reticulum and plasma membrane, and the Ca^{2+} -dependent replenishment of membrane phospholipids. The data are consistent with a function in extracellular signal transduction and cell adhesion, and indeed Esyt2 was previously implicated in both these functions in Xenopus. Despite this, little is known of the function of the Esyts in vivo. We have generated mouse lines carrying homozygous deletions in one or both of the genes encoding the highly homologous Esyt2 and Esyt3 proteins. Surprisingly, *esyt2*$^{-/-}$*/esyt3*$^{-/-}$ mice develop normally and are both viable and fertile. In contrast, *esyt2*$^{-/-}$*/esyt3*$^{-/-}$ mouse embryonic fibroblasts display a reduced ability to migrate in standard in vitro assays, and are less resistant to stringent culture conditions and to oxidative stress than equivalent wild type fibroblasts.

Introduction

The Extended Synaptotagmins (Esyts) are multiple C2 domain containing membrane proteins. The first member of this family of proteins was isolated from preparations of plasma membranes and high density microsome fractions of rat adipocytes [1]. However, the Esyts were not further considered until 2007, when the primary structures of the three human Esyts1 to 3 were determined and their membrane associations investigated [2]. Human Esyt1 was shown to contain five C2 domain homologies, while human Esyts 2 and 3 each contain three. The C2 domains are preceded by a ~300a.a. N-terminal region containing one or two putative membrane spanning domains and a predicted SMP domain [3-5] (Figure 1A). Solution studies of the C2 domains of Esyt2 have confirmed their structural identity and shown that, when linked, they exhibit calcium-dependent multimerization, while the domains display different abilities to coordinate Ca^{2+} [6-8]. The C2C domains of Esyt2 and 3 interact with phospholipids driving the recruitment of these Esyts to phospholipids within the plasma membrane [2, 9]. In previous studies, we identified Xenopus ESyt2 as an endocytic adapter that determines the timing of ERK activation in blastula embryos by binding both Fibroblast Growth Factor Receptor (FGFR) and Adaptin 2 (AP-2) to catalyze rapid receptor endocytosis via the Clathrin pathway [9]. We further showed that ESyt2 recruits the cytoskeleton regulator p21-Activated-Kinase-1 (PAK1) to modulate local actin polymerization **[10]**, a function required during endocytosis [11]. Most recently it was shown that the ESyts and the related yeast Tricalbins are in fact found inserted into the endoplasmic reticulum (ER) at sites of contact with the Plasma Membrane (ER-PM junctions) [12-14]. This has given rise to the model of the ESyts as two-pass ER membrane proteins that link the ER to the PM via a C2C-domain-$PI(4,5)P_2$ (PIP2) interaction. Most recently, ESyt1 was shown to stimulate the formation of ER-PM junctions in a Ca^{++}-dependent manner, and in this way to promote recruitment of the phosphatidylinositol transfer protein (PITP) Nir2 and phospholipid incorporation into the PM [14].

To date the demonstration that Esyt2 is required for mesoderm formation in early Xenopus embryos remains the only demonstrated biological requirement for any of the Esyt proteins. The mouse and human genomes encode three Esyt proteins, one of which represents the obvious ortholog of Xenopus Esyt2. In order to relate our studies in Xenopus to the apparently more complex mouse and human situation we have studied the requirements for ESyt2 and 3 in mouse and in cultured mouse cells. Unexpectedly, we find that inactivation of either or both the genes for the highly similar ESyts -2 and -3 has no discernible effect on mouse development, viability, reproduction or longevity. However, *esyt2*$^{-/-}$ and *esyt2*$^{-/-}$/*esyt3*$^{-/-}$ embryonic fibroblasts (MEFs) display defects in both migration and resistance to culture stresses consistent with the previously proposed functions in growth factor response and the cytoskeleton regulation.

Results

Targeted disruption of the mouse ESyt2 and ESyt3 genes.

ES cells carrying insertions in the *esyt2* gene (#CA0077 and AN0678, International Gene Trap Consortium (IGTC)) (Figure 1B to D), and "Knockout First" ES cells carrying a potentially conditional insertion in *esyt3* (EPD0458_5_A10, European Conditional Mouse Mutagenesis Program (EUCOMM)) (Figure 1E to G) were used to generate chimeric mice. Southern blotting and targeted PCR analysis showed that transmission of the mutant alleles was obtained in each case.

ESyt2, -3 and 2/3 null mice are viable.

We found that not only were the *esyt2*$^{-/-}$ and *esyt3*$^{-/-}$ mice viable, but the frequency of wild-type, heterozygous and homozygous null genotypes followed a Mendelian pattern of inheritance (Table 1A). Moreover, we found that the *esyt2*$^{-/-}$ and *esyt3*$^{-/-}$ mice were fertile, produced litters of normal size and did not show any overt morphological defects compared to their heterozygous and wild-type littermates. When *esyt2*$^{-/-}$ and *esyt3*$^{-/-}$ mice were crossed they also generated viable *esyt2*$^{-/-}$/*esyt3*$^{-/-}$

offspring at near Mendelian ratios (Table 1B). The ratios did however show some skewing towards *esyt2*$^{+/-}$/*esyt3*$^{+/-}$ double heterozygotes at the expense of *esyt2*$^{+/+}$/*esyt3*$^{+/-}$ and *esyt2*$^{-/-}$/*esyt3*$^{-/-}$, suggesting minor effects on viability during development. As expected, the *esyt2*$^{-/-}$/*esyt3*$^{-/-}$ mice expressed no detectable level of the corresponding mRNAs, but continued to express ESyt1 mRNA at wildtype levels (Figure 2). *Esyt2*$^{-/-}$, *esyt3*$^{-/-}$, and *esyt2*$^{-/-}$/*esyt3*$^{-/-}$ mice also displayed a normal life span, several being kept for 18 months with no premature signs of senescence. Thus, the *esyt2* and *esyt3* genes are not essential for mouse development, viability, survival or reproduction.

Expression pattern of the ESyts in mouse adult tissues.

Expression of the *esyt2* and particularly of *esyt3* genes were found to be highly tissue specific in adults. ESyt2 mRNA was predominantly detected in lung, spleen, testis and stomach, and at much lower levels in all the other tissues tested (Figure 2). The same tissue specific expression pattern was reflected for ESyt1 mRNA with the sole exception of testis, which showed low levels of ESyt1 mRNA. In contrast, ESyt3 mRNA was only expressed strongly in lung and testis, and was present at low levels only in stomach and possibly brain. The strongly overlapping expression profiles may provide some explanation for the lack of an ESyt2/3-null phenotype if ESyt1 can functionally replace the other two ESyts.

Expression of ESyt2 and 3 in mouse embryos.

It was possible that the lack of a developmental phenotype simply correlated with a lack of expression of *esyt2* and/or *-3*. However, using hetero- and homozygous embryos expressing β-galactosidase from the respective endogenous gene promoters we found that the *esyt2* gene was expressed throughout the 10.5 to 12.5dpc embryo with little regional specificity. Expression was, however, highest in the neural tube and later in the dorsal root ganglia (Figure 3). In complete contrast, at 10.5dpc the *esyt3* gene was expressed only at the midbrain-hindbrain border (mhb), at the level of the rhombomeres (r2-r6) possibly within the cranial ganglia, and at the apical

ectodermal ridge (aer) of the forelimb bud (fb) and probably the hindlimb bud. The apical ectodermal ridge is a well-documented site of FGF signaling, FGF from this region is required to maintain cell proliferation in the underlying mesenchyme [19]. The specific expression of ESyt3 in this region, therefore, provides a tentative link with the demonstrated function of ESyt-family members in FGF signaling during early Xenopus development [9]. The broad and strong embryonic expression of ESyt2 could explain why ESyt3 inactivation causes no obvious phenotype, but similar studies of ESyt1 will be necessary to determine if its embryonic expression is sufficiently broad to compensate for loss of both ESyt2 and 3.

Esyt2 and Esyt3 deficiency does not impair organ development.

It was possible that the ESyt2/3 null mice harboured minor organ defects that did not affect their viability. Hence, we studied the structure of a range of organs from adult mice. However, we failed to detect anything unusual in the histology of lung, testis or spleen, in which ESyt2 and 3 are strongly expressed, or kidney, in which ESyt1 and 2 are expressed only weakly and ESyt3 was not detected (Figure 4). Similarly, cursory inspection of brain and muscle histology detected no abnormalities (data not shown).

ESyt2 loss does not affect FGF activation of ERK in MEFs.

Given that previous data had implicated Xenopus ESyt2 in FGF signaling in early Xenopus embryos [9], we generated embryonic fibroblasts from both ESyt2 and ESyt2/3 null mice and studied their response to FGF and other stimulations. As shown in Figure 2, MEFs do not contain ESyt3 mRNA, hence we first determined whether or not activation of signaling pathways were affected in *esyt2*$^{-/-}$ MEFs. After overnight serum withdrawal, FGF, EGF and serum (FBS) induced robust and similar levels of activation of ERK and AKT in both *wt* and *esyt2*$^{-/-}$ MEFs (Figure 5).

ESyt2/3 loss does affect migration of MEFs and their viability under stress.

Despite the lack of effect on signal transduction, "scratch-test" assays to determine the ability of cells to migrate when stimulated by FGF revealed that both *esyt2*$^{-/-}$*esyt3*$^{-/-}$ MEFs (Figure 6A) and the *esyt2*$^{-/-}$ MEFs (not shown) tended to migrate in a far less coordinated fashion and maintained little cell-cell contact during their migration as compared to *wt* (*esyt*$^{+/+}$*esyt3*$^{+/+}$) MEFs. The *esyt2*$^{-/-}$ and *esyt2*$^{-/-}$*esyt3*$^{-/-}$ MEFs also migrated far less rapidly (Figure 6A & B). As would be expected given the lack of esyt3 expression in MEFs (Figure 2), *esyt2*$^{-/-}$*esyt3*$^{-/-}$ MEFs displayed the same migration defect as the *esyt2*$^{-/-}$ MEFs (Figure 6B).

The *esyt2*$^{-/-}$*esyt3*$^{-/-}$ MEFs were also significantly less resistant to serum withdrawal or oxidative stress as compared to the *wt* ones. Withdrawal of serum over 4 days of incubation caused a 75% reduction in viability in *wt* MEFs, while less than 3% of *esyt2*$^{-/-}$*esyt3*$^{-/-}$ MEFs survived this treatment (Figure 6C). Despite this, FGF afforded a similar level of protection in both cell types, consistent with its ability to activate signaling pathways in both. The *esyt2*$^{-/-}$*esyt3*$^{-/-}$ MEFs were also extremely sensitive to oxidative damage as compared to the *wt*, and again here FGF provided some degree of protection in both cases. These data show that inactivation of the *esyt2*$^{-/-}$ and *esyt2*$^{-/-}$*esyt3*$^{-/-}$ genes does indeed affect aspects of cell migration and viability. These defects must, however, be compensated for in the in vivo context of the mouse.

Discussion

Given the apparent importance of Esyt2 during Xenopus development and the recent demonstrations of the role of the Esyts in ER-PM junction formation and phospholipid generation, the lack of phenotypic effects due to the loss of Esyt2 and 3 in mouse was fully unexpected. It is, however, not without precedent. Yeast contains three Tricalbin (Tcb) proteins that are structurally closely related to the mammalian Esyts [13]. Deletion studies in yeast of the Tricalbin family show that they are highly functionally redundant and in concert with other membrane tethering proteins they promote ER-PM junction formation [13, 20, 21]. Indeed, deletion of all three Tcbs was not

in itself sufficient to eliminate ER-PM tethering and this required deletion of three other proteins, Ist2 (a TMEM16 ion channel family member) and the vesicle-associated membrane protein-associated protein (VAP) orthologs Scs2 and Scs22. We previously demonstrated a requirement for Xenopus Esyt2 in FGF signal transduction, receptor endocytosis and mesoderm induction [9, 10]. Why very early Xenopus development was sensitive to Esyt2 depletion, while mouse is clearly not, is still unclear. This said, the expression profiles of the Xenopus Esyts suggest that only Esyt2 mRNA is present maternally (NCBI Unigene EST_Profiler, Xenbase [22]). Thus, Esyt2 may be the only family member present during early cleavage divisions.

Despite the apparent lack of a requirement for Esyt2 and -3 in mouse, MEFs carrying homozygous deletion of one or both genes display clear migration deficits in "scratch test" assays and are significantly more susceptible to stringent culture conditions and to oxidative stress than otherwise isogenic *wt* MEFs. Given the connection with the PAK1 function, it is tempting to suggest that this is due to defects in cytoskeletal dynamics. We note that mRNA levels of Esyt1, the only remaining Esyt in the *esyt2*$^{-/-}$ and *esyt2*$^{-/-}$*esyt3*$^{-/-}$ MEFs, are low. Possibly then this level of Esyt1 is insufficient to compensate. Clearly, these issues will only be resolved by the generation of Esyt1-null and possibly Esyt1/2/3 null mice.

Materials And Methods

Genotype analysis of targeted ES cells and mice. *esyt2*$^{+/-}$ (gene trapped clones Esyt2$^{Gt(AN0678)Wtsi}$ and Esyt2$^{Gt(CA0077)Wtsi}$) and *esyt3*$^{+/-}$ (targeted clone Esyt3$^{tm1a(EUCOMM)Wtsi}$) embryonic stem (ES) cells were generated respectively by SIGTR and EUCOMM from Wellcome Trust Sanger Institute with the targeting vectors shown in Figure 1. These clones were each used to generate two independent mouse lines. Southern blot analysis was used to determine the genotype of single *esyt2* or *esyt3* mutant ES cell lines and mice. For the Esyt2 clone AN0678, genomic DNA was restricted with BamHI and probed with a ^{32}P-labeled 400bp probe isolated from a region located between exons 9 and 10. For the Esyt2 clone CA0077, genomic

DNA was restricted with BamHI and probed with a ^{32}P-labeled 510bp probe isolated from a region located immediately after exon 13. For the *ESyt3* locus, BamHI-restricted genomic DNA was analysed using a ^{32}P-labeled 380 bp 3' probe subcloned from a region immediately after exon 10 (Figure 1), and EcoRV restricted DNA was analysed using a 350bp 5' probe from intron 2 (data not shown). Subsequently, genotypes of animals born from crosses of *esyt2*$^{-/-}$ and *esyt3*$^{-/-}$ mice were determined by PCR amplification of genomic DNA. For clone AN0678, primers AN-A (5'-CCAATCAGCAGTCTTACCAT), AN-B (5'-CGTCTCAAGGGAAGGAAATAA) and AN-C (5'-CGCCATACAGTCCTCTTCAC) were used. Primers AN-A and AN-B amplified a fragment of 803 bp from the wild type allele whereas primers AN-A and AN-C amplified a fragment of 541 bp from the targeted allele. Primers CA-D (5'-GTTCACTCTGGACGAGGTT), CA-E (5'-CAGCTCTGATGTCTGCCAGCA) and CA-F (5'-GTAAGGAGAAAATACCGCATC) were used for the CA0077 clone. A 513 bp fragment from the wild type allele was amplified with oligonucleotides CA-D and CD-E whereas primers CA-E and CA-F amplified a fragment of 383 bp from the targeted allele. For *esyt3*, primers A (5'- CTGAAGCCTCCCAGTAGGTG), B (5'-CCATCACCCCTAGTTGTTGC), C (5'- CCACAACGGGTTCTTCTGTT), D (5'-GAGGCTCCAGGCCTTAGTTT), E (5'- CAAAAGGCAACCTCAAGGAG) and F (5'- CGGTCGCTACCATTACCAGT) were used. Primers A and B amplified a fragment of 275 bp from the wild type allele, primers A and C amplified a fragment of 367 bp from the targeted allele, primers A and D amplified a fragment of 400 bp from the delta (Δ) allele, the primers E and D amplified a fragment of 200 bp and 180 bp from the wild type and the targeted allele and the primers F and D amplified a fragment of 446 bp from the ß-gal allele. The mice were housed and manipulated according to the guidelines of the Canadian Council on Animal Care and experiments were approved by the institutional animal care committee.

Gene expression analysis by RT-PCR. Total RNA was extracted from mouse tissues using Trizol (Invitrogen) and quantified by absorbance at 260nm. 2 μg of total RNA was reverse transcribed using random primers (GE Healthcare) and mMLV reverse transcriptase (Invitrogen). PCR was performed using the primers designed

with Primer3 (Untergasser et al. 2007) and the number of PCR cycles was optimized to be within the linear range of amplification. The primers used were:

mESyt1.FOR (5'-TGGGATCCTGGTATCTCAGC),
mESyt1.REV (5'-CTGGGAGATCACGTCCATTT),
mESyt2.FOR (5'- CGAATCACCGTTCCTCTTGT),
mESyt2.REV (5'- GCTCTGGAAGATTTGGTTGC),
mESyt3.FOR (5'- CAAGCCCTTCATAGGAGCTG),
mESyt3.REV (5'- AGCAAATGGACTCGGATCAC),
mGAPDH.FOR (5'- AACTTTGGCATTGTGGAAGG),
mGAPDH.REV (5' ACACATTGGGGGTAGGAACA).

Amplicons were of the expected sizes of 296 bp for ESyt1, 192 bp for ESyt2, 246 bp for ESyt3 and 223 bp for GAPDH. Products were sub-cloned and sequenced to confirm their specificity.

X-gal Staining. Mouse embryos were isolated at E10.5 to E12.5 and fixed for 30 minutes in 1% Formaldehyde, 0.2% Gluteraldehyde, 0.02% NP-40 in 1 x PBS, washed three times 20 min. each in Wash Solution (2mM MgCl2, 0.02% NP40, 1 x PBS). Embryos were protected from light and incubated overnight at R/T in the Staining buffer solution (5mM potassium ferricyanide, 5mM potassium ferrocyanide and 1 mg/ml X-gal in Wash Solution). Embryos were rinsed three times, 20 min. each, in 1 x PBS. Clarification was performed with "Sca*l*e" solution as described previously [15].

Histopathology. Organs were dissected from 11-month old adult mice and fixed for more than 24 hours in 4% paraformaldehyde in PBS. Samples were progressively dehydrated and embedded in paraffin. Cross sections of 5 to 20 microns were cut and stained with hematoxylin and eosin.

Cell culture and migration assay. Primary mouse embryo fibroblasts (MEFs) from

E14.5 embryos were prepared as described [16, 17] and cultured in Dulbecco's modified Eagle medium (DMEM) – high glucose (Invitrogen), supplemented with 10% fetal bovine serum (FBS, Wisent) and Penicillin/Streptomycin/Antimycotic (Anti-Anti, Invitrogen). The effects of ESyt2 and ESyt3 loss on MEF's migration were determined in a wound-healing assay (Scratch Test) [18]. Cells were seeded in a multi-6 well plate, 12h later serum was withdrawn and cells incubated for a further 16h before the assay. After scratching with a 2µl pipette tip, cells were incubated for the indicated times in the presence or absence of 20ng/ml bFGF (Sigma-Aldrich) and 5 µg/ml heparin (Sigma-Aldrich). Images were taken using a Nikon TE2000 inverted microscope.

Cell viability was also determined after serum withdrawal, inhibition of FGF signaling and oxidative stress. On day 0, cells were seeded at a density of 75,000/well in 6-well plates. On day 1, cells were rinsed twice with serum-free and antibiotic-free medium (SFM) and then cultured for 6h in the same medium. Culture medium was replaced with SFM alone or supplemented by 10% FBS, bFGF (5 µg/ml heparin, 20ng/ml bFGF (Invitrogen)), 25 mM SU5402 (EMD/Merck), or bFGF plus SU5402. On day 3 cells were briefly rinsed twice in SFM and cultured until day 5 in fresh aliquots of the respective media. Finally, media were replaced with PBS containing 0.001% resazurin (Sigma-Aldrich) and incubated for a further 2h before estimating the viable cell count using the relative fluorescence units (RFU) of resofurin in the cell supernatant (ex. 544nm, em. 590nm, Fluoroskan Ascent, Thermo Biolabs). The effects of oxidative stress were measured in a similar way, except that on day 1, cells were treated for 2h with the indicated concentrations of H_2O_2 or H_2O_2 plus bFGF in SFM. Cells were then briefly rinsed twice in SFM before addition of medium containing 10% FBS. At day 3, cells were then subjected to the resazurin assay as above.

Signal transduction assays. Serum was withdrawn from cultures of *Esyt2*$^{+/+}$ and $^{-/-}$ MEFs for 16h prior to stimulation with bFGF (20ng/ml)/heparin (5 µg/ml), EGF (100 ng/ml) or FBS (10%). Whole cell extracts were prepared using Triton lysis buffer (50

mM Tris [pH 7.5], 1% Triton X-100, 10% glycerol, 150 mM NaCl, 1 mM EDTA, 1 mM sodium orthovanadate, 1 mM phenylmethylsulfonyl fluoride, and 1 μg/ml of aprotinin, leupeptin and pepstatin), and cleared by centrifugation (20min., 20,000g, 4deg.C). Activation of ERK and AKT was examined by Western Blotting using 20μg of protein extract and the antibodies to phospho-ERK1/2 (Sigma), phospho-AKT (Cell Signaling) and ERK2 (J. Grose). Immune complexes were detected using HRP-conjugated secondary antibodies and ECL+ (GE HealthCare).

Acknowledgements

We thank Dr J. Grose for kindly providing the anti-ERK2 peptide antibody, and Profs Jean Charron and Lucie Jeannotte for advice. We also wish to thank R. Janvier of the Histology Unit of the RSVS (Université Laval) for wax sectioning and staining, and to acknowledge the excellent services provided by the McGill University Transgenic Core Facility and the staff of the St Patrick animal house, within the Quebec University Hospital Research Centre (RC-CHU de Québec). This work was supported most recently by an operating grant from the Cancer Research Society (CRS/SRC), but was started with support from the Canadian Cancer Society (CCS). The Research Centre of the CHU de Québec is supported by a grant from the FRSQ (Québec).

References

1. Morris NJ, Ross SA, Neveu JM, Lane WS, Lienhard GE. Cloning and preliminary characterization of a 121 kDa protein with multiple predicted C2 domains. Biochimica et Biophysica Acta (BBA) - Protein Structure and Molecular Enzymology 1999; 1431:525-30.
2. Min SW, Chang WP, Sudhof TC. ESyts, a family of membranous Ca2+-sensor proteins with multiple C2 domains. Proc Natl Acad Sci U S A 2007; 104:3823-8.
3. Toulmay A, Prinz WA. A conserved membrane-binding domain targets proteins to organelle contact sites. J Cell Sci 2012; 125:49-58.

4. Kopec KO, Alva V, Lupas AN. Homology of SMP domains to the TULIP superfamily of lipid-binding proteins provides a structural basis for lipid exchange between ER and mitochondria. Bioinformatics 2010; 26:1927-31.
5. Lee I, Hong W. Diverse membrane-associated proteins contain a novel SMP domain. Faseb J 2006; 20:202-6.
6. Groer GJ, Haslbeck M, Roessle M, Gessner A. Structural characterization of soluble ESyt2. FEBS Lett 2008.
7. Nagashima T, Hayashi F, Yokoyama S. Solution structure of the third c2 domain of kiaa1228 protein. 2009.
8. Xu J, Bacaj T, Zhou A, Tomchick DR, Sudhof TC, Rizo J. Structure and Ca-Binding Properties of the Tandem C Domains of ESyt2. Structure 2013.
9. Jean S, Mikryukov A, Tremblay MG, Baril J, Guillou F, Bellenfant S, Moss T. Extended-synaptotagmin-2 mediates FGF receptor endocytosis and ERK activation in vivo. Dev Cell 2010; 19:426-39.
10. Jean S, Tremblay MG, Herdman C, Guillou F, Moss T. The endocytic adapter ESyt2 recruits the p21 GTPase activated kinase PAK1 to mediate actin dynamics and FGF signalling. Biol Open 2012; 1:731-8.
11. McMahon HT, Boucrot E. Molecular mechanism and physiological functions of clathrin-mediated endocytosis. Nat Rev Mol Cell Biol 2011; 12:517-33.
12. Giordano F, Saheki Y, Idevall-Hagren O, Colombo SF, Pirruccello M, Milosevic I, Gracheva EO, Bagriantsev SN, Borgese N, De Camilli P. PI(4,5)P(2)-dependent and Ca(2+)-regulated ER-PM interactions mediated by the extended synaptotagmins. Cell 2013; 153:1494-509.
13. Manford AG, Stefan CJ, Yuan HL, Macgurn JA, Emr SD. ER-to-plasma membrane tethering proteins regulate cell signaling and ER morphology. Dev Cell 2012; 23:1129-40.
14. Chang CL, Hsieh TS, Yang TT, Rothberg KG, Azizoglu DB, Volk E, Liao JC, Liou J. Feedback regulation of receptor-induced ca(2+) signaling mediated by ESyt1 and nir2 at endoplasmic reticulum-plasma membrane junctions. Cell Rep 2013; 5:813-25.

15. Hama H, Kurokawa H, Kawano H, Ando R, Shimogori T, Noda H, Fukami K, Sakaue-Sawano A, Miyawaki A. Scale: a chemical approach for fluorescence imaging and reconstruction of transparent mouse brain. Nat Neurosci 2011; 14:1481-8.
16. Giroux S, Tremblay M, Bernard D, Cadrin-Girard JF, Aubry S, Larouche L, Rousseau S, Huot J, Landry J, Jeannotte L, et al. Embryonic death of Mek1-deficient mice reveals a role for this kinase in angiogenesis in the labyrinthine region of the placenta. Curr Biol 1999; 9:369-72.
17. Bisson N, Tremblay M, Robinson F, Kaplan DR, Trusko SP, Moss T. Mice lacking both mixed-lineage kinase genes Mlk1 and Mlk2 retain a wild type phenotype. Cell Cycle 2008; 7:909-16.
18. Coomber BL, Gotlieb AI. In vitro endothelial wound repair. Interaction of cell migration and proliferation. Arteriosclerosis 1990; 10:215-22.
19. Thisse B, Thisse C. Functions and regulations of fibroblast growth factor signaling during embryonic development. Developmental Biology 2005; 287:390-402.
20. Creutz CE, Snyder SL, Schulz TA. Characterization of the yeast tricalbins: membrane-bound multi-C2-domain proteins that form complexes involved in membrane trafficking. Cell Mol Life Sci 2004; 61:1208-20.
21. Zuniga S, Boskovic J, Jimenez A, Ballesta JP, Remacha M. Disruption of six Saccharomyces cerevisiae novel genes and phenotypic analysis of the deletants. Yeast 1999; 15:945-53.
22. Bowes JB, Snyder KA, Segerdell E, Jarabek CJ, Azam K, Zorn AM, Vize PD. Xenbase: gene expression and improved integration. Nucleic Acids Res 2010; 38:D607-12.

Figure Legends

Figure 1. Targeted disruptions of the *esyt2* and *esyt3* genes in mouse. A) Domain structures of the mouse Esyt proteins. The C2 domains and the putative membrane spanning domains (TM) and "synaptotagmin-like, mitochondrial and lipid binding protein (SMP) domains are indicated. B) and E) Maps of the partial *esyt2* and *esyt3* genomic loci and the positions the gene trap ßGal-Neo insertions (AN0678 and CA0077), the EUCOMM Knockout First (Targeted) insertion and the deletion and bGal insertional recombination products. Positions of genotyping PCR primers (thick arrows) and hybridization probes are also indicated. C) & F) and D) & G) Respectively, Southern analyses of BamH1 digests and PCR genotyping analyses of *esyt2* and *esyt3* mutant mice.

Figure 2. Expression of Esyt1, -2 and -3 mRNA in adult mouse tissues and MEFs. RT-PCR analyses are shown for tissues from both wild type $esyt2^{+/+}/esyt3^{+/+}$ and $esyt2^{-/-}esyt3^{-/-}$ mice as compared with GAPDH.

Figure 3. Expression pattern of the *esyt2* and *-3* genes in early mouse embryos. Expression was determined by conversion of X-Gal (blue-green) by ß-galactosidase produced from the gene inserted into the *esyt2* and *esyt3* gene loci. Enlarged panels on the right show a limb-bud and the hindbrain region of $esyt3^{+/ß\text{-}Gal}$ embryos. "aer" apical ectodermal ridge, "mhb" midbrain-hindbrain boundary, "fb" forelimb bud, "hb" hindlimb bud, "url" and "lrl" upper and lower rhombomere lips, "r2-6" rhombomeres, "ov" otic vesicle, "nt" neural tube, "drg" dorsal root ganglion.

Figure 4. Representative Haematoxylin-Eosin staining of sections obtained from two 11 month old $esyt2^{-/-}esyt3^{-/-}$ sibling males and two 11 month old $esyt2^{+/+}esyt3^{+/+}$ sibling males. Organs displayed were those that showed a strong or differential expression of ESyt1, 2 and 3, see Figure 2. A) The renal cortex of WT and DKO mice are essentially indistinguishable. Renal tubules (RT) and renal corpuscles (RC) with

glomeruli (G) and Bowman's space (BS) are indicated. Scale bars 100µm. B) Top panels: Lung sections with pleura (P), bronchioles (B) and alveoli (A) indicated, scale bars 200µm. Bottom: higher magnification of alveoli, scale bars 100µm. C) Testis morphology also appears normal, seminiferous tubules (T) and the surrounding Leydig cells (L) are indicated, scale bars 100µm. D) White pulp (WP- encircled) with central arteries (CA) and red pulp (RP) of spleen samples are indicated, scale bars 100µm.

Figure 5. Response of ERK and AKT to extracellular stimulation in *esyt2*$^{-/-}$ MEFs. Esyt2$^{+/+}$ and esyt2$^{-/-}$ MEFs were treated at 0 min. with FGF, EGF and FBS and activation of ERK and AKT followed at the indicated times using phospho-specific antibodies (pERK (-1 and -2) and pAKT). ERK2 was detected using a specific antibody and was used as loading control.

Figure 6. Migration and viability assays of *esyt2*$^{-/-}$*esyt3*$^{-/-}$ and *esyt2*$^{+/+}$*esyt3*$^{+/+}$ MEFs. A) Examples of time-course from single image fields after addition of FGF during a standard Scratch Test assay. B) Quantitation of cells migrating into the "Scratch". Data for *esyt2*$^{-/-}$ was obtained from the mean of 3 image fields and for *esyt2*$^{-/-}$*esyt3*$^{-/-}$ from 10 image fields. C) Serum withdrawal/replacement assays. Cells were grown 4 days in medium either containing FBS, bFGF, SU5402 (SU), SU plus SU or without serum (SFM), before assaying cultures for viable cells via enzymatic reduction of resazurin to resorufin. Results are given in arbitrary relative fluorescence units (RFU). D) Cells were treated for 2h with the indicated concentrations of H2O2 in serum free medium in the presence or absence of bFGF. Subsequently cells were grown in FBS supplemented serum for 2 days before determining viable cells via resazurin conversion as in C. In B) to D) Error bars indicate the standard deviation, see Materials and Methods for assays.

TABLE 1

Genotype analysis of the progeny born A) from *esyt2*$^{+/-}$/*esyt2*$^{+/-}$ (alleles CA0077 and AN0678) and *esyt3*$^{+/-}$/*esyt3*$^{+/-}$ crosses, and B) from *esyt2*$^{+/-}$/*esyt3*$^{+/-}$ crosses as compared with the expected Mendelian frequencies.

Figure 1. Targeted disruptions of the *esyt2* and *esyt3* genes in mouse.

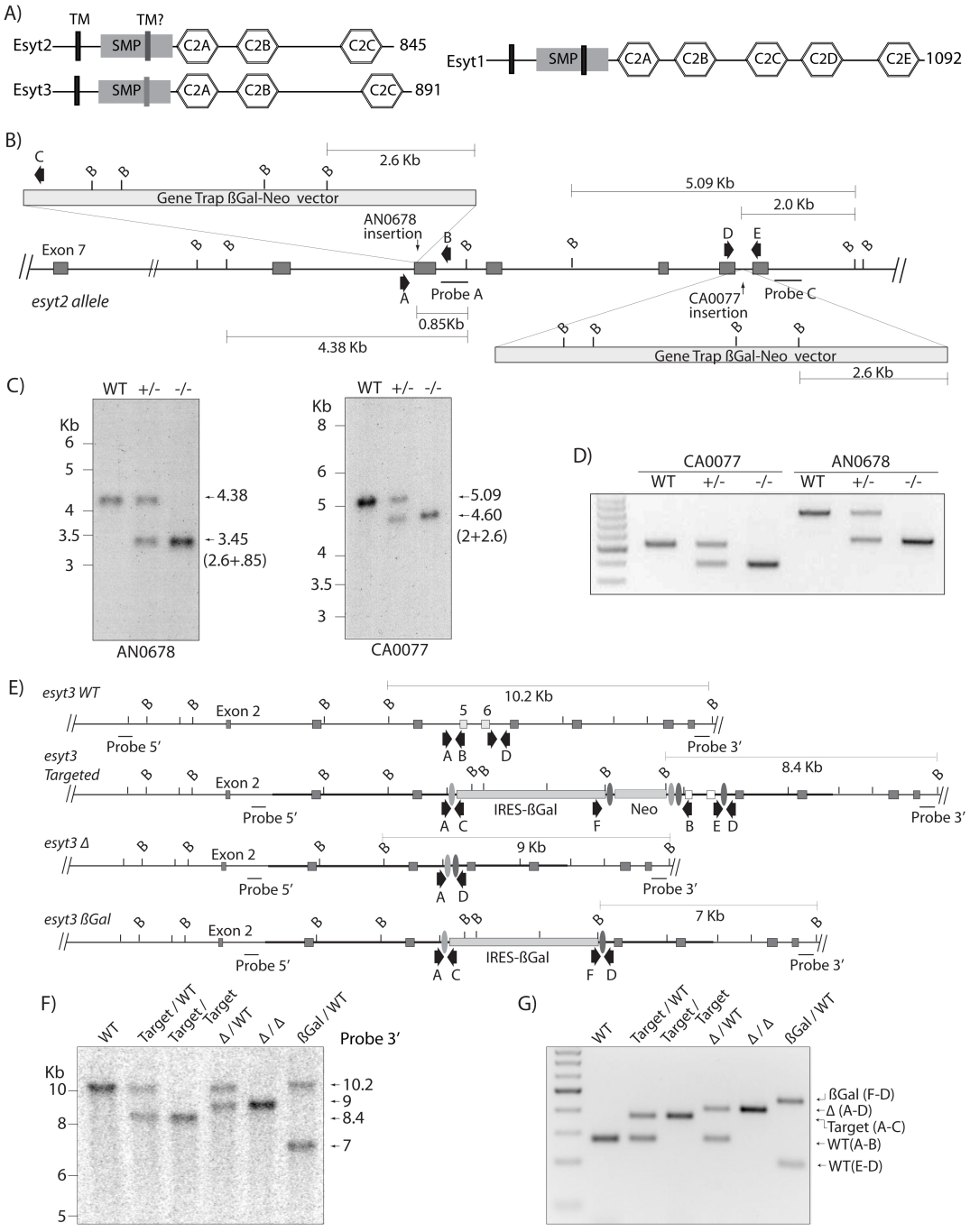

Figure 2. Expression of Esyt1, -2 and -3 mRNA in adult mouse tissues and MEFs.

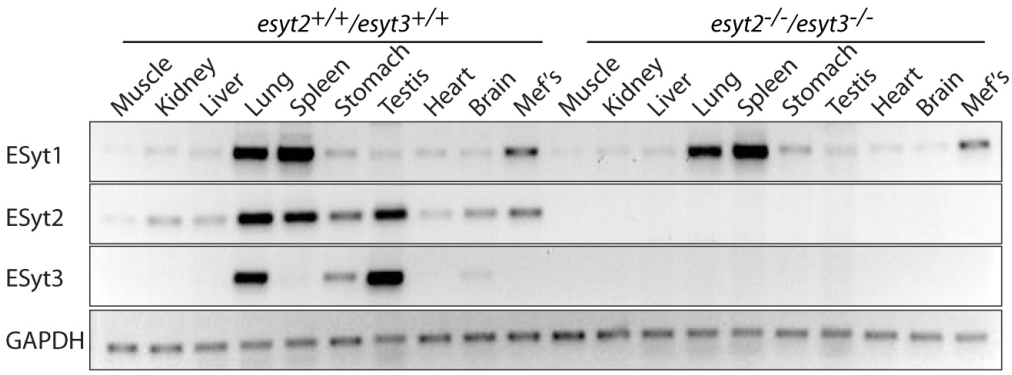

Figure 3. Expression pattern of the *esyt2* and *-3* genes in early mouse embryos.

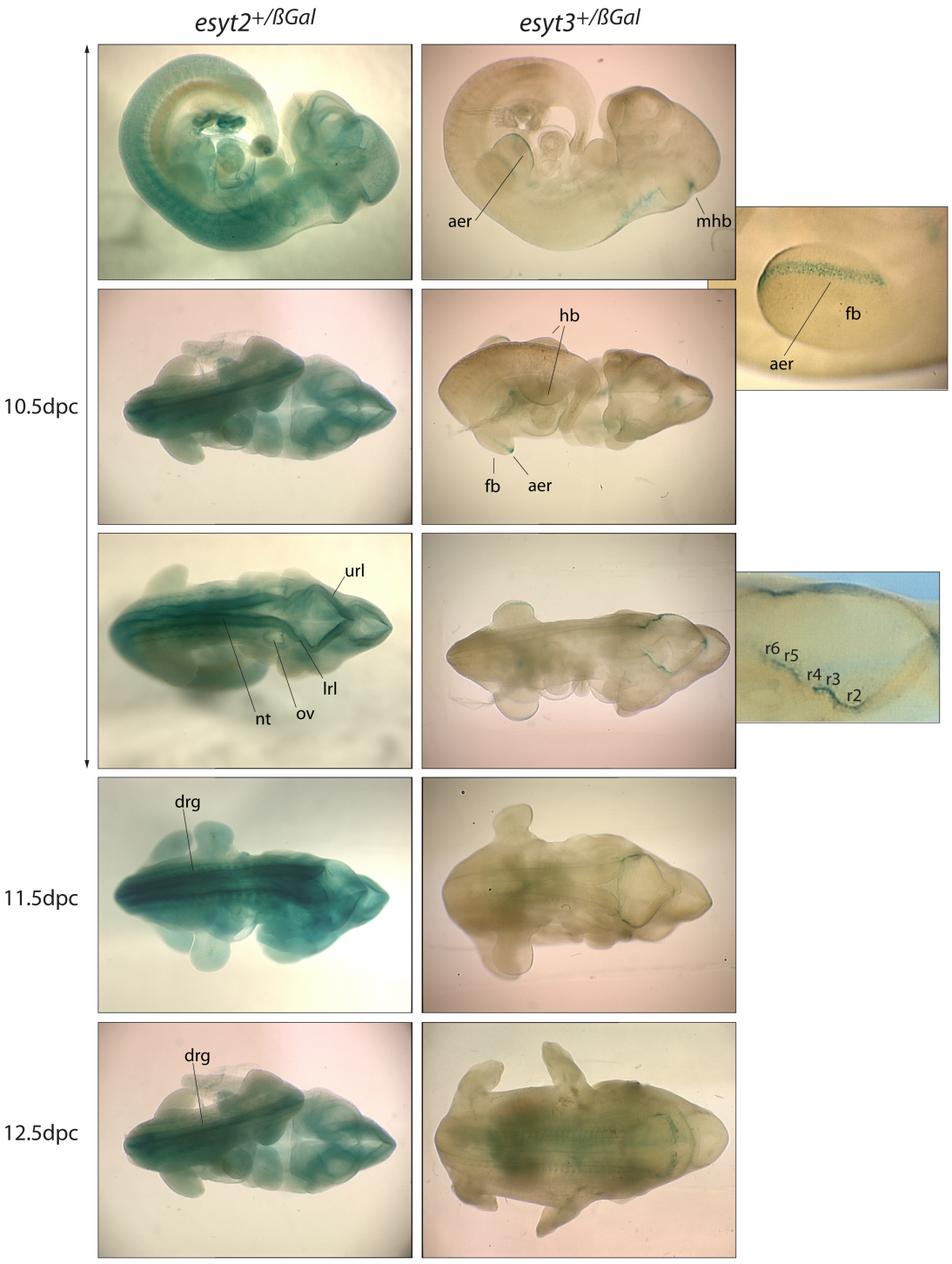

Figure 4. Representative Haematoxylin-Eosin staining of sections obtained from two 11 month old *esyt2*$^{-/-}$*esyt3*$^{-/-}$ sibling males and two 11 month old *esyt2*$^{+/+}$*esyt3*$^{+/+}$ sibling males.

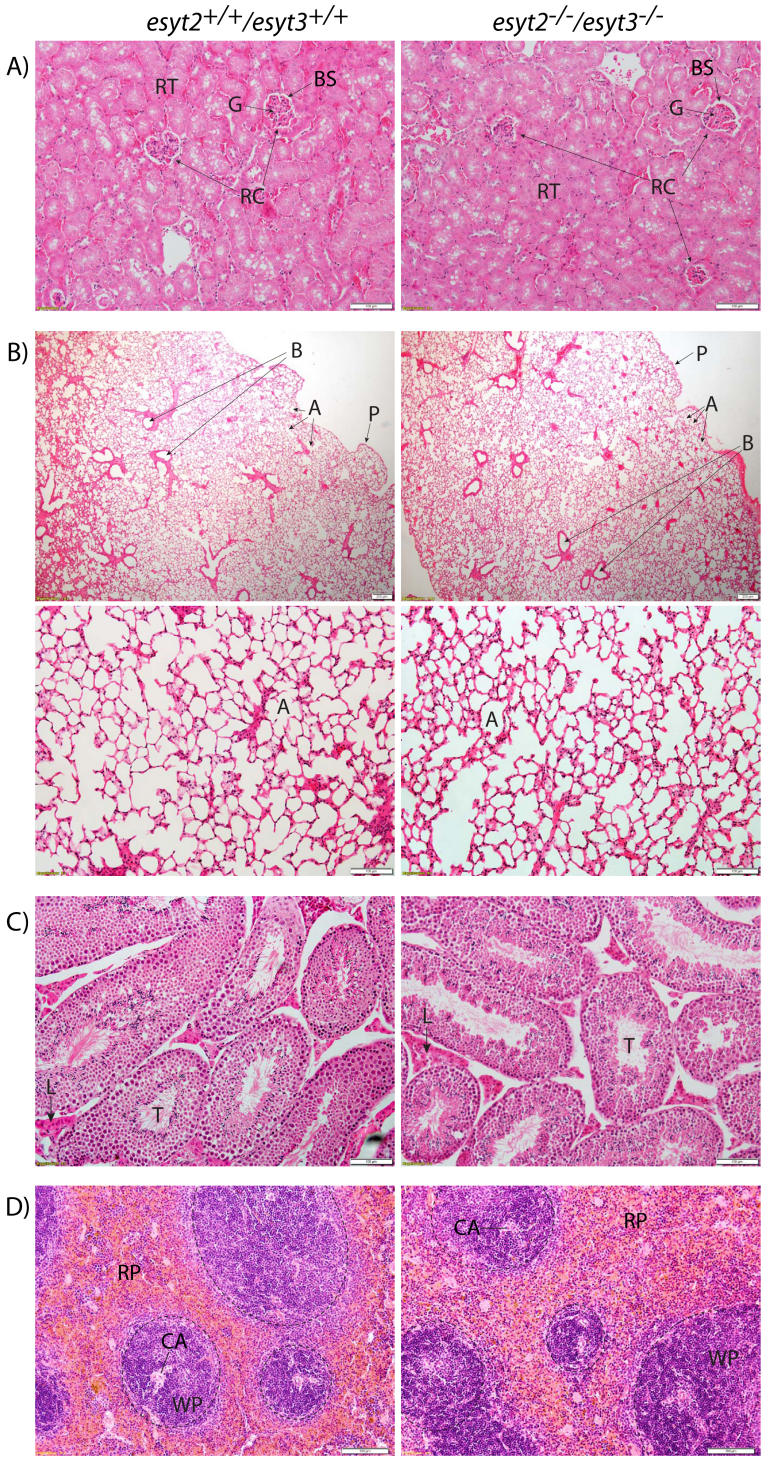

Figure 5. Response of ERK and AKT to extracellular stimulation in *esyt2*$^{-/-}$ MEFs.

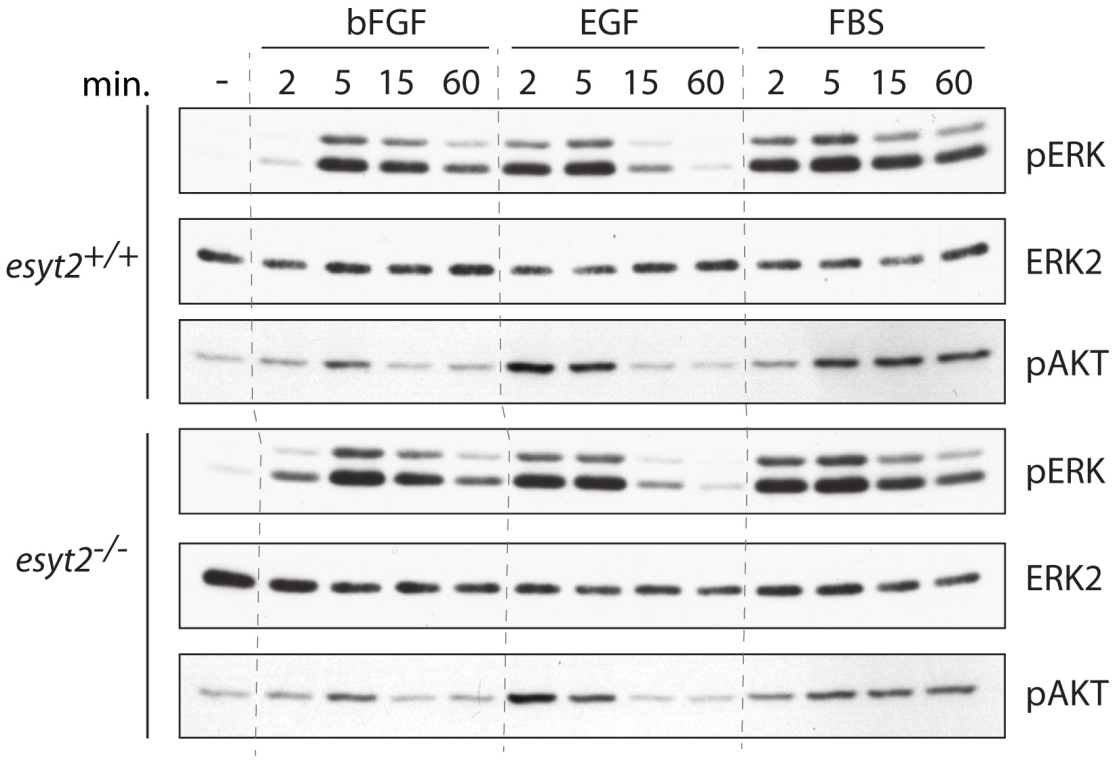

Figure 6. Migration and viability assays of *esyt2*$^{-/-}$*esyt3*$^{-/-}$ and *esyt2*$^{+/+}$*esyt3*$^{+/+}$ MEFs.

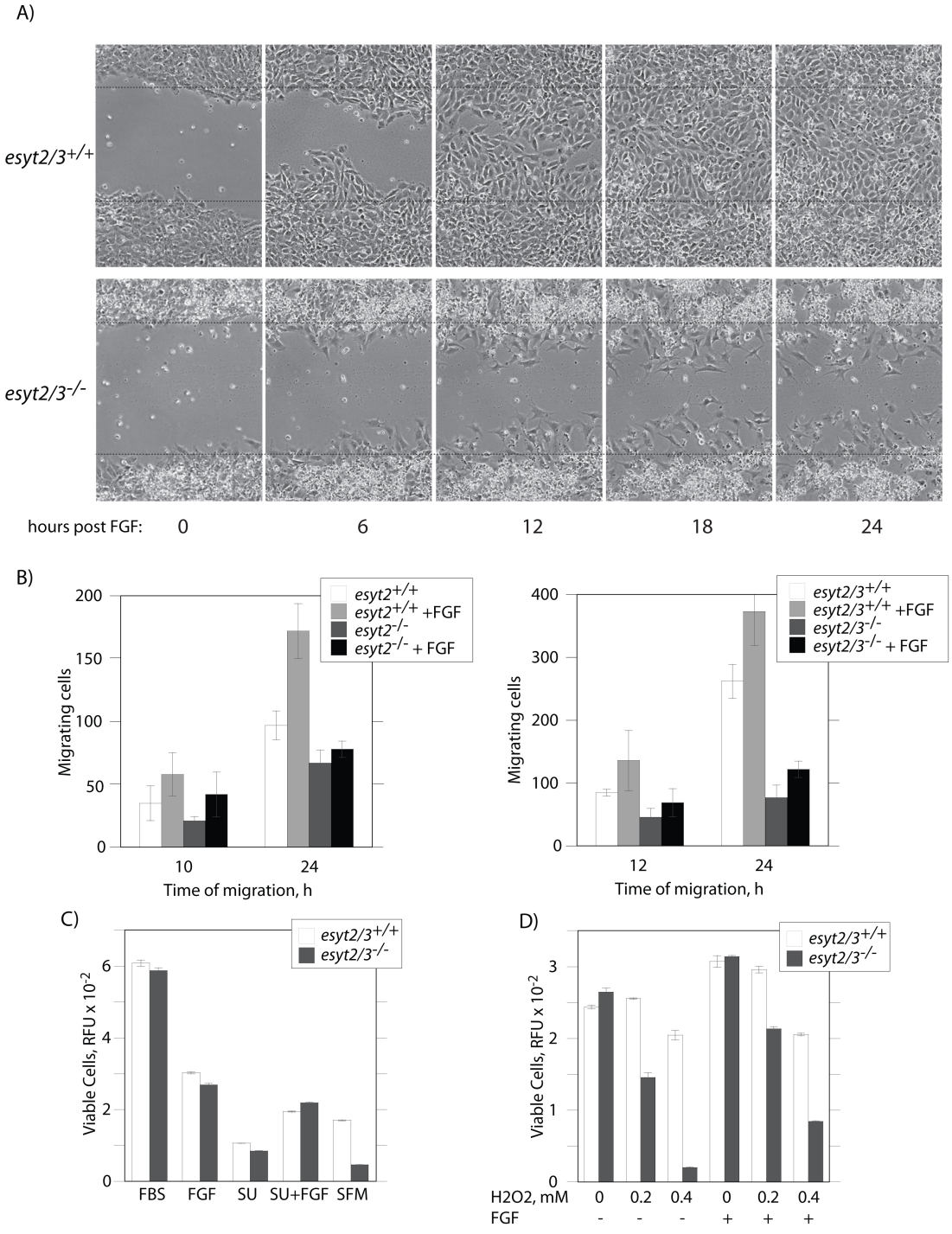

Table 1. Genotype analysis of the progeny born A) from *esyt2*$^{+/-}$/*esyt2*$^{+/-}$

A)

Gene	Number of pups	WT/WT	+/-	-/-
ESyt2 (CA0077)	171	41 (24%)	86 (50%)	44 (26%)
ESyt2 (AN0678)	180	53 (29%)	87 (48%)	40 (22%)
ESyt3	143	18 (23%)	43 (55%)	17 (22%)
	% Expected	25%	50%	25%

B) ESyt2/ESyt3

Number pups	+/+ +/+	+/+ +/-	+/+ -/-	+/- +/+	+/- +/-	+/- -/-	-/- +/+	-/- +/-	-/- -/-
143	10 (7.0%)	17(11.9%)	9(6.3%)	10(7.0%)	45(31.5%)	15(10.5%)	12(8.4%)	18(12.6%)	7(4.9%)
% Expected	6.25%	12.50%	6.25%	12.50%	25.00%	12.50%	6.25%	12.50%	6.25%